

Realistic bending stiffness of diaphragm walls for structural analysis

*A comparison with the uncracked and totally cracked stiffness for the case of
The Waalbrug Nijmegen*



Master of Science Thesis

Ranjana Soekhoe
Delft, 15-12-2015



Gemeente Rotterdam

© Ranjana Soekhoe, 2015

Graduation Committee

Chair:

Prof.dr.ir. D.A. Hordijk
TU Delft, Civil Engineering and Geosciences
Department Design & Construction
Structural and Building Engineering
Concrete Structures

Members:

Dr.ir. C.B.M. Blom
Daily Supervisor
• TU Delft, Civil Engineering and Geosciences
Department Design & Construction
Structural and Building Engineering
Concrete Structures
• Ingenieursbureau Gemeente Rotterdam

Dr.ir. R. Spruit
External Supervisor
• TU Delft, Civil Engineering and Geosciences
Department Geoscience & Engineering
Geo-Engineering
• Ingenieursbureau Gemeente Rotterdam

Ir. L.J.M. Houben
Thesis Coordinator
TU Delft, Civil Engineering and Geosciences
Department Structural Engineering
Road and Railway Engineering

Realistic bending stiffness of diaphragm walls for structural analysis

*A comparison with the uncracked and totally cracked stiffness for the case of
The Waalbrug Nijmegen*

Thesis

Submitted in partial fulfilment of the
requirements for the degree of

Master of Science

in

Civil Engineering

by Ranjana Soekhoe

Acknowledgements

I would like to extend my sincere gratitude to the graduation committee for their supervision and availability during the realization of this thesis. First and foremost, I would like to thank my two supervisors. My daily supervisor, Dr.ir. C.B.M. Blom, for giving me the opportunity to formulate a thesis subject together, which also had my keen interest. I indeed conducted this project with great pleasure. The questions about the subject often led me to new insights and solutions for problems I encountered. I thank my external supervisor, Dr.ir. R. Spruit, for guiding me through the geotechnical related part of this project and the given suggestions to lift the analyses made to a higher level.

I would like to thank the Engineering Office of Rotterdam (IGR) for supporting the graduation project and the employees for the great experience. I address a special word of gratitude towards Bas Govindasamy and Tako Heukels, not only for sharing their knowledge and given support, but also for the inspiring and great talks.

Last but not least, I would like to thank my family and friends. A special thank you to my parents, brother and two sisters. Your endless support and encouragement made the journey a whole lot easier.

Ranjana Soekhoe
Delft, 15 December 2015

Abstract

For a safe structure design standards mainly emphasize on calculations based on the uncracked and fully cracked stiffness of concrete structures. In the common design practice an uncracked stiffness (EI_0) is applied for the SLS and a fully cracked stiffness (EI_∞) for the ULS, where the reduced stiffness $EI_\infty \approx 1/3EI_0$. However, in reality it is unlikely for a structure to remain uncracked or to become fully cracked; it is more common to find members consisting of cracked and uncracked zones. This implies the existence of a realistic variable bending stiffness (EI_{var}) along the reinforced concrete member. The Eurocode 2 states that members which are expected to crack, but may not be fully cracked, will behave in a manner intermediate between the uncracked and fully cracked conditions. Insufficient elaboration on the impact of EI_{var} on the safety of concrete structures and whether the applied design models using EI_0 and EI_∞ are indeed conservative models, led to the formulation of this research project.

By means of the ‘Waalbrug-project’, this thesis investigates the impact of a realistic bending stiffness on the structural behaviour. For this particular project the safety of the parking structure, consisting of diaphragm walls and a roof structure, is analyzed. The bending stiffness of diaphragm walls is not constant over the height, but it varies as a function of the magnitude of the occurring bending moment and the amount of reinforcement. As soon as the wall is cracked the wall stiffness decreases at an increasing bending moment, which is explained in literature by means of the M-(N)- κ diagram. A reduced wall stiffness results in greater wall deformations, but on the other hand the deformations on their turn influence the wall stiffness. For the influence of the soil behaviour on the stiffness of the diaphragm wall the ‘interaction’ model Plaxis 2D was used.

Different calculation models were set up to determine whether the structural behaviour at EI_{var} lies indeed within the behaviour of an uncracked and fully cracked structure. The impact of the boundary condition (hinged or clamped connection) was also studied. The Half Model and Total Model in the calculation programs PCSheetPileWall and Plaxis 2D were used for structural analysis. The structural behaviour was expressed in terms of the bending moment (M_{Ed}), settlement (δ_v) and lateral wall displacement (U_x), which were calculated at the bending stiffnesses EI_0 , EI_∞ and EI_{var} as a function of an axial compressive force $N = 0$ kN and $N \neq 0$ kN for the following calculation models:

- Walls only; hinged
- Walls only; clamped
- Walls and roof; clamped.

EI_{var} based calculations turned out to be an iterative procedure. During this research two iteration procedures were developed to find the actual EI-distribution over the diaphragm wall height. An evaluation of the load distribution and cracked zones according to both iteration procedures, finally led to the conclusion that the results of iteration procedure 2 were valid for EI_{var} and that too for every calculation model. In iteration procedure 2 the actual EI-distribution over the wall height is obtained by considering the average M-line and average cracked zones based on EI_0 and EI_∞ .

In this research a safety analysis was performed for:

- The basic case (‘basic reinforcement ratio’ for the hinged and clamped case) and for;
- The hinged case in particular, where a variation was made in the soil stiffness and the reinforcement ratio of the diaphragm wall.

In the calculation models a ‘basic reinforcement ratio’ was the main input for determining EI_{var} . For the ‘Walls only; hinged’- model it was found that the parking structure was totally safe if the walls were designed based on EI_∞ , while for the ‘Walls and roof; clamped’- model a safe structure was reached if the walls were designed based on EI_0 . The ‘Walls only; clamped’- model showed that a fully clamped connection is only an academic case, which is not realizable. The chosen connection type was found to have a major impact on the structural safety.

Due to limited freedom of movement with regard to the reinforcement in the clamped case, variations were only studied for the hinged case. If stiffer diaphragm walls, achieved by applying a high reinforcement ratio, were used in the hinged case a model based on EI_{∞} still proved to be conservative. At a higher reinforcement ratio the behaviour tended even faster towards EI_{∞} (occurrence of greater cracked zones). When the soil properties (lower soil stiffness) were changed for the hinged case, EI_{∞} still proved to be a safe approach for the bending moment. However, for the deformations an EI_{var} based calculation was a safer method, because the actual deformations proved to be larger than what followed from the lower bound stiffness EI_{∞} .

All analyses taken into account, it can be concluded that considering both the outer boundaries EI_0 and EI_{∞} is not always a guarantee for a safe structure. Therefore, EI_{var} based calculations are necessary. It has been proven that the axial force (N) has no significant impact on EI_{var} .

Especially, when designing the reinforcement a load distribution according to EI_{var} should be considered. Otherwise, there is a great risk of placing less reinforcement over a certain part of the wall, in particular for the hinged case. An EI_0 based calculation for reinforcement design is only conservative if the maximum occurring bending moment of both walls is considered over the total wall height. However, this is a too safe approach. Of more practical relevance for (similar) future projects would be to design the reinforcement based on the 'dekkingslijn'-principle using (1) the bending stiffness EI_0 , but then with 30-50% extra reinforcement at the bottom part of the wall or (2) the bending moment envelope based on different simulations with EI_{var} .

TABLE OF CONTENTS

Acknowledgements	iii
Abstract	v
List of Figures	xi
List of Tables	xiv
Abbreviations	xvi
List of Symbols	xvi
1. INTRODUCTION	1
1.1. Background	1
1.2. Problem description	2
1.2.1. Diaphragm wall stiffness	2
1.2.2. Boundary condition diaphragm wall - roof structure.....	4
1.2.3. Packing structure in total – calculation models.....	5
1.3. Work approach	5
1.3.1. Problem statement	5
1.3.2. Aim and Scope of the research project	6
1.3.3. Objectives and research questions	6
1.4. Outline	8
2. LITERATURE SURVEY	10
2.1. Introduction	10
2.2. Diaphragm walls	10
2.2.1. Deformations and settlements	10
2.2.2. Soil-structure interaction.....	11
2.3. Soil models.....	12
2.3.1. Calculation methods	12
2.3.2. Material models.....	15
2.3.2.1. Real soil response vs. constitutive models	15
2.3.2.2. Choice of constitutive model.....	16
2.3.2.3. Soil parameters	16
2.4. The M-(N)-κ diagram.....	17
2.4.1. Characteristics in M-(N)- κ diagram	19
2.4.2. EC2: Minimum and maximum reinforcement ratio diaphragm walls	21
2.4.3. Software programs using M-N- κ diagram: PCSheetPileWall.....	21

2.5.	Design standards: Cracked vs. Uncracked bending stiffness.....	22
2.5.1.	EC2: Behaviour of not fully cracked member	22
2.5.2.	Bending stiffnesses: EI_0 , EI_{var} and EI_∞	23
3.	RESEARCH STRATEGY.....	24
3.1.	Geometry	24
3.2.	The loading combinations in SLS	25
3.2.1.	LC1.....	26
3.2.2.	LC2.....	26
3.2.3.	LC3.....	27
3.3.	Assumptions	29
3.4.	Calculation software – input	30
3.4.1.	PCSheetPileWall	30
3.4.1.1.	The material properties of the structure and the soil in PCSheetPileWall	31
3.4.1.2.	The calculation model in PCSheetPileWall	32
3.4.2.	Plaxis 2D.....	32
3.4.2.1.	The material properties of the structure and the soil in Plaxis 2D	33
3.4.2.2.	The calculation model in Plaxis 2D	34
3.5.	Roof structure – Equivalent Beam Model	36
3.6.	Calculation strategy	39
4.	RESULTS AND DISCUSSION.....	40
4.1.	Walls only; hinged.....	40
4.1.1.	Case a: EI (κ).....	40
4.1.1.1.	PCSheetPileWall – Half Model	40
4.1.1.2.	Plaxis 2D – Half Model	42
4.1.1.3.	Plaxis 2D – Total Model	44
4.1.1.4.	Iteration procedure 1 – right wall	44
4.1.1.5.	Problem left wall	48
4.1.1.6.	Iteration procedure 2 – both walls	49
4.1.1.7.	Final results EI (κ)	50
4.1.2.	Case b: EI (κ , N).....	52
4.1.2.1.	PCSheetPileWall – Half Model	52
4.1.2.2.	Plaxis 2D – Half Model	54
4.1.2.3.	Plaxis 2D – Total Model	55

4.1.2.4.	Iteration procedure 1 – right wall	56
4.1.2.5.	Problem left wall	59
4.1.2.6.	Iteration procedure 2 – both walls	59
4.1.2.7.	Final results EI (κ , N).....	61
4.2.	Walls only; clamped	62
4.2.1.	The clamped connection: A design case	62
4.2.2.	Defining the reinforcement for the clamped case.....	62
4.2.3.	Case a: EI (κ).....	66
4.2.3.1.	PCSheetPileWall – Half Model	66
4.2.3.2.	Plaxis 2D – Half Model	68
4.2.3.3.	Plaxis 2D – Total Model	69
4.2.3.4.	Iteration procedure 1 – right wall	70
4.2.3.5.	Iteration procedure 2 – both walls	73
4.2.3.6.	Final results EI (κ)	75
4.2.4.	Case b: EI (κ , N).....	76
4.2.4.1.	PCSheetPileWall – Half Model	76
4.2.4.2.	Plaxis 2D – Half Model	78
4.2.4.3.	Plaxis 2D – Total Model	79
4.2.4.4.	Iteration procedure 1 – right wall	80
4.2.4.5.	Iteration procedure 2 – both walls	82
4.2.4.6.	Final results EI (κ , N).....	84
4.3.	Evaluation iteration procedure EI_{var}	85
4.4.	Walls and roof; hinged	85
4.5.	Walls and roof; clamped	85
4.5.1.	Case a: EI (κ).....	86
4.5.2.	Case b: EI (κ , N).....	86
4.5.3.	Impact roof stiffness	87
5.	EVALUATION: SAFETY ANALYSIS	89
5.1.	Basic reinforcement ratio – safety analysis	89
5.2.	Variations hinged connection.....	93
5.2.1.	High reinforcement ratio.....	93
5.2.2.	Different soil type.....	93
5.2.3.	Hinged case in particular – safety analysis	94

5.3.	Risk analysis required reinforcement ratio for EI_{var}	97
5.4.	Evaluation cracked zones for EI_{var}	99
5.5.	Overview and answering of research questions	99
6.	CONCLUSIONS AND RECOMMENDATIONS.....	103
6.1.	Introduction	103
6.2.	Conclusions.....	103
6.3.	Recommendations	104
	References.....	106

Appendices

Appendix A	: Literature survey
Appendix B	: Geotechnical Soil Profiles
Appendix C1	: Iteration process right wall – ‘Walls only; hinged’, Case a: $EI (\kappa)$
Appendix C2	: Iteration process right wall – ‘Walls only; hinged’, Case b: $EI (\kappa, N)$
Appendix C3	: Iteration process right wall – ‘Walls only; clamped’, Case a: $EI (\kappa)$
Appendix C4	: Iteration process right wall – ‘Walls only; clamped’, Case b: $EI (\kappa, N)$
Appendix D	: Properties Stiff Structure
Appendix E1	: Variation hinged connection 1 – $\rho_{l,tot} = 1\%$, Case a: $EI (\kappa)$
Appendix E2	: Variation hinged connection 1 – $\rho_{l,tot} = 1\%$, Case b: $EI (\kappa, N)$
Appendix F1	: Variation hinged connection 2 – Soil Type 2, Case a: $EI (\kappa)$
Appendix F2	: Variation hinged connection 2 – Soil Type 2, Case b: $EI (\kappa, N)$

List of Figures

Figure 1: Location of the construction [1]	1
Figure 2: Railway bridge over the Waal at Nijmegen [1]	1
Figure 3: Packing structures around the existing foundation of the 3 bridge pillars [1]	2
Figure 4: Detail packing structure, consisting of diaphragm wall structure and a roof structure [1]	2
Figure 5: 3D-model of the roof structure [2].....	4
Figure 6: Calculation models: (a) Hinged connection; (b) Clamped connection.....	5
Figure 7: Measuring the structural safety.....	7
Figure 8: Thesis outline	9
Figure 9: Interaction model: (a) Distribution of soil reactions on the wall; (b) Behaviour according to theoretical model; (c) Behaviour of real structure.	13
Figure 10: Influence of the wall stiffness (EI) for an unanchored wall. The occurring moment is equal for both cases	14
Figure 11: Influence of the wall stiffness (EI) and the soil stiffness (k_s) for an anchored wall	14
Figure 12: Deformed mesh in Plaxis 2D.....	14
Figure 13: Comparison of HS- and MC-model with real soil response [8].....	15
Figure 14: The M-(N)- κ diagram	18
Figure 15: The influence of tension-stiffening on the bending stiffness	19
Figure 16: The M-(N)- κ diagram with reinforcement ratio (ρ_l) as variable	20
Figure 17: The M-N- κ diagram with normal compressive force ($N = N'_c$) as variable	21
Figure 18: Moment-curvature relation in a reinforced concrete section under pure bending before reinforcement yielding [9]	23
Figure 19: Geometry of the situation.....	24
Figure 20: Floor map of existing foundation surrounded by diaphragm wall structure	25
Figure 21: Loading conditions in SLS.....	28
Figure 22: Panel layout diaphragm wall	30
Figure 23: Output PCSheetPileWall.....	31
Figure 24: Impression calculation model in PCSheetPileWall (Hinged case – LC3).....	32
Figure 25: Impression Half Model in Plaxis 2D (Hinged case – LC3).....	34
Figure 26: Impression Total Model in Plaxis 2D (Hinged case – LC3).....	35
Figure 27: Equivalent beam model using 1 m strip at representative mid-section	36
Figure 28: Determining EA.....	37
Figure 29: Determining EI for 1-sided loaded structure	38
Figure 30: Determining EI for 2-sided loaded structure	38
Figure 31: M-line both walls from PCSheetPileWall (hinged connection, $N = 0$ kN).....	41
Figure 32: EI-distribution both walls from PCSheetPileWall. Left wall characterized by “EI-bite” in cracked zone.....	41

Figure 33: M- κ diagram both walls (hinged connection, $N = 0$ kN).....	41
Figure 34: (a) Deformed mesh and (b) M-line of left wall for EI_{var} (cracked_3 zones) in Plaxis 2D – Half Model ...	43
Figure 35: Hinged case - (a) Deformed mesh and (b) M-line for the walls only at $N = 0$ kN.....	44
Figure 36: Results for even and uneven iterations of right wall for $N = 0$ kN.....	46
Figure 37: The assumed ‘average result’ for the right wall based on iteration #13 and #14.	46
Figure 38: Final result EI_{var} according to iteration procedure 1 in Plaxis 2D – Total Model.	47
Figure 39: Contradicting cracked zones for the left wall	48
Figure 40: The ‘average result’ based on EI_0 and EI_∞	49
Figure 41: Final result EI_{var} according to iteration procedure 2 in Plaxis 2D – Total Model.	50
Figure 42: Hinged case – The M-line for EI_0 , EI_∞ and EI_{var} for $N = 0$ kN	51
Figure 43: M-line both walls from PCSheetPileWall (hinged connection, $N \neq 0$ kN).....	53
Figure 44: EI-distribution both walls from PCSheetPileWall. Left wall characterized by “EI-bite” in cracked zone.	53
Figure 45: M-N- κ diagram both walls (hinged connection, $N \neq 0$ kN).....	53
Figure 46: (a) Deformed mesh and (b) M-line of left wall for EI_{var} (cracked_3 zones) in Plaxis 2D – Half Model ...	55
Figure 47: Hinged case - (a) Deformed mesh and (b) M-line for the walls only at $N \neq 0$ kN.....	55
Figure 48: Results for even and uneven iterations of right wall for $N \neq 0$ kN.....	57
Figure 49: The assumed ‘average result’ for the right wall based on iteration #12 and #13.	57
Figure 50: Final result EI_{var} according to iteration procedure 1 in Plaxis 2D – Total Model.	58
Figure 51: The ‘average result’ based on EI_0 and EI_∞	59
Figure 52: Final result EI_{var} according to iteration procedure 2 in Plaxis 2D – Total Model.	60
Figure 53: Hinged case - The M-line for EI_0 , EI_∞ and EI_{var} for $N \neq 0$ kN	61
Figure 54: Model in PCSheetPileWall.....	63
Figure 55: Results case 2	64
Figure 56: Results case 3	65
Figure 57: Results case 4	65
Figure 58: M-line both walls from PCSheetPileWall (clamped connection, $N = 0$ kN)	67
Figure 59: M- κ diagram both walls for the Stiffened Region (I).....	67
Figure 60: M- κ diagram both walls for the Field (II)	68
Figure 61: (a) Deformed mesh and (b) M-line of left wall for EI_{var} in Plaxis 2D – Half Model.....	69
Figure 62: Clamped case - (a) Deformed mesh and (b) M-line for the walls only at $N = 0$ kN	70
Figure 63: Cracking pattern at an uneven and even iteration step	71
Figure 64: The assumed ‘average result’ for the right wall based on iteration #10 and #11.	72
Figure 65: Final result EI_{var} according to iteration procedure 1 in Plaxis 2D – Total Model.	73
Figure 66: The ‘average result’ based on EI_0 and EI_∞	73
Figure 67: Final result EI_{var} according to iteration procedure 2 in Plaxis 2D – Total Model.	74
Figure 68: Clamped case – The M-line for EI_0 , EI_∞ and EI_{var} for $N = 0$ kN.....	75

Figure 69: M-line both walls from PCSheetPileWall (clamped connection, $N \neq 0$ kN)	76
Figure 70: M-N- κ diagram both walls for the Stiffened Region (I).....	77
Figure 71: M-N- κ diagram both walls for the Field (II)	77
Figure 72: (a) Deformed mesh and (b) M-line of left wall for EI_{var} in Plaxis 2D – Half Model.....	79
Figure 73: Clamped case - (a) Deformed mesh and (b) M-line for the walls only at $N \neq 0$ kN.....	80
Figure 74: The assumed ‘average result’ for the right wall based on iteration #5 and #6.	81
Figure 75: Final result EI_{var} according to iteration procedure 1 in Plaxis 2D – Total Model.	82
Figure 76: The ‘average result’ based on EI_0 and EI_{∞}	82
Figure 77: Final result EI_{var} according to iteration procedure 2 in Plaxis 2D – Total Model.	83
Figure 78: M-line for EI_0 , EI_{∞} and EI_{var} for $N \neq 0$ kN.....	84
Figure 79: Clamped case – (a) Behaviour of the total packing structure and (b) the corresponding M-line configuration.....	85
Figure 80: Clamped case – The M-line and cracked zones of the total structure for EI_0 , EI_{∞} and EI_{var} at $N = 0$ kN ..	86
Figure 81: Clamped case – The M-line and cracked zones of the total structure for EI_0 , EI_{∞} and EI_{var} at $N \neq 0$ kN ..	87
Figure 82: Impact roof stiffness on bending moment distribution.....	88
Figure 83: Basic reinforcement ratio – Maximum occurring bending moment of the walls for the hinged and clamped case.....	90
Figure 84: Basic reinforcement ratio – Maximum settlement of the foundation for the hinged and clamped case	90
Figure 85: Basic reinforcement ratio – Maximum lateral wall displacement for the hinged and clamped case.....	91
Figure 86: Maximum occurring bending moment of the walls for the hinged case at different reinforcement ratios and soil types	95
Figure 87: Maximum settlement of the foundation for the hinged case at different reinforcement ratios and soil types	95
Figure 88: Maximum lateral wall displacement for the hinged case at different reinforcement ratios and soil types	96
Figure 89: The ‘Waalbrug-project’: Example of ‘dekkingslijn’ bending moments used for reinforcement design over the wall height of the starter panel [11]	97

List of Tables

Table 1: Specification of levels	25
Table 2: Horizontal (point) loads on diaphragm wall for LC1	26
Table 3: Uniform load – LC1	26
Table 4: Surcharge load – LC1	26
Table 5: Vertical load from spread foundation – LC1	26
Table 6: Horizontal (point) loads on diaphragm wall for LC2	26
Table 7: Uniform load LC2.....	27
Table 8: Surcharge loads LC2.....	27
Table 9: Vertical load spread foundation	27
Table 10: Properties panel types	29
Table 11: Properties diaphragm wall in PCSheetPileWall.....	31
Table 12: Material properties sand	31
Table 13: Material properties of the concrete diaphragm wall.....	33
Table 14: Material properties of the sand and interface.....	33
Table 15: Material properties spread foundation.....	34
Table 16: Diaphragm wall properties for EI_0 and EI_∞	39
Table 17: Cracked and uncracked zones of both walls for the considered loading combinations	40
Table 18: EI-distribution of both walls obtained from PCSheetPileWall	42
Table 19: Results for Plaxis 2D – Half Model, using 3 different approaches for the EI_{var} of the cracked zone	42
Table 20: Results iteration process right wall for $N = 0$ kN - hinged connection.....	45
Table 21: EI-distribution for both walls used as input in Plaxis 2D – Total Model for iteration procedure 1.....	47
Table 22: Comparison of the assumed ‘average result’ and the Plaxis-result for the right wall.....	48
Table 23: EI-distribution for both walls used as input in Plaxis 2D – Total Model for iteration procedure 2.....	49
Table 24: Hinged case - Final results for EI_0 , EI_∞ and EI_{var} for $N= 0$ kN.....	51
Table 25: Cracked and uncracked zones of both walls for the considered loading combinations	52
Table 26: EI-distribution of both walls obtained from PCSheetPileWall	54
Table 27: Results for Plaxis 2D – Half Model, using 3 different approaches for the EI_{var} of the cracked zone	54
Table 28: Results iteration process right wall for $N \neq 0$ kN – hinged connection	56
Table 29: EI-distribution for both walls used as input in Plaxis 2D – Total Model for iteration procedure 1.....	58
Table 30: Comparison of the assumed ‘average result’ and the Plaxis-result for the right wall.....	59
Table 31: EI-distribution for both walls used as input in Plaxis 2D – Total Model for iteration procedure 2.....	60
Table 32: Hinged case - Final results for EI_0 , EI_∞ and EI_{var} for $N \neq 0$ kN.....	61
Table 33: The clamped moment at different lengths for the stiffened region.....	64
Table 34: EI-distribution of both walls obtained from PCSheetPileWall	68

Table 35: Results in Plaxis 2D – Half Model for EI_0 , EI_∞ and EI_{var}	69
Table 36: Results iteration process right wall for $N = 0$ kN – clamped connection.....	71
Table 37: EI-distribution for both walls used as input in Plaxis 2D – Total Model for iteration procedure 1.....	72
Table 38: EI-distribution for both walls used as input in Plaxis 2D – Total Model for iteration procedure 2.....	74
Table 39: Clamped case - Final results for EI_0 , EI_∞ and EI_{var} for $N = 0$ kN	75
Table 40: EI-distribution of both walls obtained from PCSheetPileWall	78
Table 41: Results in Plaxis 2D – Half Model for EI_0 , EI_∞ and EI_{var}	78
Table 42: Results iteration process right wall for $N \neq 0$ kN – clamped connection.....	80
Table 43: EI-distribution for both walls used as input in Plaxis 2D – Total Model for iteration procedure 1.....	81
Table 44: EI-distribution for both walls used as input in Plaxis 2D – Total Model for iteration procedure 2.....	83
Table 45: Clamped case - Final results for EI_0 , EI_∞ and EI_{var} for $N \neq 0$ kN	84
Table 46: Clamped case - Final results for the total structure for EI_0 , EI_∞ and EI_{var} at $N = 0$ kN	86
Table 47: Clamped case - Final results for the total structure for EI_0 , EI_∞ and EI_{var} at $N \neq 0$ kN	87
Table 48: Basic reinforcement ratio – Overview of results for the hinged and clamped case.....	89
Table 49: Material properties ‘Soil Type 2’ in Plaxis 2D.....	94
Table 50: Overview of results for the hinged case at different reinforcement ratios and soil types	94
Table 51: Risk with regard to required reinforcement ratio for EI_{var}	98
Table 52: Cracked zones for EI_{var} as a function of the connection type, wall properties and soil properties	99

Abbreviations

EC2	Eurocode 2
BEF	Beam on Elastic Foundation Method
FEM	Finite Element Method
HS-model	Hardening Soil Model
LE-model	Linear Elastic Model
MC-model	Mohr-Coulomb Model
N.A.P.	The Normal Amsterdam Level (in Dutch: Normaal Amsterdams Peil)
SLS	Serviceability Limit State
ULS	Ultimate Limit State

List of Symbols

Upper case letters

A_c	Cross sectional area of concrete
A_{sv}	Area of the vertical reinforcement
A_s	Cross sectional area of tension reinforcement
A'_s	Cross sectional area of compression reinforcement
$E_{c,eff}$	Effective modulus of elasticity of concrete (for long-term loading)
E_{cd}	Design value of modulus of elasticity of concrete
E_{cm}	Secant modulus of elasticity of concrete (for short-term loading)
E_f	Fictitious modulus of elasticity
E_s	Design value of modulus of elasticity of reinforcing steel
E_{50}^{ref}	Secant stiffness in standard drained triaxial test
E_{oed}^{ref}	Tangent stiffness for primary oedometer loading
E_{ur}^{ref}	Unloading and reloading stiffness
EA	Normal stiffness
EI	Bending stiffness
EI_0	Uncracked bending stiffness
EI_∞	Fully or totally cracked bending stiffness
EI_{var}	Realistic (variable) bending stiffness
I_g	Moment of inertia of the gross concrete section, neglecting reinforcement
I_{cr}	Moment of inertia of the fully cracked section
$I_{c,eff}$	Effective moment of inertia
M	Bending moment
M_a	Maximum bending moment in member
M_e	Yield moment
M_{Ed}	Occurring bending moment
M_{pl}	Crushing moment
M_r	Cracking moment
M_u	Ultimate moment
M_x	Arbitrary bending moment
N'_c	Axial compressive force
R_{inter}	Strength reduction factor
U_x	Lateral wall displacement
W	Section modulus

Lower case letters

b	Width
c	Cohesion
$c_{concr.}$	Concrete cover

d	Diaphragm wall thickness
d_{eq}	Equivalent plate thickness
f_c	Compressive strength of concrete
f_{cd}	Design value of concrete compressive strength
f_{ck}	Characteristic compressive cylinder strength of concrete at 28 days
f_{ctm}	Mean value of axial tensile strength of concrete
f_{yd}	Design yield strength of reinforcement
f_{yk}	Characteristic yield strength of reinforcement
$k_{x,y}$	Soil permeability in x,y-direction
k_s	Modulus of subgrade reaction or soil spring stiffness
m	Power for stress-level dependency of stiffness
n	Modular ratio of steel and concrete (E_s/E_c)
q	Partially distributed surface loading
w	Displacement
w_{line}	Line load due to self-weight diaphragm wall
x	Height of concrete compression zone
x_e	Height of concrete compression zone when reinforcement starts yielding
x_{pl}	Height of concrete compression zone when concrete starts to crush
x_u	Maximum height of the concrete compression zone
x_{uncr}	Height of concrete compression zone in the uncracked phase

Greek lower case letters

$\gamma_{concrete}$	Specific weight concrete
γ_{dry}	Soil unit weight above phreatic level
γ_{sat}	Soil unit weight below phreatic level
δ	Wall friction angle
δ_v	Settlement
ε'_c	Compressive strain in concrete
ε_c	Tensile strain in concrete
ε'_s	Compressive strain in steel
ε_s	Tensile strain in steel
$\varepsilon_{c3} = \varepsilon'_{c,pl}$	Crushing strain of concrete (compressive strain in concrete at peak stress f_c)
$\varepsilon_{cu3} = \varepsilon'_{cu}$	Ultimate compressive strain in the concrete
$\varepsilon_{s,pl}$	Yielding strain of reinforcement
ε_{su}	Ultimate strain of reinforcement
κ	Curvature
κ_e	Curvature corresponding to the yield moment
κ_{pl}	Curvature corresponding to the crushing moment
κ_r	Curvature corresponding to the cracking moment
κ_u	Curvature corresponding to the ultimate moment
ρ	Radius of curvature
$\rho_{l,min}$	Minimum reinforcement ratio
$\rho_{l,max}$	Maximum reinforcement ratio
σ'_c	Compressive stress in concrete
σ_c	Tensile stress in concrete
σ'_s	Compressive stress in steel
σ_s	Tensile stress in steel
ν	Poisson's ratio
$\varphi(\infty, t_0)$	Final value of creep coefficient
ψ	Dilatancy angle
ϕ	Internal friction angle

1. INTRODUCTION

1.1. Background

The Waalbrug in Nijmegen concerns a bridge from the 1880s. Due to rising water levels and a higher risk of flooding, it was decided to create an ancillary channel in the flood plains at the approach bridges in the 'Uiterwaarden'.

The realization of the ancillary channel below the existing approach bridge fell within the scope of the project "Room for the Nijmegen - Waal". Due to the construction of the ancillary channel the strength of the foundation of the existing pillars of the approach bridge became an issue. Since the bottom of the ancillary channel was scheduled to be approximately 3 meters below the existing foundation level, the pillars of the railway bridge had to be made suitable for the construction of the ancillary channel. The existing structure is a spread foundation with a stone bearing support structure on it (pillar). In order to be able to excavate a "packing structure" was devised consisting of a diaphragm wall structure around the existing foundation, where a roof structure connects the 1.5 m thick diaphragm walls with each other. This construction would prevent large settlements of the existing foundation and disruption of the rail traffic (rail Arnhem - Nijmegen). The roof structure is characterized by a high tensile force (shear from the diaphragm wall construction on the roof structure (axial force)). The trenches for the diaphragm walls have a depth of 23 m. This project has already been completed. In Figure 1 and Figure 2 the location of the construction and an impression of the bridge indicating the 3 bridge pillars for which the packing structure has been applied are given, respectively. Figure 3 and Figure 4 give a more detailed view of the packing structure.

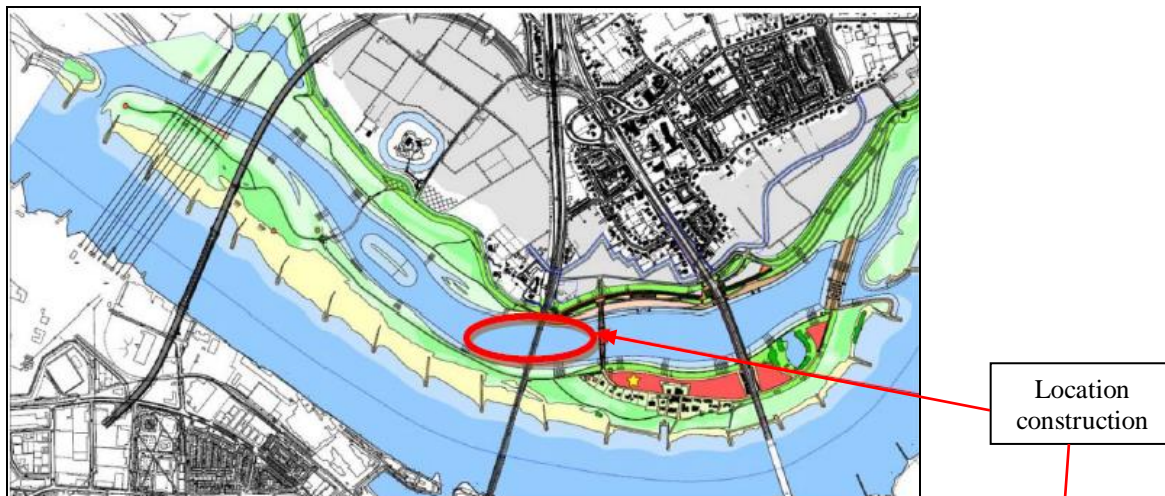


Figure 1: Location of the construction [1]¹

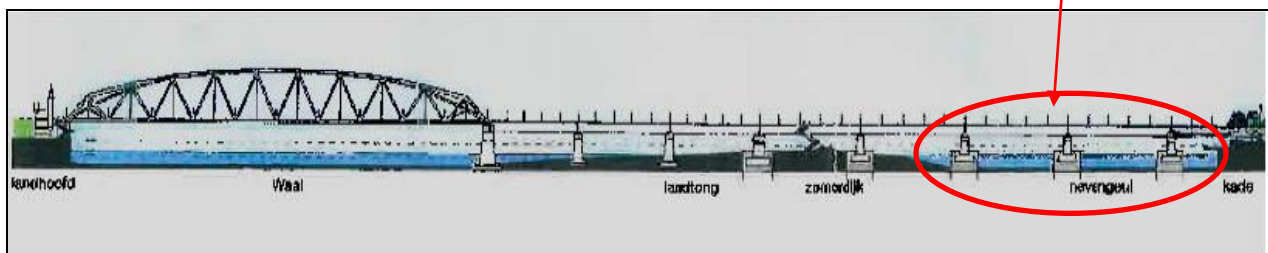


Figure 2: Railway bridge over the Waal at Nijmegen [1]

¹ Source from Intranet (not publicly available) of Engineering Office of Rotterdam (IGR)

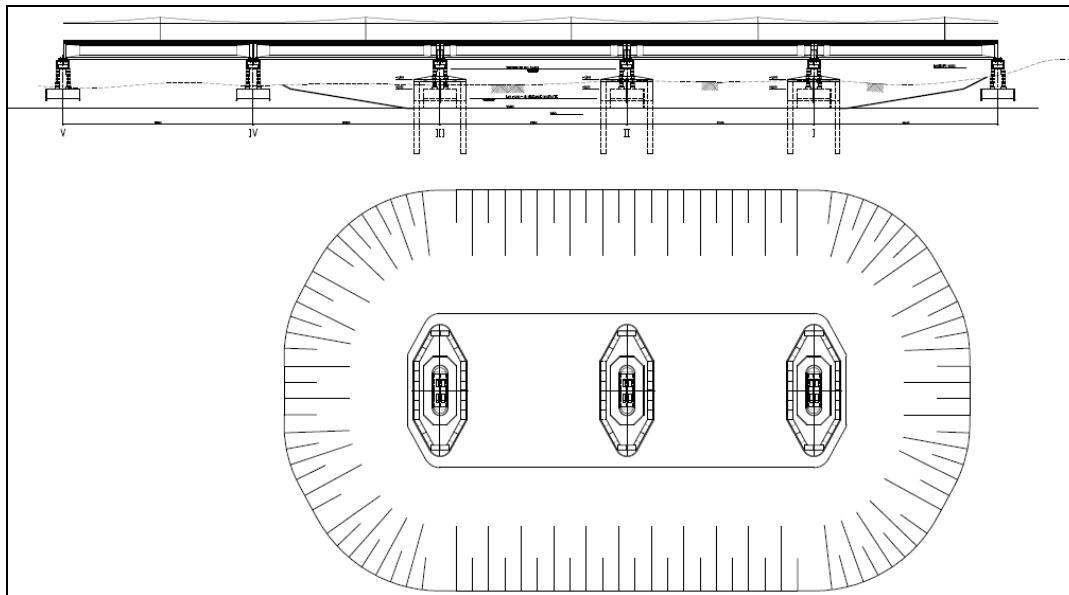


Figure 3: Packing structures around the existing foundation of the 3 bridge pillars [1]

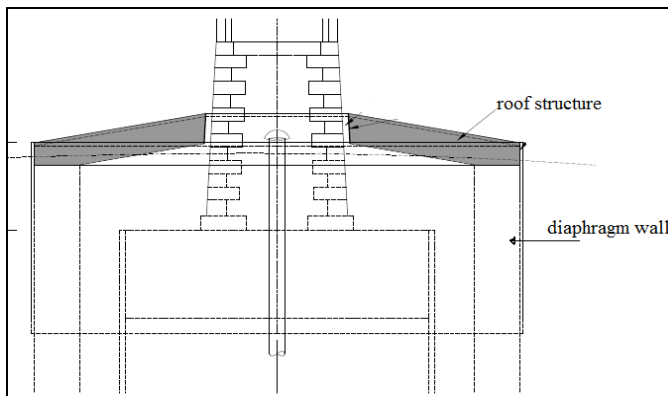


Figure 4: Detail packing structure, consisting of diaphragm wall structure and a roof structure [1]

1.2. Problem description

The description of the problem has been split up into three parts, namely from the point of view of:

- The diaphragm wall stiffness: Calculating with a variable stiffness;
- The boundary condition diaphragm wall – roof structure: The impact thereof in combination with a variable stiffness for the wall;
- The total packing structure: The structural safety and the most appropriate model to choose.

1.2.1. Diaphragm wall stiffness

The diaphragm walls are quite deep in the ground and can deform. Due to the deformation of the diaphragm wall the ground within the packing structure will relax, resulting in settlements which will cause the pillar to go down further. Coupled to this phenomenon is the risk of train derailment. It is therefore important to design a diaphragm wall where the relaxation of the ground is minimal, expressed in a limited lateral wall displacement and a limited foundation settlement.

Since the diaphragm wall is surrounded by ground, not only can it be looked at as a concrete structure, but also as a geotechnical structure. This implies that the deformations and settlements largely depend on the soil-structure interaction or, in others words, on both the diaphragm wall stiffness (EI) and the soil

stiffness. In the geotechnical design a certain bending stiffness EI had to be implemented as point of departure for the diaphragm wall. In the common design practice, the following is applied:

- An uncracked stiffness (EI_0) for the SLS;
- A fully cracked stiffness (EI_∞) for the ULS, where the reduced stiffness $EI_\infty \approx 1/3 * EI_0$.

The largest settlements are actually expected for the ULS with a totally cracked wall, as a result of which the settlements form a ULS-boundary! But, in the common design practice the settlement is an SLS-boundary, for example the deflection of a floor.

In reality, however, it is unlikely for a structure to remain uncracked or to become fully cracked. The diaphragm wall will consist of both cracked and uncracked parts, implying a variation in the bending stiffness (EI_{var}) over the height of the diaphragm wall. In the application of diaphragm walls it needs to be noted that, due to crack formation, there is a relationship between the occurring bending moment in the diaphragm wall and the bending stiffness EI . In case of exceeding the cracking moment (M_r), the stiffness of the wall will reduce. For the reduced bending stiffness the M - (N) - κ diagram of the concrete cross-section of the diaphragm wall should be considered. The bending stiffness EI of the diaphragm wall is not only influenced by crack formation, but also by the soil behaviour. When due to crack formation the bending stiffness of the wall is reduced, the wall deformation will increase. As the wall deforms, the soil in its turn also exerts a load on the diaphragm wall which also influences the bending stiffness. Because of the interaction between the diaphragm wall and the soil behind it, the stiffnesses of both depend on each other.

Insufficient elaboration in the design standards with regard to structures with a variable stiffness – the design standards mainly emphasize on calculations based on uncracked or fully cracked cross-sections – and a lack of studies on this matter, are a reason to consider the impact of the variable stiffness on the safety of the structure. Modelling with an uncracked section is not justified; for the “Waalbrug-project” the diaphragm wall appeared to crack over a section of 4-5m at the top part of the wall in an extreme situation (e.g. unexpected higher loads), while the rest remained uncracked. The disadvantage of modelling with a fully cracked wall is that it is technically irrelevant for it leads to a relatively large thickness for the diaphragm wall. A variation in the EI over the height may be an interesting point, since for instance too stiff designed diaphragm walls (with a constant EI) attract much more load leading to excess reinforcement in the structure. Actually, it also remains a question whether the correct force distribution and deformations are calculated when a constant EI is considered over the entire height of the diaphragm wall. Therefore, it is not known whether the applied design model using a constant EI is conservative.

For a safe construction one needs to calculate, in accordance with the standards, with a constant EI . As mentioned before, two extremes can be distinguished here: EI_0 and EI_∞ . For the “Waalbrug-project” the reinforcement and wall thickness were designed such that the diaphragm walls would remain uncracked. Thus, calculations with EI_0 resulted in sufficient strength and the settlement requirements were also met. For EI_∞ the settlement requirements were not met. Despite the fact that the walls were made so rigid and were not expected to crack, a sensitivity analysis was done assuming that the wall would crack locally in an extreme situation. In that case it was found that:

- A local cracked zone in the wall (local reduction of the wall stiffness creating a ‘hinge’ in the wall) resulted in a redistribution of forces towards the stiff soil. As a result the deformations and settlements were still quite acceptable;
- Due to the geometry of the packing structure (3D-arrangement wall panels) the actual deformations were less than in case one only considers the 2D-calculation of a representative wall panel.

For the “Waalbrug-project” a variable EI was implemented over the entire wall height just to check the settlement requirements in an extreme case. However, the problem one encounters is that:

Problem 1:

Calculations based on a variable EI are not defined in the standards and thus it is not clear how to deal with the safety in that case.

1.2.2. Boundary condition diaphragm wall - roof structure

The roof structure is a shell structure which is applied to keep the diaphragm walls all together after excavation of the surrounding ground. For the “Waalbrug-project” the connection between the 1.5 m thick diaphragm wall and the 0.9 m thick roof structure is schematized as a concrete hinge. Due to the hinged connection the shear force in the diaphragm wall results in a relatively large tensile force on the roof structure. The tensile force acts on the entire circumference of the structure, causing the roof structure to act as a ‘tensile body’ in both directions (X and Y in Figure 5). Due to the presence of a recess in the roof structure, the tensile force is led around the hole. This causes a tensile force concentration along the edge (‘edge stresses’) of the bridge pillar. The masonry structure of the pillar protrudes through the recess. A flexible covering separates the pillar from the roof structure. As a result of this the braking force (from the rail traffic) on the pillar is transferred via rotation to the soil under the foundation level (within the packing structure) instead of directly into the roof structure. In this way, stress concentrations in the existing masonry structure are avoided.

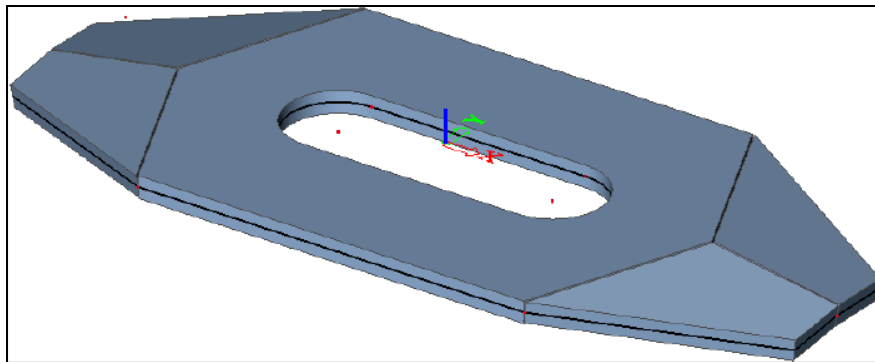


Figure 5: 3D-model of the roof structure [2]²

It was found that a clamped connection between the top of the diaphragm wall and the roof structure would result in very high bending moments, which would make it practically impossible to reinforce the roof structure. Calculations showed that a clamped connection was not necessary for the proper functioning of the packing structure. Therefore, a moment-free connection (hinge) was finally chosen. Because of the hinged connection the span-moment in the diaphragm wall would obviously be higher than in the case of a clamped connection. As a result of the schematized concrete hinge at the top and full fixity of the diaphragm wall in the soil, the greatest part of the load distribution takes place over the height of the diaphragm wall and not across the width.

Obviously, the type of wall-roof connection is decisive for the force distribution and the deformation of the structure. Just like for a constant EI, this phenomenon also holds for a variable EI. The influence of the EI_{var} on the safety of the construction elements changes as a function of the boundary condition: hinged or clamped. This was not investigated further. After looking into this matter, an evaluation should be made whether it was necessary to zoom in on the boundary condition.

Problem 2:

More detailed investigation is required on the influence of EI_{var} as function of the boundary condition (hinged, clamped) on the safety of construction elements.

² Source from Intranet (not publicly available) of Engineering Office of Rotterdam (IGR)

1.2.3. Packing structure in total – calculation models

When the possibilities regarding the bending stiffness of the diaphragm wall and the connection between the diaphragm wall – roof structure are considered, different calculation models can be set up. There is no clear information on how the packing structure should be calculated correctly and what impact the different calculation models have on the structural safety. Therefore it is necessary to compare the safety related to each of the calculation models with each other. The safety will be considered for the “walls only” and for the “walls + roof” for both a hinged and a clamped connection. For each case, one distinguishes 6 possibilities (1a-b, 2a-b, 3a-b). The different research models are depicted in Figure 6. Adherent to these calculation models the following 3 limits will be distinguished with regard to the safety, namely the:

1. Bending moment (M_{Ed});
2. Settlement (δ_v);
3. Lateral wall displacement (U_x).

It is possible that these limits will contradict each other in terms of safety. For instance, one calculation model may predict a better safety with regard to the occurring bending moment, while another calculation model works better for the settlements. It is therefore important to investigate the different parameters which have an impact on the structural safety.

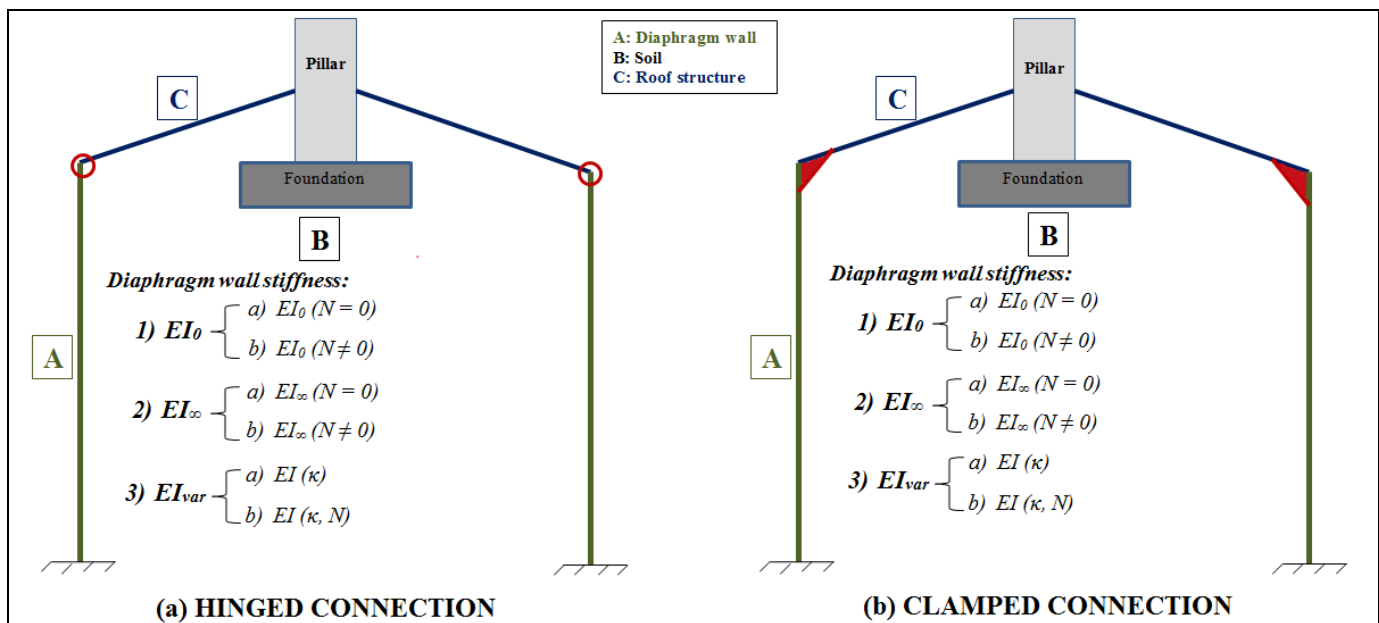


Figure 6: Calculation models: (a) Hinged connection; (b) Clamped connection

1.3. Work approach

In this section the problem statement, the overall aim and scope of this research project are defined. From the overall aim, the objectives and in more detail the research questions are formulated.

1.3.1. Problem statement

Based on the described problems in section 1.2, the problem statement reads as follows:

It is not known to which extent one is compromising the safety of the structure by calculating with EI_{var} . The impact of the boundary condition with regard to the safety of construction-elements and the packing structure in total is thereby also not known.

1.3.2. Aim and Scope of the research project

The overall aim of this research is to:

Determine the impact of calculating with EI_{var} on the safety of the structure.

Since this research concerns a sensitivity analysis, in which the focus is mainly on the variable stiffness of the diaphragm wall, it is important not to make too many variations. In this study the following limitations are set with regard to:

- **2D/3D – calculations:** Only 2D-calculations will be performed;
- **Diaphragm wall panels:** In practice, several types of panels have been applied for the diaphragm wall, but only the representative (most heavily loaded) panel is considered for calculation;
- **Reinforcement ratio:** In practice, the amount of reinforcement applied by the contractor is variable over the height. As a result, several sections with a different reinforcement ratio are discerned over the height. However, for this study a constant reinforcement ratio will be used for the ‘hinged case’ and two reinforcement ratios (for the stiffened region and for the field) will be applied for the ‘clamped case’;
- **Soil layers:** From the geotechnical profile the soil is found to consist of 13 different soil layers. However, for this study the soil type which is mainly present will be used for the calculations, namely sand;
- **Stresses roof structure:** The variation in stresses of the roof structure (especially at the recess) as a function of the variable stiffness, boundary condition, temperature loading and roof inclination will not be dealt with in this research. The roof structure will be modelled as a simple beam for 2D-calculations.

1.3.3. Objectives and research questions

In order to reach the above-mentioned aim, it is decomposed into objectives and related research questions. These are the following:

I. Determine the structural safety for different calculation models

- 1) What is the safety level for each of the calculation models with regard to:
 - a) The diaphragm walls only;
 - b) The total packing structure;

Note: In order to answer this question the bending moment, settlement and lateral wall displacement must be calculated for each model and plotted in diagrams as depicted in Figure 7. Based on question I.1, the remaining questions (I.2 – I.7) can be answered.

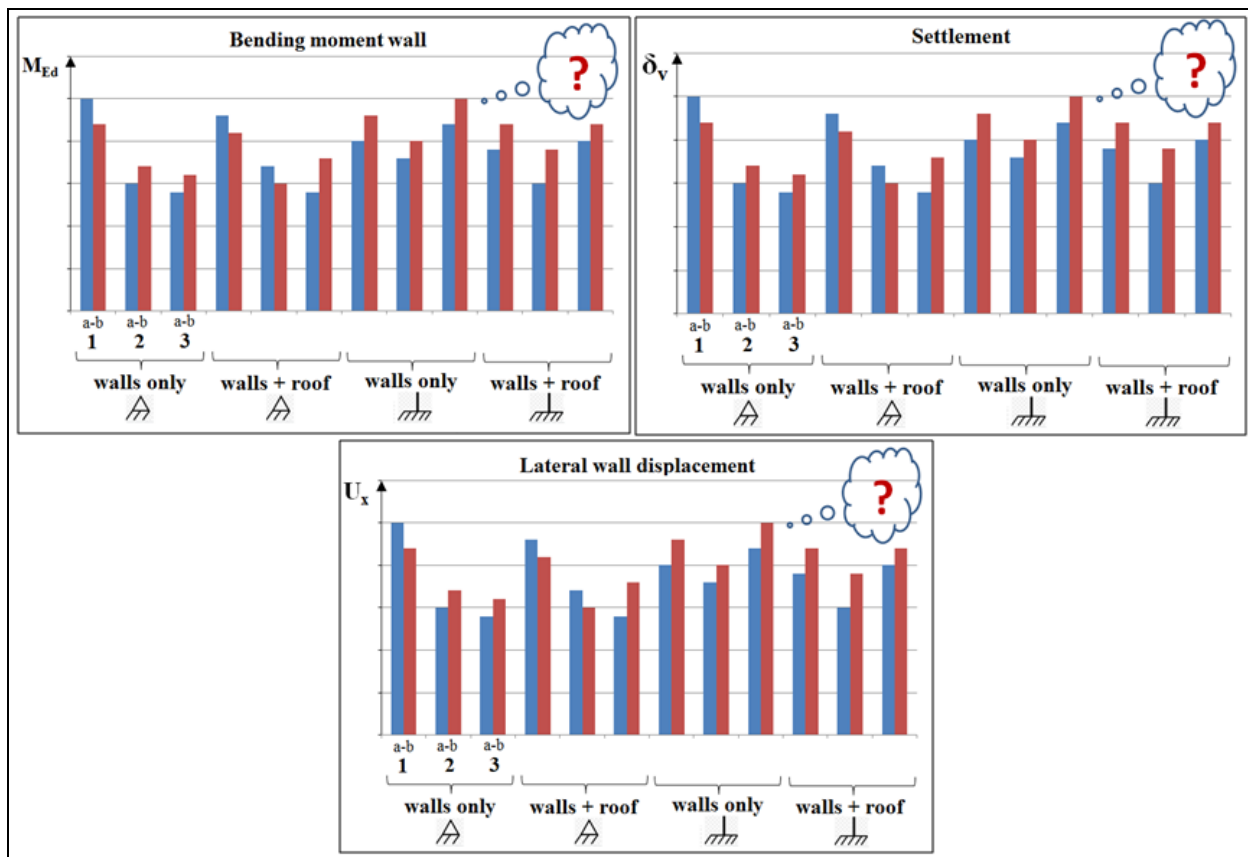


Figure 7: Measuring the structural safety

- 2) Should EI_{var} indeed be accounted for?
 - a) Should EI_{var} be accounted for as a function of the deformation (κ) or as a function of both (κ) and the axial force (N) ?
 - b) What is the contribution of the axial force (N) to EI_{var} ?
- 3) Are the applied models, based on EI_0 and EI_{∞} , conservative?
- 4) Does the safety level change for stiffer diaphragm walls (e.g. thicker wall, higher reinforcement ratio), and if so how much does it change?
- 5) Based on the structural safety, which calculation model is the most adequate for this project and why?
- 6) Which parameters have an impact on the structural safety?
- 7) If a calculation model forms an unsafe approach, how can this be dealt with?

II. Knowledge building and guidelines for similar conditions as the ‘Waalbrug-project’

A. **Interaction concrete structure (diaphragm wall) – soil:**

- 1) How is the EI -variation over the wall height and/ or how does the wall crack (location cracked zones):
 - a) As a function of the loading, soil condition and boundary condition?
 - b) With/ without the roof structure at the given soil and loading condition?
- 2) How does EI_{var} influence the soil reaction, e.g.: relaxation, settlements?
- 3) Does the interaction soil-wall change for another loading or soil condition, and if so, how does it change?

B. **Boundary condition w.r.t. connection diaphragm wall – roof structure:**

- 1) What is the influence of the boundary condition on the diaphragm wall?
- 2) Was it necessary to consider the impact of the boundary condition?

C. Response of total packing structure:

- 1) What is the influence of EI_{var} and the boundary condition on the safety of the total structure?
- 2) Under which circumstances is it (not) necessary to take EI_{var} into account?
- 3) Which calculation model gives the most optimized design w.r.t. safety?

1.4. Outline

This report consists of 6 chapters and is organized as follows (see also Figure 8) :

Chapter 1 provides background information which led to the formulation of this research project and outlines the problem description, objectives, research questions and scope related to this project.

Chapter 2 deals with the literature study, providing information relevant for this research. Theoretical background information regarding diaphragm walls, soil-structure interaction and different soil models is given. The derivation of the reduced bending stiffness of a diaphragm wall (due to crack formation) using the M-(N)- κ diagram is also dealt with. Furthermore, some background information is provided for the behaviour of a not fully cracked concrete member according to the design standards (Eurocode 2).

The applied research strategy to obtain the aimed results is enlightened in Chapter 3. The aimed results concern the load distribution and deformations related to the variable bending stiffness over the diaphragm wall height. The calculation strategies and different calculation models used in the software programs PCSheetPileWall and Plaxis 2D are dealt with. Four main calculation models are set up: “Walls only; hinged”, “Walls + Roof; hinged”, “Walls only; clamped” and “Walls + Roof; clamped”.

Chapter 4 discusses the differentiation in the different calculation models and the obtained results corresponding to each of the valid models. For the validity of the results two different iteration procedures are applied and validated for each calculation model.

All the results obtained from the different calculation models are presented and discussed in Chapter 5. A safety analysis is performed for the different calculation models based on the realistic bending stiffness of the diaphragm wall. A comparison is made with the uncracked and fully cracked stiffness according to the standards. Furthermore, a risk analysis of the applied reinforcement ratio and an evaluation of the cracked zones are presented in case the realistic bending stiffness of the wall is considered. Based on the findings practical relevant suggestions are made for future projects concerning diaphragm walls with a realistic EI-distribution.

Conclusions and recommendations are finally presented in Chapter 6.

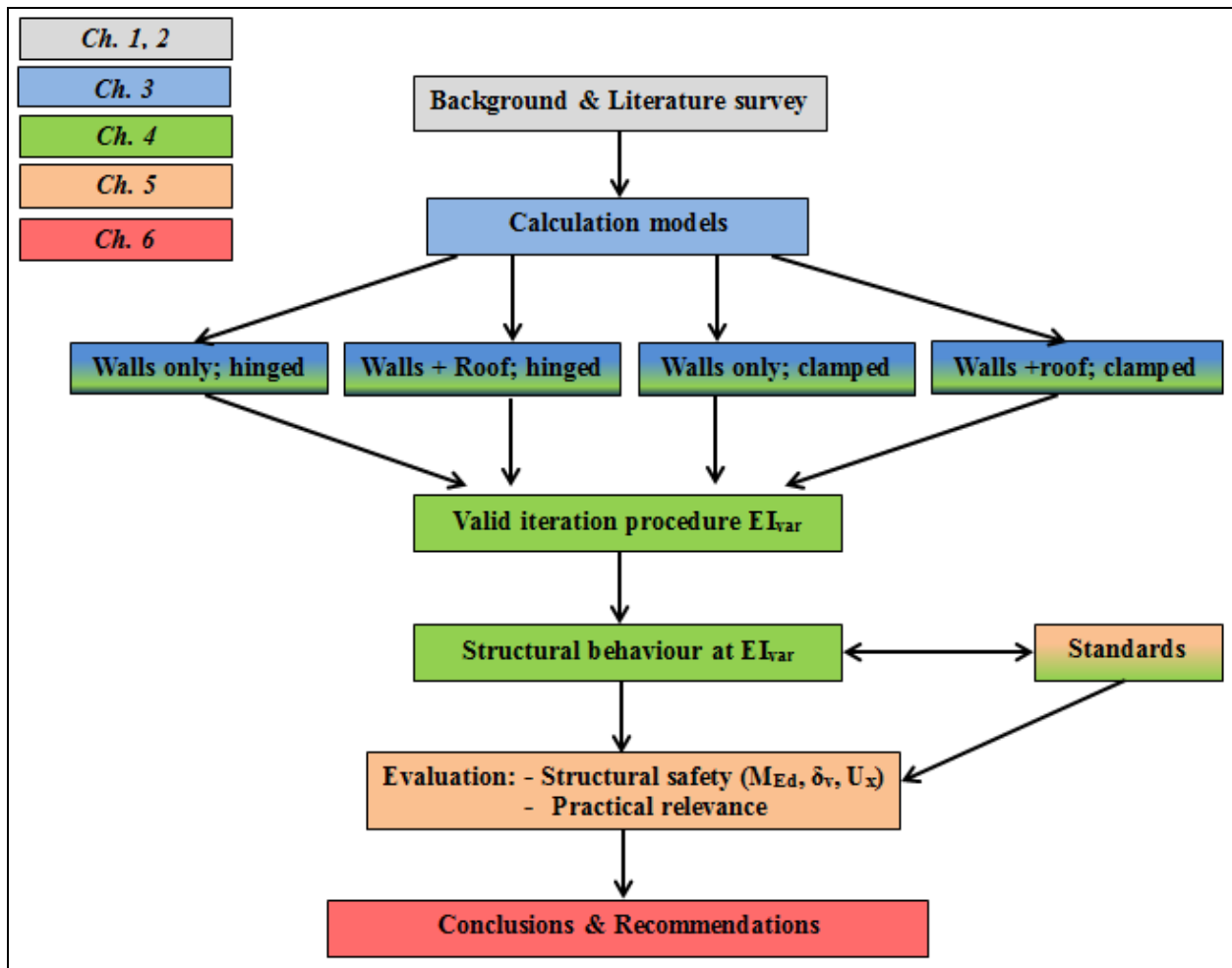


Figure 8: Thesis outline

2. LITERATURE SURVEY

2.1. Introduction

For the extensive literature study performed for this research reference is made to Appendix A. This chapter gives a summary thereof.

2.2. Diaphragm walls

Diaphragm walls are reinforced in-situ concrete elements formed in the ground, which by placing multiple elements in line with each other form a continuous unanchored wall. They have an earth-retaining, water-retaining and/ or load-bearing function. Instead of reinforced concrete, the diaphragm walls can also be executed, totally or partially, in prestressed concrete. The application of prestressing would particularly be useful in the SLS, since a more rigid wall can be accounted for (no cracking). In this research reinforced concrete diaphragm walls are dealt with.

The strength and stability of a diaphragm wall structure are determined by the material (reinforced concrete) and the surrounding soil. The wall acts as a cantilever beam which is clamped into the soil or as a beam supported at both ends (at the bottom the soil and at the top an anchor). When compared to other wall types, e.g. a single steel sheet pile wall, diaphragm walls are considered to be very stiff. The high bending stiffness of the wall results in low soil deformations just behind the wall.

2.2.1. Deformations and settlements

For the deformation state of the diaphragm wall, distinction is made between:

- The settlements;
- The horizontal deformations of the wall (or: ‘lateral wall displacement’).

Deformations and settlements can lead to collapse of the structure. Large deformations of the diaphragm wall result in large settlements of the surface level and also of the foundations of adjacent buildings. The settlement of the soil in response to the deformation of the diaphragm wall is also highly dependent on the soil properties and geological profile.

Several factors affect the deformation of the diaphragm wall. The most important factors are the:

- *Soil properties*: The occurring deformations and settlements are highly dependent on the available soil properties. Stiff soil is relatively less sensitive to deformations and settlements compared to soft soil.
- *Water pressure*: The difference in water pressure against the diaphragm wall has large effects on the deformation of the wall. Higher pressure differences will lead to greater deformations.
- *Surface load*: Just like deformations of the wall affect the settlements of the surface level, so does the loading on the surface level affect the deformations of the wall. The higher the surface load, the greater the deformations.

The above-mentioned factors are imposed factors, which can be influenced very limitedly. The following factors can be influenced during the design and realization of the project:

- *Wall stiffness*: The bending stiffness of the diaphragm wall has a large impact on the deformations of the wall. Here it holds that: the stiffer the wall, the smaller the deformation.
- *Construction method and construction phases*: The construction method and construction phases have an effect on the occurring deformations of the wall. Careful construction procedures may result in limited deformations.

- *Excavation depth:* The excavation depth is highly dependent on the design, the construction method and the construction phases. The greater the excavation depth, the greater the deformations will be due to the greater soil and water pressures.

The occurring settlements can be reduced by limiting the deformation of the structure. In order to reduce the deformations of the diaphragm wall, the following measures can be taken:

- *Apply temporary struts;*
- *Increase the bending stiffness of the diaphragm wall by means of:*
 - Increasing the wall thickness;
 - Applying more reinforcement;
 - Applying prestressing;
 - Applying steel profiles (e.g. HEM-profiles) in the diaphragm wall.

It is common practice to apply temporary struts and more reinforcement, instead of prestressing in the diaphragm walls.

In the soil, next to the diaphragm wall, deformations can be caused by:

- Relaxation of the soil;
- Deflection of the wall as a result of the excavation;
- Decrease of the water table (groundwater level) which leads to settlement.

In order to determine the lateral wall displacement, one needs to take into account:

- The deformation of the wall itself;
- The deformation of the soil;
- The deformation of anchors or struts, if applicable.

In the service state, the deformations can increase due to:

- Time effects in the soil (creep and consolidation);
- Changes in the bending stiffness of the concrete wall due to creep and crack formation.

2.2.2. Soil-structure interaction

Soil is a complicated material that behaves non-linearly and often shows anisotropic and time-dependent behaviour when subjected to stresses. The non-linear behaviour implies that the soil deformations do not increase linearly with the increasing soil stresses. In compression soil becomes stiffer. Sand, which at the surface shows no cohesion, exhibits an increasing stiffness and strength when subjected to all-sided compression. The explanation can be found in the fact that the space between the particles decreases as the soil is compressed. This leads to an increase of the forces between the particles, an increase of the number of contacts between the particles and an increase of the contact surface between the particles, resulting in a higher soil stiffness. Since in general the stresses increase with the depth, it can be expected that the soil stiffness increases with the depth. A pile foundation embedded in deep sand for instance, extracts a large part of its bearing capacity from the high stiffness of the soil (deep sand) lying under high pressure. The upper lying layers cause a high pressure in the deep sand, which now acts as a very stiff layer, making it possible to allow very large forces on the pile. It can be concluded that the soil stiffness depends significantly on the stress-level; the soil stiffness increases with compression and generally increases with the depth (higher stresses).

Diaphragm walls are in direct contact with the soil. When external forces act on the structure, neither the structural displacements nor the soil displacements, are independent of each other. The soil-structure interaction is a process in which the response of the soil influences the motion of the structure and the motion of the structure influences the response of the soil.

For the modelling of soil behaviour, several models are available which are based on the material behaviour in terms of stiffness and strength. Stiffnesses of soil and structural elements obviously play a role in the distribution of forces. On one hand, an accurate determination of the soil stiffnesses is important to obtain a proper load distribution in the structure; the stiffness behaviour of the soil mainly depends on the stress state present therein. On the other hand, the bending stiffness of the diaphragm wall plays an important role in the equilibrium of forces between the soil and the diaphragm wall, because the deformation of the diaphragm wall depends on the horizontal soil pressures.

2.3. Soil models

A description of the different calculation methods for soil-structure interaction and the different applicable material models for the soil are enlightened in this section.

2.3.1. Calculation methods

In general three calculation methods, incorporating the soil-structure interaction, are available for retaining walls. The calculation-based approaches can be used to predict stresses, loads, and system movements. These calculation methods are:

- Blum's Equivalent Beam Method;
- Beam on Elastic Foundation Method (BEF);
- Finite Element Method (FEM).

Since the Blum method cannot be used for walls with a very high bending stiffness, such as diaphragm walls, this will not be dealt with further. The other two methods will be addressed briefly. For this research the following calculation programs were used:

- PCSheetPileWall, which is based on the BEF-model;
- Plaxis 2D, which is based on the FEM-model.

❖ Beam on Elastic Foundation Method (BEF):

The soil-structure interaction is taken into account by modelling the wall as an elastic beam resting on uncoupled springs. The soil medium is represented as a system of identical but mutually independent, linearly elastic springs (Figure 9a). Hence, this model does not include the effects of arching within the soil mass. The spring constant is the ratio of stress (p) to displacement (w), which can be expressed as follows:

$$k_s = \frac{p}{w} \quad (\text{Eq. 1})$$

where the constant k_s is called the modulus of subgrade reaction or soil spring constant.

In general, the soil behaviour is linear and the model lacks continuity among the springs. According to this idealization, deformation of the structure due to the applied load is confined to loaded regions only. If the structure is subjected to a partially distributed surface loading (q), the springs will not be affected beyond the loaded region. For such a situation, an actual foundation is observed to have the surface deformation as shown in Figure 9b. Hence, by comparing the behaviour of a theoretical model and an actual structure (Figure 9c), it can be seen that this model essentially suffers from a complete lack of continuity in the supporting medium. The fundamental problem with the use of this model is to determine the stiffness of the elastic springs used to replace the soil. The predicted wall displacements are very sensitive to the values of subgrade modulus used in the analysis. The BEF-method does not directly estimate vertical ground movements behind the wall. Ground movements behind the wall are evaluated using the calculated wall displacement from the model. An empirical relationship between wall movement and ground movements must then be used [3, 4, 5].

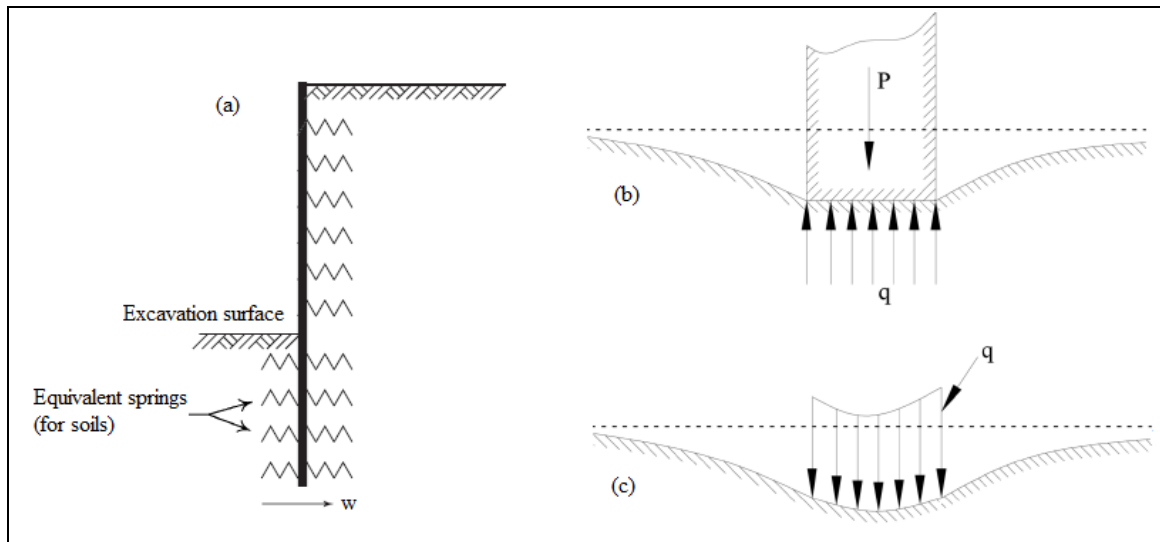


Figure 9: Interaction model: (a) Distribution of soil reactions on the wall; (b) Behaviour according to theoretical model; (c) Behaviour of real structure.

Based on the displacement method, the following differential equation needs to be solved:

$$EI \frac{d^4 w}{dx^4} + kw = f \quad (\text{Eq. 2})$$

This formula consists of three terms, where:

Term 1: Represents the bending stiffness of the wall

Term 2: Represents the spring supports for soil and anchors.

Term 3: Represents the external load, other than from the subsoil.

Influence of EI and k_s on the wall behaviour

For the BEF-analysis it is found that the calculated load distribution over the wall is usually closer to reality than the calculated displacements. The occurring load distribution and the displacements are not only determined by the soil spring stiffness, but are rather a result of the mutual relationship between the wall stiffness (EI), the soil spring stiffness (k_s) and the spring stiffness of anchors.

Assuming a homogeneous soil profile at an unanchored wall, the magnitude of k_s has a negligible influence on the maximum moment and a great influence on the deformation. The effect of EI on both the moment and the deformation remains small in absolute terms, which is made clear in Figure 10. For an anchored wall this interaction between EI, k_s , the bending moments and the deformations is not so obvious. In Figure 11 the influence of variations of the above-mentioned factors is outlined schematically. For anchored walls with a relatively low bending stiffness the deformation pattern of the wall is strongly influenced by the anchor stiffness.

❖ Finite Element Method (FEM)

The finite element method is based on a model in which the behaviour of soil and structure is integrated. With this method fundamental calculations of stresses and deformations of soil and structural members can be made. In contrast to the BEF-analysis, the FEM-analysis can provide direct information on the ground movements outside of and inside the excavation. Another difference between the FEM- and BEF-methods is that variations in the soil stiffness (modulus) can have a greater effect on predicted loadings and movements due to the inclusion of soil arching in the FEM-model [3, 6]. An example is shown in Figure 12.

Because the FEM-analysis gives, compared to the BEF-analysis, a more accurate prediction of the soil-structure interaction, this calculation method will mainly be used throughout this research for determining the load distribution and deformations. Herewith, the software package Plaxis 2D will be used to analyse and calculate geotechnical structures.

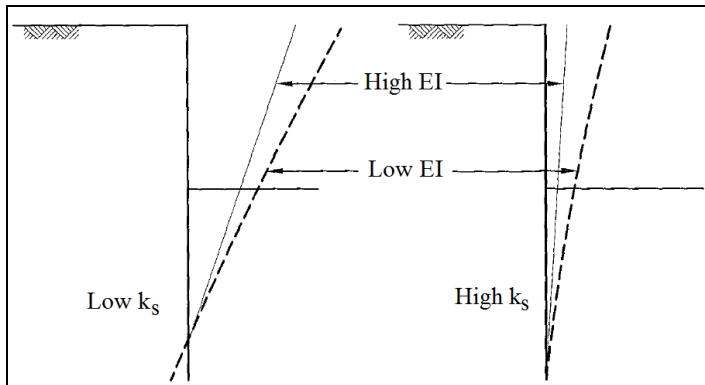


Figure 10: Influence of the wall stiffness (EI) for an unanchored wall. The occurring moment is equal for both cases

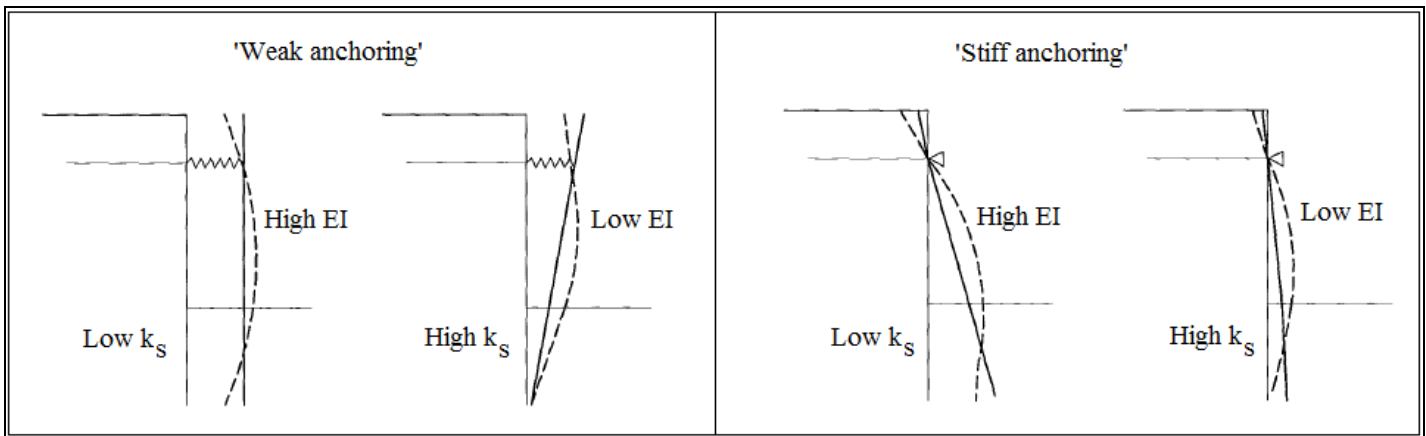


Figure 11: Influence of the wall stiffness (EI) and the soil stiffness (k_s) for an anchored wall

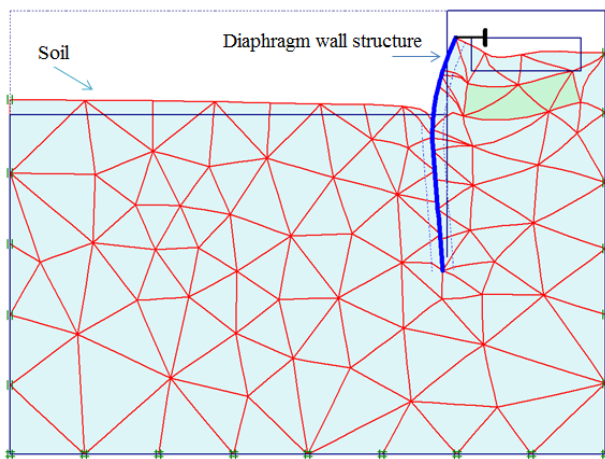


Figure 12: Deformed mesh in Plaxis 2D

2.3.2. Material models

Different constitutive soil models are available in FEM. The models listed in the following are based on the material models in Plaxis, as the latter can be considered to be the most commonly used FEM in the geotechnical field in the Netherlands. For a detailed description of the various models with their corresponding features and capabilities, reference is made to Appendix A and the Plaxis Manuals. The difference between these models lies in the manner in which the material behaviour is described in terms of stiffness and strength. The different material models are:

- The Linear Elastic Model (LE)
- The Mohr-Coulomb Model (MC)
- The Hardening Soil Model (HS)
- The Hardening Soil Small Strain Model (HSS)
- The Soft Soil Creep Model (SSC)

Generally speaking the HS-model (with or without small strain stiffness) is considered to be the most suitable model for retaining structures. This model is suitable for all soils (soft and stiff soils), but does not account for viscous effects (e.g. creep). The LE-model is very limited for the simulation of soil behaviour and it is primarily used for stiff structures in the soil. The MC-model should only be used for a relatively quick and simple first analysis of the problem considered. When good soil data is lacking, there is no use in further more advanced analyses. The SSC-model should be used whenever time-dependent behaviour becomes dominant due to the presence of pre-dominantly soft soils. The HSS-model must be considered especially when it is important that deformations are calculated with higher accuracy [6, 7].

2.3.2.1. Real soil response vs. constitutive models

The HS-model is an elasto-plastic soil model represented by a hyperbolic stress-strain relationship as depicted in Figure 13, resulting in more realistic displacement fields compared to for instance the linear-elastic perfectly-plastic MC-model. The MC-model is ideal for a stability test, but the displacements obtained are not realistic because of the constant stiffness. For real soils the stiffness depends on the stress level. Control of the stress level dependency, implying that the stiffness moduli increase with pressure, is taken into account by the HS-model. Figure 13 represents the stress-strain relationship for the MC-model, the HS-model and real soil. With the HS-model the real soil behaviour is approximated more accurately.

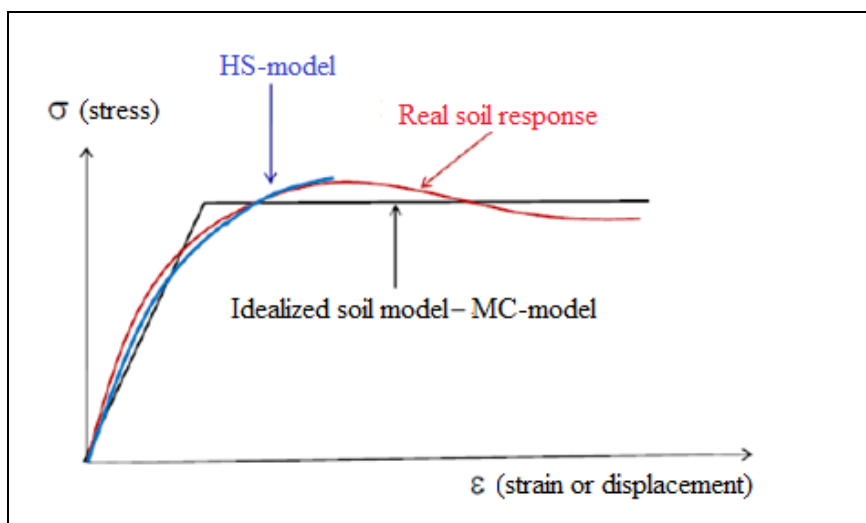


Figure 13: Comparison of HS- and MC-model with real soil response [8]

2.3.2.2. Choice of constitutive model

The choice of a constitutive model depends on many factors but, in general, it is related to the type of analysis that needs to be performed, expected precision of predictions and available knowledge of soil. Geo-engineering analyses can be distinguished into 2 groups:

- Bearing capacity and stability analyses. These are related to the ULS-analysis, using basic linear models e.g. MC-model (but this is not a rule) and;
- Deformation analyses. These are related to the SLS-analysis, using advanced non-linear constitutive models e.g. HS-model.

Deformation analyses or situations where differences in stiffness play a significant role in the distribution of forces require a more advanced constitutive model. In such cases the HS-model is preferred above the MC-model. It should be noted that the HS-model requires more detailed data. If these data are not available the MC-model may be applied. However, in that case the uncertainties in the finite element calculation with regard to the bending moments in the retaining wall can be quite large.

In this research the emphasis lies mainly on the deformation analysis, where a good prediction of the occurring displacements is required. As the soil deformations will affect the bending stiffness and thus the force distribution in the diaphragm wall and vice versa, the urge for a realistic displacement field is of great importance. Not only this, but also the fact that the geotechnical profile of this project consists mostly of sand layers, led to the choice for the HS-model as representative soil model throughout this research. In the context of this research the following material models are used: LE- and HS-model. The LE-model will be used for structural elements (foundation and diaphragm wall), whereas the HS-model will be used for the soil.

2.3.2.3. Soil parameters

When designing geotechnical structures, it is necessary to know the pertinent parameters controlling the soil behaviour. The soil model parameters can be distinguished into stiffness parameters and strength parameters. For a detailed description of the soil parameters used in this research reference is made to Appendix A. The considered soil parameters are:

- Horizontal soil pressure coefficient (K);
- Cohesion (c);
- Internal friction angle (ϕ);
- Wall friction angle (δ);
- Dilatancy angle (ψ);
- Permeabilities (k_x and k_y);
- Saturated and unsaturated weight (γ_{sat} and γ_{unsat});
- Modulus of subgrade reaction (k_s) – Secant;
- Over-Consolidation Ratio (OCR);
- Pre-Overburden Pressure (POP);
- Stiffness moduli (E):
 - The triaxial loading stiffness or secant modulus (E_{50});
 - The triaxial unloading stiffness (E_{ur});
 - The oedometer loading stiffness (E_{oed}).

2.4. The M-(N)- κ diagram

The bending stiffness (EI) is the resistance to a curvature (κ) when a structural component is loaded with a bending moment (M) and possibly an axial compressive force (N'_c). The relationship between M and κ , whether or not combined with an axial compressive force, is expressed by means of M-(N)- κ diagrams. The actual nonlinear bending moment-curvature relationship is idealized by means of a simple piece-wise linear relationship as depicted in Figure 14.

For reinforced concrete the bending stiffness can vary considerably. There appears to be a large difference in the bending stiffness of an uncracked and a cracked concrete cross-section. As soon as the concrete has cracked, the bending stiffness decreases with increasing deformation. Due to a varying bending moment, the structure contains a variable bending stiffness (EI_{var}) over its length; every bending moment has a different EI belonging to it.

To put it briefly, the M-(N)- κ diagram is a simplified representation of the varying bending stiffness of a reinforced concrete structure, or in other words the resistance of a concrete cross-section to deformation in the different loading phases. To determine the M-(N)- κ diagram 4 loading phases are considered from the moment of loading till the moment of failure of the reinforced concrete structure. In Figure 14 these loading phases can be distinguished as:

- P_1 : The **cracking moment** M_r , with the accompanying curvature κ_r .
The (mean) tensile strength of the concrete has been reached and the first crack appears ($\sigma_c = f_{ctm}$).
- P_2 : The **yield moment** M_e , with the accompanying curvature κ_e .
The (tensile) reinforcement starts to yield ($\sigma_s = f_{yd}$).
- P_3 : The **crushing moment** M_{pl} , with the accompanying curvature κ_{pl} .
The concrete in the compression zone starts to crush ($\epsilon_{c3} = 1,75\%$ for normal concrete, thus $\leq C50/60$).
- P_4 : The **ultimate moment** M_u , with the accompanying curvature κ_u .
The concrete has reached its ultimate compressive strain ($\epsilon_{cu3} = 3.5\%$ for normal concrete)

This order of the loading phases is common. However, the points P_2 and P_3 can appear in reversed order; the reinforcement does not necessarily have to yield before the concrete starts to crush. This depends on the applied amount of reinforcement. However, for a ductile failure it is necessary that the reinforcement yields before the concrete compression zone fails, thus before reaching point P_4 . This can be achieved by applying the maximum reinforcement ratio ($\rho_{l,max}$).

See Figure 14. From the moment of loading till the moment of failure of the structure, the M-(N)- κ diagram can be well approximated by means of 4 straight lines which connect the points M_r , M_e , M_{pl} and M_u . By means of the M-(N)- κ diagram one can determine the bending stiffness EI of a reinforced concrete structure at an arbitrary bending moment (M_x). From the origin a line is drawn to M_x and the corresponding curvature κ_x is read off. The bending stiffness (EI) $_x$, which is the slope of the line, can now

be determined. For an arbitrary moment the bending stiffness becomes: $(EI)_x = \tan(\alpha_x) = \frac{M_x}{\kappa_x}$. By

definition the slope is taken from the line that starts from the origin and not from, for instance the line in the M-(N)- κ diagram with an angle of inclination α_e . Otherwise, the EI would be constant for the branch P_1 - P_2 , implying that every cracked part of the structure has the same EI which is not very likely. The EI derived for the branch P_3 - P_4 , between M_{pl} and M_u , would in that case be reduced to an absolute minimum (α_u). Of course, it is obvious that as long as the moment has not reached M_r , the bending stiffness EI remains constant for the uncracked concrete cross-section. Logically, in the uncracked phase the EI is also the largest. From Figure 14 it is clear that the bending stiffness EI decreases as the load is increased. The

reason behind this phenomenon is the increasing crack formation and the yielding of the reinforcement from a certain point onward.

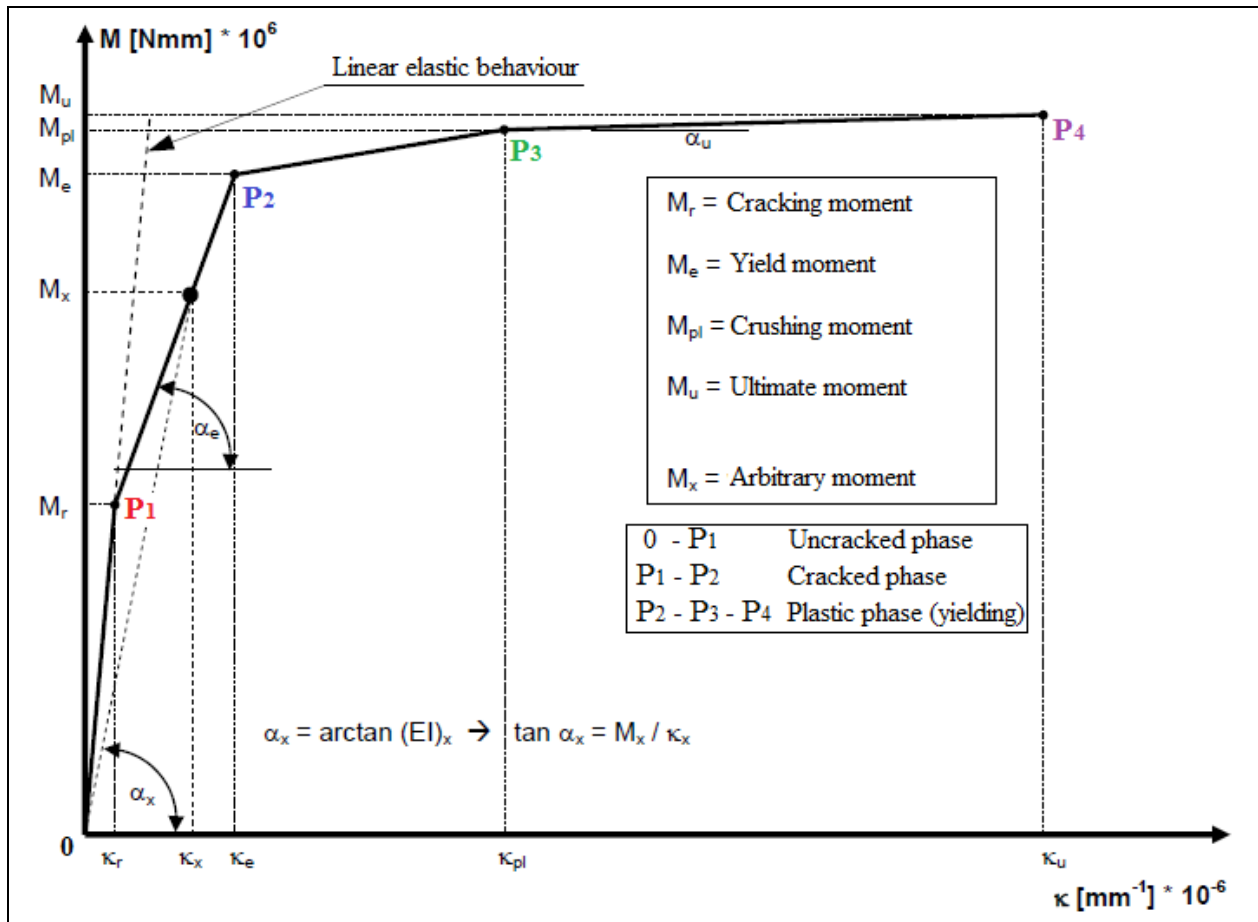


Figure 14: The M-(N)- κ diagram

As stated before, the points P_2 and P_3 can appear in reversed order. This implies that concrete crushing (M_{pl}) can occur before yielding of the reinforcement (M_e). At a relatively low reinforcement ratio it is usual that yielding of the steel (M_e) occurs before the concrete crushing (M_{pl}), while at a high reinforcement ratio M_{pl} is obtained before M_e . In determining the M-N- κ diagram, yielding of the tension reinforcement will occur first in case of small compressive forces and relatively large bending moments, while in case of large compressive forces and relatively small bending moments crushing of the concrete will be obtained before yielding of the steel.

In this research the influence of tension-stiffening (the positive contribution of the stiff uncracked concrete parts between the cracks) on the overall bending stiffness of the structure is taken into account. This implies that according to Figure 15 the path to follow starts from the origin to ①-③. If the tension-stiffening (shaded area) is not considered, this signifies that as soon as the first crack occurs the tension reinforcement takes over the total tensile force and the contribution of the tensile strength of the concrete in the stiff uncracked concrete sections is totally neglected. In that case the path from the origin to ①-②-③ has to be followed. Since this is not very realistic in practice (and it has also not been established by research) that after the first crack the curvature increases excessively, it is more likely to apply the diagram with tension stiffening. For a clear understanding Figure 15 shows a beam subjected to bending, where due to crack formation one can distinguish sections with an uncracked stiffness and sections with a cracked stiffness with or without the contribution of tension-stiffening.

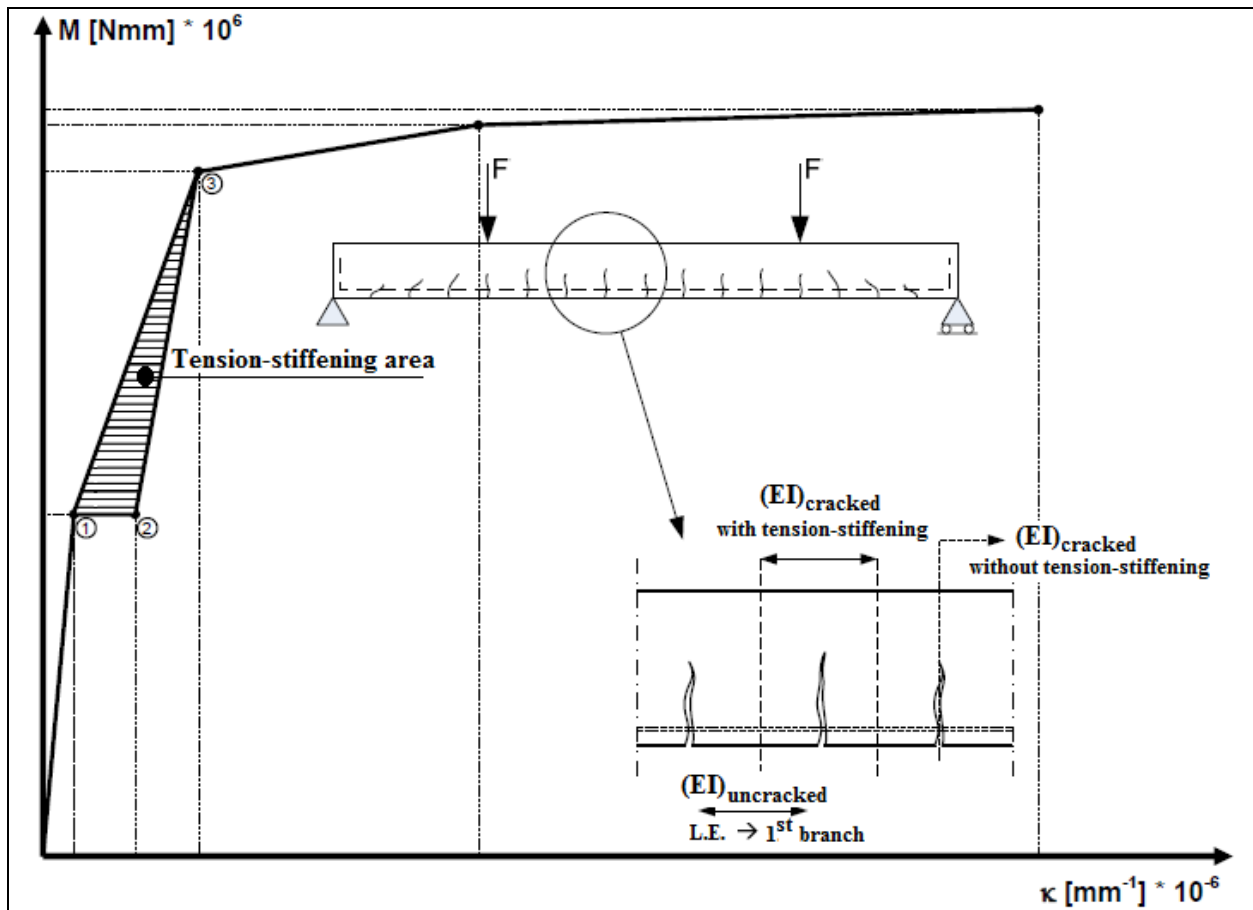


Figure 15: The influence of tension-stiffening on the bending stiffness

2.4.1. Characteristics in M-(N)-κ diagram

In this section both the influence of the reinforcement ratio (ρ_l) and an axial compressive force (N'_c) on the M-(N)-κ diagram are dealt with.

❖ Influence reinforcement ratio (ρ_l)

Figure 16 depicts an M-κ diagram for a reinforced concrete section with ρ_l as the only variable. The first branch, the uncracked section, goes until the cracking moment M_r . For convenience's sake this point is kept constant as starting point for the next phase at every ρ_l .

The following details can be noted in the diagram of Figure 16:

- With a decreasing ρ_l , the difference between M_u and M_r becomes smaller. To avoid brittle fracture, it is therefore necessary to define a $\rho_{l,min}$;
- With an increasing ρ_l , the 'horizontal' branch between M_c/M_{pl} and M_u becomes smaller. The yield path becomes smaller and at a very high reinforcement ratio there will be no yielding at all. This form of failure is also undesirable and therefore a $\rho_{l,max}$ must be defined;
- With an increasing ρ_l , the tension-stiffening effect reduces. Eventually, the points origin-①-③ as shown in Figure 15 are lying approximately on one line and there is no shaded area anymore;
- The ability to deform plastically increases with a decreasing ρ_l .

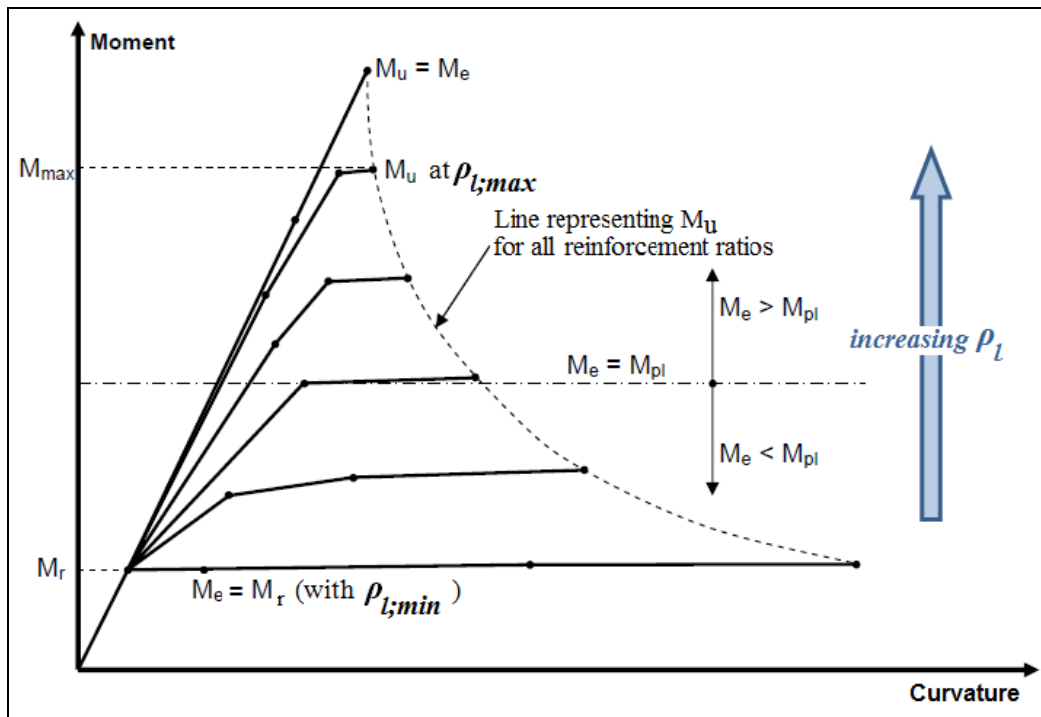


Figure 16: The M-(N)-κ diagram with reinforcement ratio (ρ_l) as variable

In Figure 16 the (almost) horizontal branch represents the curvature distance between $M_e - M_u$ or between $M_{pl} - M_u$. The longer this branch, the more a structure can deform (rotational capacity). The dividing line is shown in the middle of the diagram; on this line it holds that $M_e = M_{pl}$. Below this line the yielding of the reinforcement will always occur before the crushing of concrete, so $M_e < M_{pl}$. While above this line the opposite holds; the concrete will crush before the reinforcement yields, so $M_{pl} < M_e$. Often M-κ diagrams are based on the situation where yielding of the reinforcement occurs first, but this only holds for relatively low reinforcement ratios.

❖ Influence axial compressive force (N'_c)

An axial compressive force (N'_c) causes a reduction of the tensile stress in the concrete cross-section. The compressive stress (indirectly) provides for an increase in the stiffness of the element. This is clearly seen in Figure 17, when comparing the case $N = 0$ with $N \neq 0$ kN. The presence of an axial compressive force in the cracked cross-section leads to an increased bending stiffness EI, which is clearly reflected by the steepening of the slope of branches ①-② and ②-③ with increasing N. The "enlarged view" in Figure 17 also shows that an increased N leads to an increased cracking moment M_r and a shorter yield path. The presence of a higher N shows more brittle behaviour, reflected by a shorter 'horizontal branch' (③-④). The stiffness of the uncracked cross-section remains constant, regardless of whether or not the element is loaded by an axial compressive force. For deformation calculations it is safer to assume a lower bending stiffness. Therefore, it is preferred to use M-κ diagrams ($N'_c = 0$) above M-N-κ diagrams in calculating deformations.

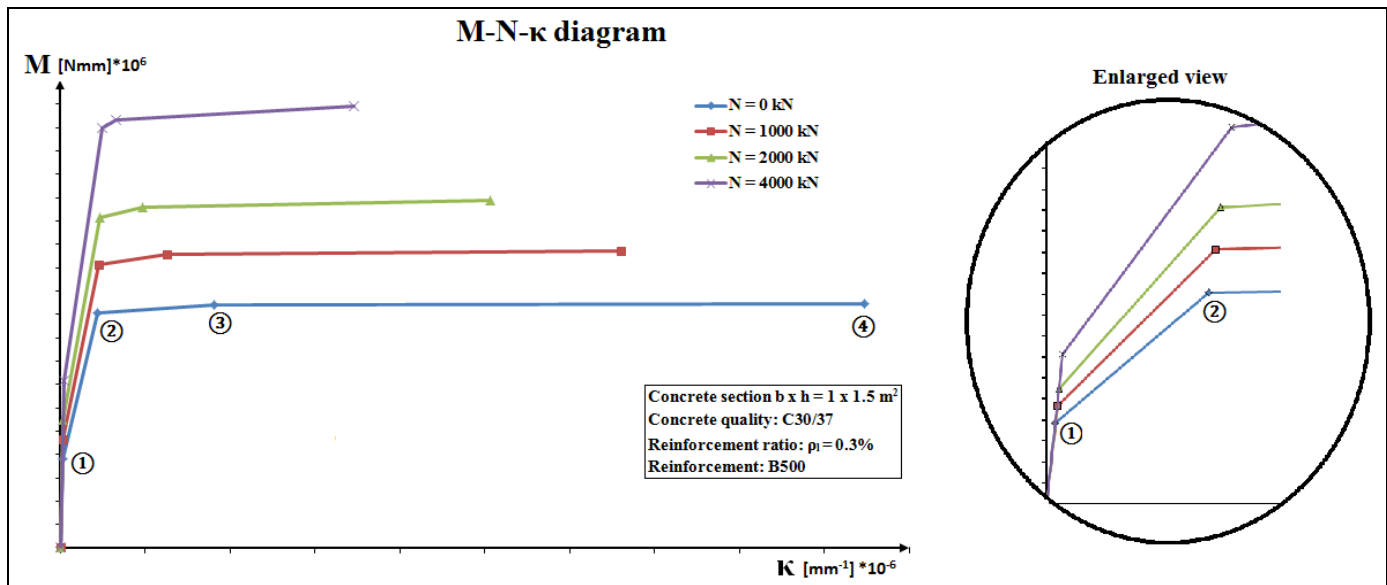


Figure 17: The M-N- κ diagram with normal compressive force ($N = N'$) as variable

2.4.2. EC2: Minimum and maximum reinforcement ratio diaphragm walls

In order to prevent brittle failure by steel rupture and to ensure sufficient ductility, a minimum reinforcement ratio ($\rho_{l,\min}$) and a maximum reinforcement ratio ($\rho_{l,\max}$) are required, respectively. If the reinforcement ratio is defined based on A_c (total cross-sectional area of concrete), one finds according to EC2, clause 9.6.2 that $\rho_{l,\min} = 0.2\%$ and $\rho_{l,\max} = 4\%$ for a diaphragm wall

2.4.3. Software programs using M-N- κ diagram: PCSheetPileWall

The bending stiffness EI of diaphragm walls is not constant over the height, but it varies as a function of the magnitude of the *occurring bending moment and the amount of reinforcement*. As soon as the cracking moment M_r has been exceeded, the wall stiffness decreases at an increasing bending moment. The stiffness which is reached in each stage of construction depends on the calculated moment. However, if the wall stiffness is adjusted, this in its turn influences the calculated moment again. In order to gain a clear insight into the actual occurring moment distribution of the wall, it is necessary to apply the reduced bending stiffness following from an M-N- κ diagram, based on the amount of reinforcement.

Currently, there are almost no retaining wall calculation programs available in which the reinforced concrete wall stiffness is included based on the bending moment. The only known exception is formed by the program PCSheetPileWall, where the use of M- κ diagrams is supported with or without an axial force. Optionally, creep effects can be considered while effects of unloading with respect to a previous construction phase are taken into account automatically.

It is most realistic to calculate the bending moment in a diaphragm wall using an "interaction" model in which the soil behaviour is also taken into account. The wall deformation depends on both the soil stiffness (k_s) and the wall stiffness (EI). *A reduced wall stiffness results in greater wall deformations, but on the other hand the deformations on their turn influence the wall stiffness.* For geotechnical structures the influence of the soil behaviour on the M and EI of the wall is accounted for by means of the:

- Elastic foundation model, representing the soil stiffness using elastic springs. PCSheetPileWall is based on this model;
- Finite element model, which gives a very realistic representation of the soil behaviour. In this research the program Plaxis 2D was used. This model gives a more accurate prediction of the soil-wall interaction. The only drawback of this program is that the variable stiffness over the wall height can not

be taken into account automatically, thus it is not based on the M-N- κ diagram. The varying stiffnesses (cracked and uncracked stiffnesses) must be entered manually for the various sections.

2.5. Design standards: Cracked vs. Uncracked bending stiffness

As long as the occurring moment in a reinforced concrete member does not exceed the cracking moment (M_r), the member is in the uncracked condition behaving in a linear elastic manner represented by the uncracked stiffness (EI_0). When the bending moment in a cross-section reaches M_r , flexural cracks form in the outermost layers of the tension zone. As the bending moment increases the cracks start propagating. The section becomes fully cracked, when the flexural cracks reach the neutral axis, rendering the entire tension zone ineffective in resisting the bending moment. Due to cracking the bending stiffness has decreased to the so-called cracked bending stiffness (EI_∞), which is assumed to be $1/3EI_0$ in design theory. The background concerning this approach for the cracked bending stiffness is explained in Appendix A. In practice it is more common to find members consisting of cracked and uncracked zones instead of a totally uncracked or fully cracked member. This implies the existence of a realistic variable bending stiffness (EI_{var}) along the reinforced concrete member. The decreased bending stiffnesses in the cracked zones will lead to greater deformations of the concrete member as a whole.

2.5.1. EC2: Behaviour of not fully cracked member

In structural design deformation calculations are complicated by the non-linear behaviour of concrete. The deformation calculations in Eurocode 2 (EC2) are based on the determination of the curvatures and deflections of a concrete beam corresponding to its uncracked and fully-cracked conditions. EC2 states in clause 7.4.3 that:

“Members which are expected to crack, but may not be fully cracked, will behave in a manner intermediate between the uncracked and fully cracked conditions”.

EC2, Equation (7.18) requires the calculation of a deformation value which is a weighted average of the uncracked and fully-cracked state of the member:

$$\alpha = \zeta\alpha_{II} + (1 - \zeta)\alpha_I \quad (\text{Eq. 3})$$

Where:

- α The considered deformation parameter, e.g. a strain, curvature, rotation or deflection
- α_I, α_{II} Values of the deformation parameter calculated for the uncracked and fully cracked conditions, respectively
- ζ Distribution coefficient allowing tension stiffening, where in case of pure bending it holds:

$$\zeta = 1 - \beta \left(\frac{M_r}{M} \right)^2 \quad (\text{Eq. 4})$$

With:

- $\zeta = 0$ for uncracked sections
- β is a coefficient taking account of the duration loading or repeated loading
 - = 1.0 for short-term (instantaneous) loading
 - = 0.5 for sustained loads or many cycles of repeated loading
- M_r is the cracking moment
- M is the maximum service moment

Figure 18 represents the moment-curvature relation in a reinforced concrete section under pure bending just before yielding of the reinforcement. The curvature is given by $\kappa = 1/r$. The slope of the $1/r_I$ – and $1/r_{II}$ – curve represent the stiffnesses EI_0 and EI_∞ , respectively.

According to EC2 the realistic stiffness EI_{var} along the reinforced concrete member can be calculated by interpolating between the two extremes, namely the uncracked stiffness (EI_0) and the fully cracked stiffness (EI_∞). Analogous to (Eq. 3), the realistic bending stiffness for a cracked structure can be found from:

$$EI_{var} = \zeta \cdot (EI_\infty) + (1 - \zeta) \cdot (EI_0) \quad (Eq. 5)$$

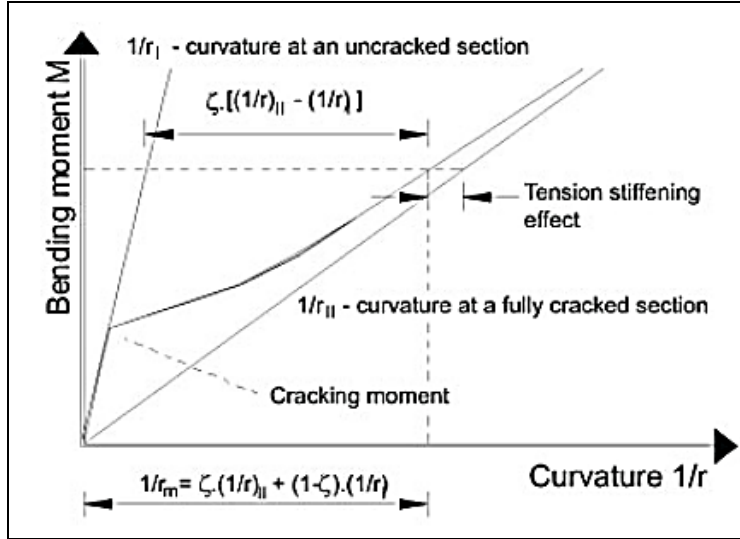


Figure 18: Moment-curvature relation in a reinforced concrete section under pure bending before reinforcement yielding [9]

2.5.2. Bending stiffnesses: EI_0 , EI_{var} and EI_∞

In this research the bending stiffness EI for the uncracked and fully cracked condition is calculated as the product of moment of inertia of the gross concrete section (I_g) and the modulus of elasticity of concrete (E_c), where according to [10] E_c is applied as follows in the design process:

- For SLS-calculations the mean value E_{cm} is used;
- For ULS-calculations a partial safety factor, γ_{cE} , is used to give a design value for the modulus, $E_{cd} = E_{cm}/\gamma_{cE}$ (where γ_{cE} is 1.2).
- For long-term deflection calculations E_{cm} is modified by creep to give an effective modulus, $E_{c,eff}$. This is calculated using the expression $E_{c,eff} = E_{cm}/(1 + \varphi)$ where φ is the creep coefficient with a value typically between 1 and 3.

Because of the deformation calculations (SLS) considered in this research, it is obvious that E_{cm} has to be applied. From this point forward the bending stiffnesses considered in this report will be addressed as follows:

- EI_0 : the uncracked bending stiffness, where $EI_0 = E_{cm} \times I_g$;
- EI_∞ : the fully cracked bending stiffness, where $EI_\infty = E_{cm} \times \frac{1}{3} I_g$. It should be noted that besides cracking, the effect of creep, is also included in the fully cracked bending stiffness.
- EI_{var} : the realistic (variable) bending stiffness, which will be determined from the M-(N)- κ diagram.

3. RESEARCH STRATEGY

3.1. Geometry

For the realization of the ancillary channel, the original surface level of NAP +10.5 m was lowered to NAP +2 m. The bottom of the ancillary channel lies 3 m deeper than the foundation level of the existing spread foundation, which consists of unreinforced concrete. In case of scour, the bottom of the ancillary channel is assumed to be at NAP +1 m. The packing structure is designed for a lifetime of 100 years. The total width (parallel to railway bridge axis) of the packing structure is 16 m (8 m from axis pillar). The diaphragm wall structure consists of 22.5 m long panels. An impression of the cross-sectional geometry and the levels specified therein are given in Figure 19 and Table 1, respectively. A floor map of the existing foundation surrounded by the diaphragm wall structure is depicted in Figure 20.

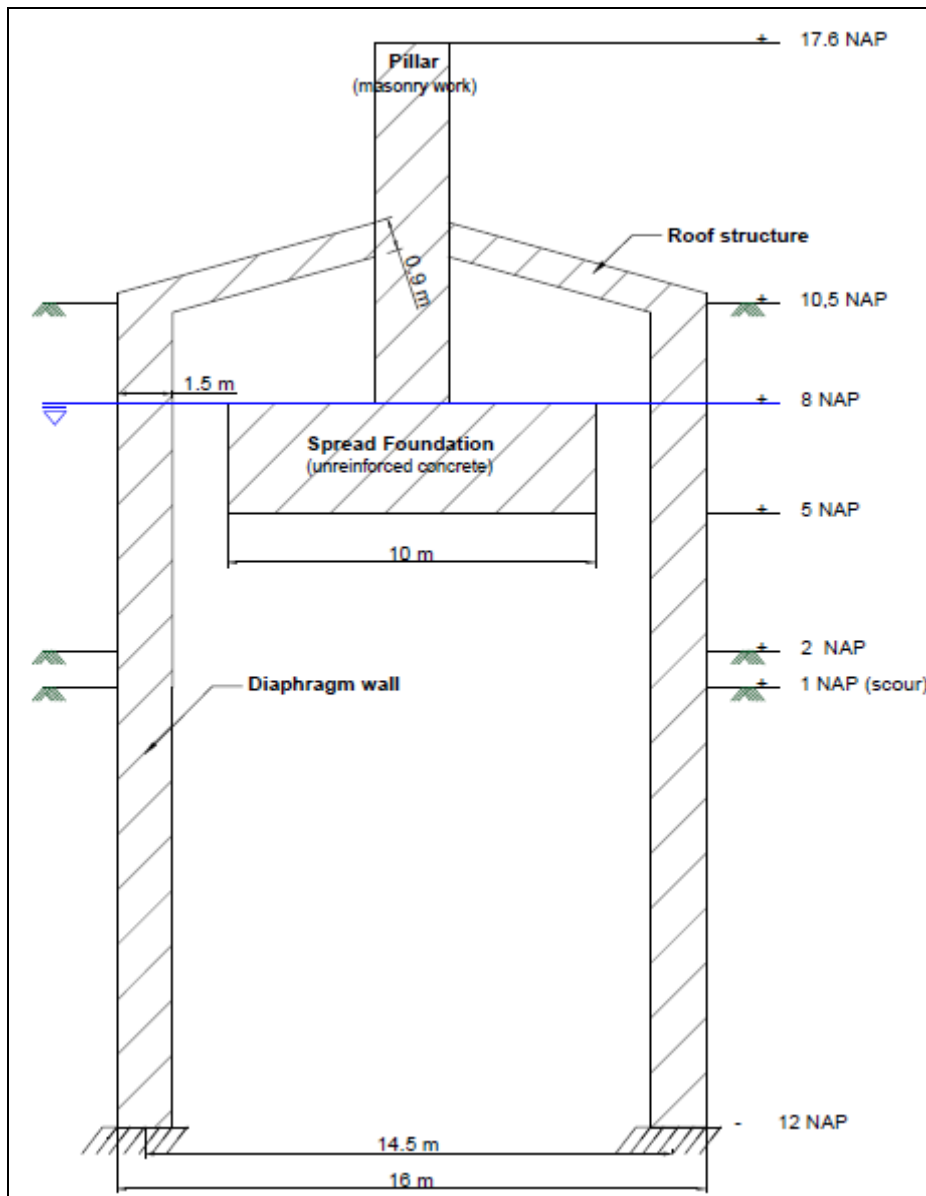


Figure 19: Geometry of the situation

Level w.r.t. NAP [m]	
+ 17.6	Rail traffic level
+10.5	Connection diaphragm wall – roofstructure / Surface level before excavation
+ 8	Assumption of groundwater level inside and outside of packing structure
+ 5	Foundation level of existing spread foundation
+ 2	Bottom of ancillary channel
+ 1	Bottom of ancillary channel due to scour
-12	Bottom of diaphragm wall

Table 1: Specification of levels

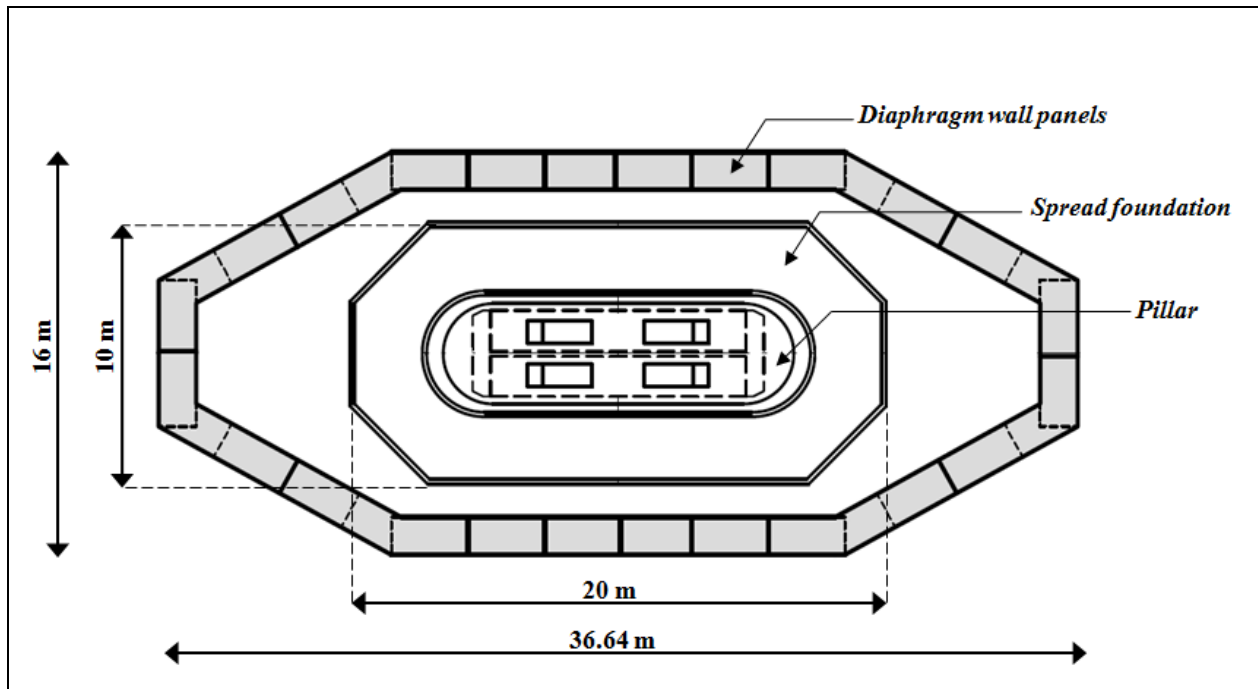


Figure 20: Floor map of existing foundation surrounded by diaphragm wall structure

3.2. The loading combinations in SLS

Since the deformations were the main issue during execution of the “Waalbrug-project”, the structure will be calculated for the SLS only. Three different loading combinations are distinguished:

- LC1: Loading from superstructure, without braking forces;
- LC2: Loading from superstructure with braking forces;
- LC3: Loading from superstructure with braking forces, and 1 m scour.

These loading conditions are depicted in Figure 21.

The values of the horizontal (point) loads and the vertical distributed load for the different loading combinations are given in 3.2.1, 3.2.2 and 3.2.3.

Note: The maximum braking force given in Table 6 is considered for the case where two trains are passing each other. At that point it is assumed that one train uses its maximum braking force, while the other train accelerates. Since the braking force is the opposite of the accelerating force, both forces work in one direction eventually.

3.2.1. LC1

Name	Level w.r.t NAP [m]	Load [kN/m ³]
Soil pressure 1	10.25	-2.25
Soil pressure 2	9.50	-9.00
Soil pressure 3	8.50	-18.00
Soil pressure 4	7.50	-25.00
Soil pressure 5	6.50	-30.00
Soil pressure 6	5.50	-35.00

Table 2: Horizontal (point) loads on diaphragm wall for LC1

The vertical load acting on the bottom level of the spread foundation consists of a uniform load (q_1), a surcharge load (q_2) and a vertical distributed load from the spread foundation (q_3) given in Table 3, Table 4 and Table 5, respectively. For the 3 m thick spread foundation it is found that $q_3 = h_{slab} \times \gamma_c = 3 \times 24 = 72 \text{ kN/m}^2$

Name	Load [kN/m ²]
q_1 (soil weight)	75

Table 3: Uniform load – LC1

Name	Distance from diaphragm wall [m]	Load [kN/m ²]
q_2 (vertical load superstructure)	1.50	174
	11.50	174

Table 4: Surcharge load – LC1

Name	Distance from diaphragm wall [m]	Load [kN/m ²]
q_3 (vertical distributed load spread foundation)	1.50	72
	11.50	72

Table 5: Vertical load from spread foundation – LC1

3.2.2. LC2

Name	Level w.r.t NAP [m]	Load [kN/m ³]
Soil pressure 1	10.25	-2.25
Soil pressure 2	9.50	-9.00
Soil pressure 3	8.50	-18.00
Soil pressure 4	7.50	-25.00
Soil pressure 5	6.50	-30.00
Soil pressure 6	5.50	-35.00
Braking force 1	6.00	-114.00
Braking force 2	7.00	-114.00

Table 6: Horizontal (point) loads on diaphragm wall for LC2

The vertical load acting on the bottom level of the spread foundation consists of a uniform load (q_1), a surcharge load (q_2) and a vertical distributed load from the spread foundation (q_3), which is equal to the one calculated in LC1. For LC2, q_2 acts over an effective width of 7.17 m of the spread foundation. These loads are given in Table 7, Table 8 and Table 9.

Name	Load [kN/m ²]
q ₁ (soil weight)	75

Table 7: Uniform load LC2

Name	Distance from diaphragm wall [m]	Load [kN/m ²]
q ₂ (vertical load superstructure)	1.50	225
	8.67	225

Table 8: Surcharge loads LC2

Name	Distance from diaphragm wall [m]	Load [kN/m ²]
q ₃ (vertical distributed load spread foundation)	1.50	72
	11.50	72

Table 9: Vertical load spread foundation

3.2.3. LC3

For LC3, the horizontal and vertical loads are the same as for case LC2. The only difference is now that due to scour the bottom of the ancillary channel is at NAP +1 m.

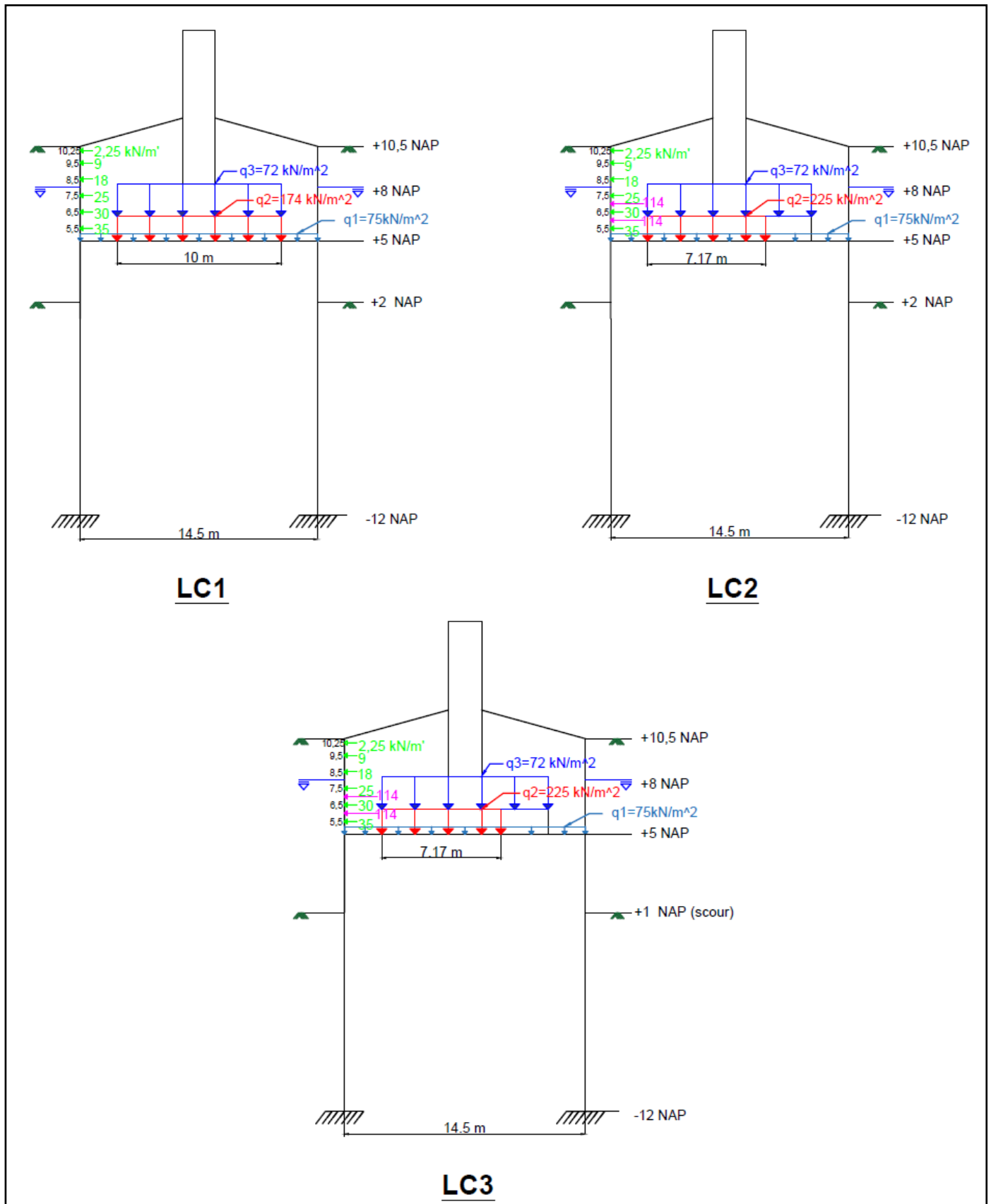


Figure 21: Loading conditions in SLS

3.3. Assumptions

For the calculations the following assumptions have been made in PCSheetPileWall and Plaxis 2D:

1. Consider only one soil layer, in particular: clean sand (firm).

Although the soil profile consists of 13 layers, the most common material to be found is sand. For calculation purposes assume the average of the soil parameter values. For the exact soil profile and the soil parameter values for the different layers reference is made to Appendix B.

2. Consider only the loading combinations in SLS.

Since the occurring settlements and lateral displacement of the diaphragm wall are studied as a function of its varying bending stiffness, the loading combinations in the SLS are of importance. Therefore the material factors and safety coefficients will be set to 1.0. The loading combinations in SLS have already been given in section 3.2.

3. No water pressure difference between the groundwater inside and outside of the packing structure. Therefore, assume 1 groundwater level inside and outside of the packing structure at NAP +8 m. In order to avoid additional loading on the diaphragm wall due to water pressure difference, a feed-through was applied in practice.

4. Consider only the representative panel type with the basic reinforcement applied within it: Starter panel of 2.8 m wide with basic reinforcement 16Ø32.

The diaphragm wall consists of 3 types of panels. The reinforcement cages used in these panel types are different. The properties of the panel types are given in Table 10. The basic reinforcement given in this table is the reinforcement present at each side of the panel thickness, in particular at the channel side and the pillar side. The applied concrete cover is 100 mm. From Figure 22 it can be noted that there are also corner panels with reinforcement cages D and G. However, only the panels lying around the mid cross-section A-A are regarded as representative, since they will be the most heavily loaded panels compared to the panels which are further away. Based on the amount of reinforcement applied, the starter panel is taken as the representative panel for calculations in PCSheetPileWall. This panel is the ‘weakest link’ among the different panel types.

Panel type	Reinforcement cage	Panel width [m]	Basic reinforcement per side
Starter panel (‘starter’)	A	2.8	16Ø32
Intermediate panel (‘volger’)	B	3.051	19Ø32
Closure panel (‘sluiter’)	C	3.051	19Ø32

Table 10: Properties panel types

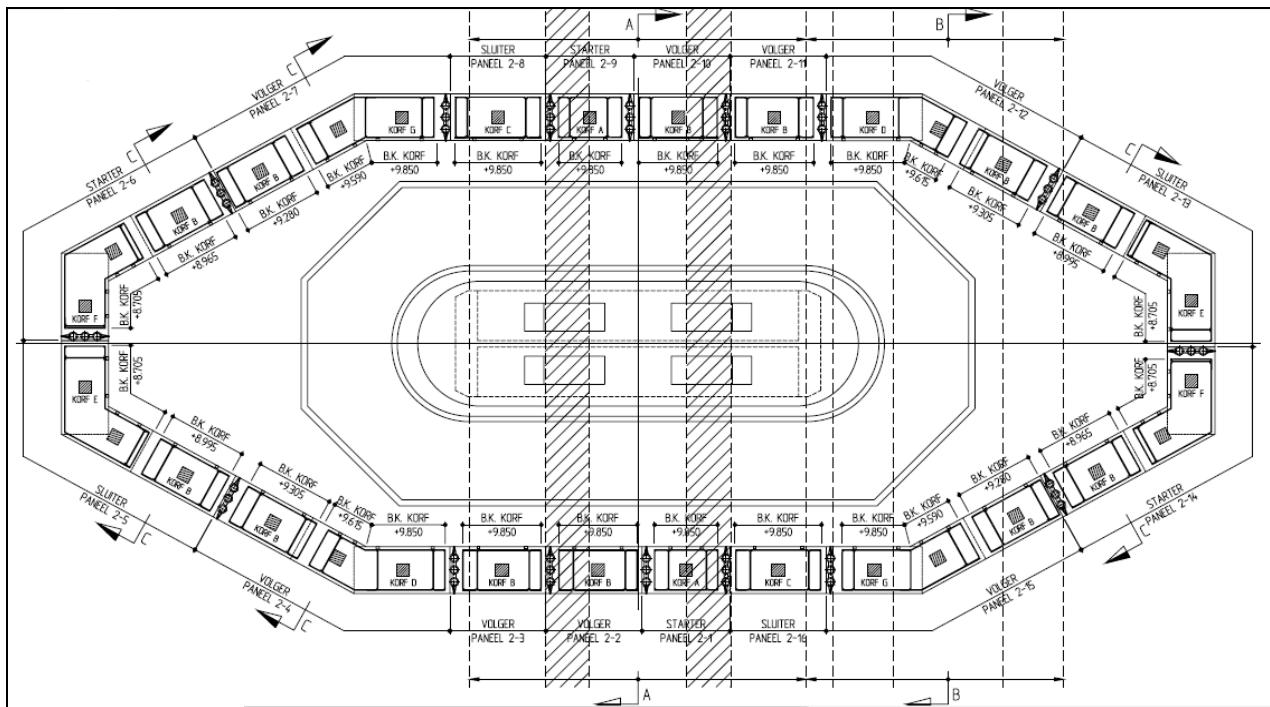


Figure 22: Panel layout diaphragm wall

3.4. Calculation software – input

In order to investigate the soil-structure interaction, two calculation software programs were used during this research, in particular:

- PCSheetPileWall (Version 1.36) – a discrete model and;
- Plaxis 2D (Version 8) – a continuous model.

The geometric and physical nonlinearities are taken care of by the software programs. In case of geometric nonlinearity the force distribution is influenced by the deformation. The physical nonlinearity concerns a changing bending stiffness EI as the load increases. In PCSheetPileWall, both the geometric and physical nonlinearity are included by the program itself. However, this is not totally the case with Plaxis 2D. This program takes the geometric nonlinearity automatically into account, but does not allow for the physical nonlinearity. In Plaxis 2D the varying bending stiffness for structural elements subjected to bending should be implemented manually. The element is divided into parts, where each part is considered to behave linear-elastic (with a constant EI).

3.4.1. PCSheetPileWall

PCSheetPileWall is a discrete numerical model based on the beam on elastic foundation method (BEF-method). Based on the properties of the reinforced concrete diaphragm wall and the occurring bending moment, the *cracked* bending stiffness is calculated by the program. The diaphragm wall can consist out of more than one section in vertical direction, where for each section the bending moment capacity is represented by an M -(N)- κ diagram for the SLS and ULS. An overview of the calculation results from this program is given in Figure 23. A representation of the lateral stiffness over the wall height (EI -distribution) together with an indication of the cracked and uncracked zones over the wall height, is regarded as one of the most important features of this program.

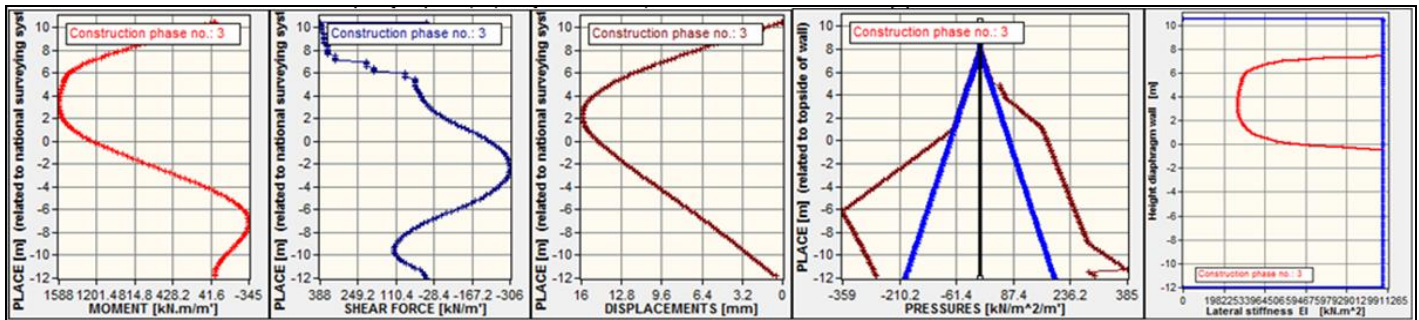


Figure 23: Output PCSheetPileWall

3.4.1.1. The material properties of the structure and the soil in PCSheetPileWall

The properties of the diaphragm wall and the input data for the sand are according to Table 11 and Table 12, respectively.

Property		
Total length	l [m]	22.5
Thickness	d [m]	1.5
Reinforcement	$A_{reinf.}$ [mm ² /m ²]	(depends on studied case)
Cover	$c_{concr.}$ [mm]	100
Concrete quality	C30/37	
Compressive strength concrete	f_{ck} [N/mm ²]	37
Tensile strength concrete	f_{ctm} [N/mm ²]	2.9
E-modulus concrete	E_{cm} [N/mm ²]	33000
Reinforcement	B500B	
Yield stress reinforcement	f_{yk} [N/mm ²]	500

Table 11: Properties diaphragm wall in PCSheetPileWall

Parameter		Value	Unit
Soil unit weight above phreatic level	γ_{dry}	19	[kN/m ³]
Soil unit weight below phreatic level	γ_{sat}	20	[kN/m ³]
Cohesion (constant)	c_{ref}	0	[kN/m ²]
Internal friction angle	φ	30	[°]
Wall friction angle	δ	30	[°]
Dilatancy angle	ψ	0	[°]
Over consolidation ratio	OCR	1	[-]
Shell factor		1	[-]
Modulus of subgrade reaction (Secant)	k_1	26000	[kN/m ³]
	k_2	13000	[kN/m ³]
	k_3	6500	[kN/m ³]

Table 12: Material properties sand

For determination of the bending stiffness (M-(N)- κ diagram) of the diaphragm wall, the following options are taken into account:

- No reinforcement holes;
- No influence of reinforcement in compression zone;
- No creep;
- Material and safety factors are equal to 1;
- N only due to self-weight, N due to shear force along wall not included:

The vertical shear forces along the wall (due to friction wall-soil) have an eccentricity equal to $0.5x$ wall thickness. By this eccentricity, extra moments are exerted onto the diaphragm wall. In case one considers $N_{\text{tot}} = N_{\text{self-weight}} + N_{\text{shear force}}$, then the N_{tot} for the left and right wall are different. In order not to complicate the calculations and iteration procedure with 2 different M-N- κ diagrams for both walls, it is assumed to consider only $N_{\text{self-weight}}$ when the impact of N is studied. The self-weight of the diaphragm wall is calculated with a specific weight of $\gamma_{\text{concrete}} = 24 \text{ kN/m}^3$;

3.4.1.2. The calculation model in PCSheetPileWall

In PCSheetPileWall it is only possible to draw one diaphragm wall (Half Model) where at both sides the surface level, groundwater level, soil layers, loading, anchors/struts and/or supports are defined for each construction phase. An impression of the calculation model for the “Waalbrug-project” is depicted in Figure 24.

Since in PCSheetPileWall it was only possible to schematize one wall with loads working at both sides of it, both walls were modelled apart. The left wall was schematized using LC1, LC2 and LC3. Since from these loading combinations it was clear that LC3 was the representative loading condition (because of the larger cracked zone in the left wall), it was not necessary to look at the impact of the other loading combinations on the right wall. So for the right wall the only loading combination applied was LC3, indicated as LC3, R.

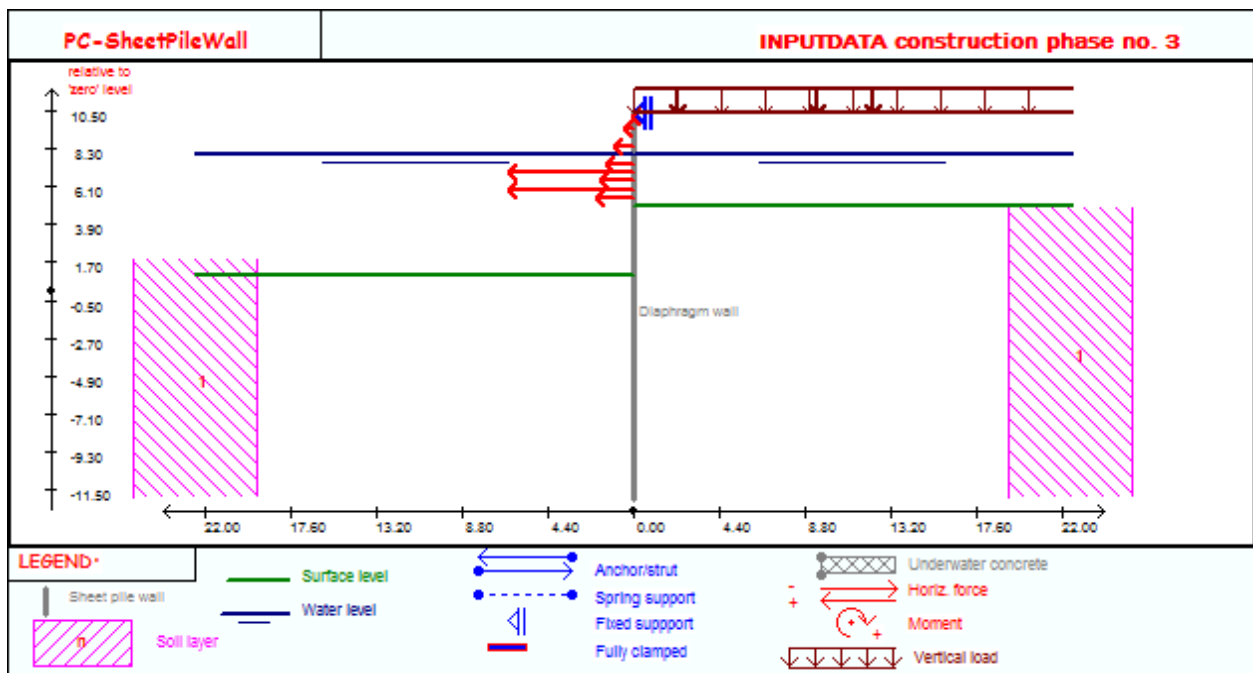


Figure 24: Impression calculation model in PCSheetPileWall (Hinged case – LC3)

3.4.2. Plaxis 2D

In a discrete (spring) model, such as PCSheetPileWall, the soil stiffness has a great influence on the deformations, while its impact on the force distribution is much smaller. A better calculation model is the finite element model (FEM), such as Plaxis 2D. It gives a qualitative good insight into the deformations of the wall and the soil. In general, the calculated deformations mainly depend on the chosen soil model and the associated soil parameters. In the context of this research the following material models are used:

- The Linear Elastic Model (LE) : for the diaphragm walls and the spread foundation;
- The Hardening Soil Model (HS) : for the soil.

3.4.2.1. The material properties of the structure and the soil in Plaxis 2D

The properties of the diaphragm wall as implemented in Plaxis 2D are given in Table 13. The material properties of the sand and the interfaces are according to Table 14.

Parameter	Name	Value	Unit
Type of behaviour	Material type	Elastic	[-]
Normal stiffness	EA	*	[kN/m]
Flexural rigidity	EI	*	[kNm ² /m]
Equivalent thickness	d	1.5	[m]
Weight	w _{line}	23	kN/m/m
Poisson's ratio	v _{concrete}	0.2	[-]

Table 13: Material properties of the concrete diaphragm wall

Notes Table 13

- * EI will be derived from the M-(N)-κ diagram and the corresponding EA is then calculated.
- w_{line} is a line load in the direction of the height of the diaphragm wall, caused by the self-weight of the wall. When considering 2.5 m of the wall to be above phreatic level and the remaining 20 m to be below the phreatic level, an average specific weight can be taken into account based on:
 - o $\gamma_{\text{concrete, dry}} = 24 \text{ kN/m}^3$
 - o $\gamma_{\text{concrete, wet}} = 24 - 10 = 14 \text{ kN/m}^3$ (assuming $\gamma_{\text{water}} = 10 \text{ kN/m}^3$)

From this an average specific weight follows: $\gamma_{\text{concrete, average}} = \frac{24 \times 2.5 + 14 \times 20}{22.5} = 15 \text{ kN/m}^3$, resulting in

w_{line} = $\gamma_{\text{concrete, average}} \times d = 15 \times 1.5 = 23 \text{ kN/m}^2$ or 23 kN/m/m (a line load per unit width of the diaphragm wall).

Parameter	Name	Value	Unit
Material model	Hardening soil model		[-]
Type of material behaviour	Drained		[-]
Soil unit weight above phreatic level	γ_{dry}	19	[kN/m ³]
Soil unit weight below phreatic level	γ_{sat}	20	[kN/m ³]
Permeability in horizontal direction	k _x	1	[m/day]
Permeability in vertical direction	k _y	1	[m/day]
Secant stiffness in standard drained triaxial test	E ₅₀ ^{ref}	37500	[kN/m ²]
Tangent stiffness for primary oedometer loading	E _{oed} ^{ref}	37500	[kN/m ²]
Unloading and reloading stiffness	E _{ur} ^{ref}	112500	[kN/m ²]
Power for stress-level dependency of stiffness	m	0.55	[-]
Cohesion (constant)	c _{ref}	*0.5	[kN/m ²]
Internal friction angle	φ	30	[°]
Dilatancy angle	ψ	0	[°]
Strength reduction factor	R _{inter}	1	[-]

Table 14: Material properties of the sand and interface

Notes Table 14:

- *For improved numerical analysis Plaxis recommends a value for the cohesion above 0.2. Therefore c_{ref} is taken as 0.5
- E_{ur}^{ref} = 3* E₅₀^{ref}
- Ψ = φ - 30
- R_{inter}: In general, for real soil-structure interaction the interface is weaker and more flexible than the associated soil layer, implying that the interface strength R_{inter} should be less than 1. In case the

interface should not influence the strength of the surrounding soil it holds that $R_{inter} = 1$ (no reduced strength properties).

The material of the spread foundation has not been modelled as reinforced concrete, but rather as a soil layer. From core samples it has been found that the material has changed in the course of time from concrete in a more or less granular material. The granular material is modelled as a soil layer using the ‘Linear Model – Drained’ model with material parameters as depicted in Table 15.

Parameter	Name	Value	Unit
Material model	Linear elastic		[-]
Type of material behaviour	Drained		[-]
Soil unit weight above phreatic level	γ_{unsat}	24	[kN/m ³]
Soil unit weight below phreatic level	γ_{sat}	24	[kN/m ³]
Stiffness	E^{rel}	1×10^5	[kN/m ²]
Poisson's ratio	ν	0.2	[-]
Strength reduction factor	R_{inter}	1	[-]

Table 15: Material properties spread foundation

3.4.2.2. The calculation model in Plaxis 2D

In Plaxis 2D it is possible to draw both the:

- Half Model, considering only the left wall with the braking forces and the;
- Total Model, considering the total packing structure.

An impression of both calculation models for the “Waalbrug-project” for the representative loading case LC3 is depicted in Figure 25 and Figure 26. The positive X-Y coordinate system is also given in these models.

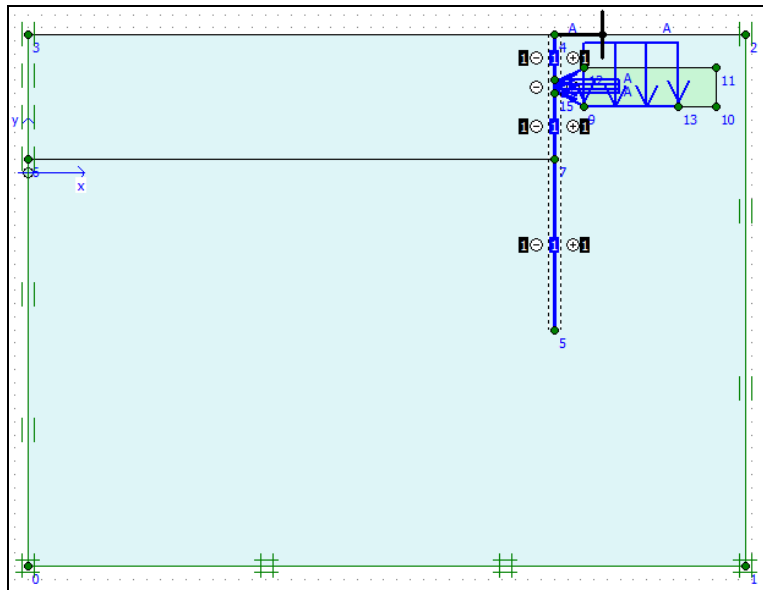


Figure 25: Impression Half Model in Plaxis 2D (Hinged case – LC3)

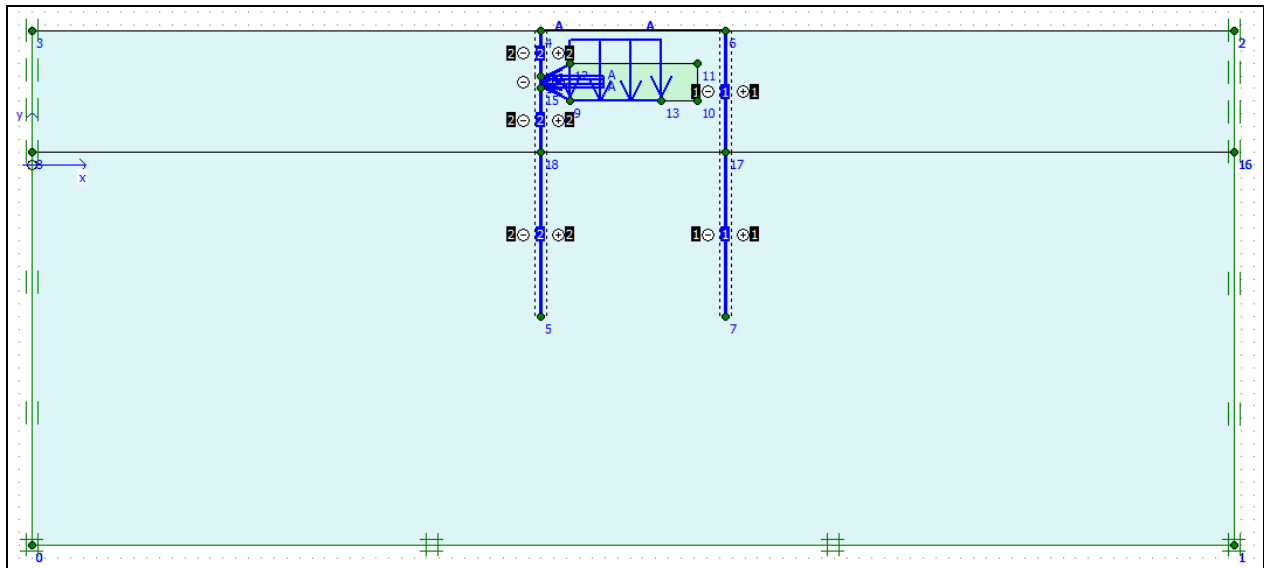


Figure 26: Impression Total Model in Plaxis 2D (Hinged case – LC3)

Load modelling PCSheetPileWall vs. Plaxis 2D

See Figure 24 vs. Figure 25: In PCSheet it is not possible to have different levels, within one construction phase, at which one can put the loading. For each construction phase there is one surface level for the left side and one for the right side at which all the loads have to be defined. Therefore it was not possible to have the same model as in Plaxis 2D, where different levels for the distributed loads are possible within one construction phase. For the model in PCSheet q_1 and q_3 are defined to account for the soil above NAP +5 m and the spread foundation, respectively. So, q_1 , q_3 and the point loads due to horizontal soil pressure, do not have to be defined in Plaxis 2D, because the soil and the foundation slab can just be drawn. The only loading to be modelled in Plaxis 2D are the braking forces and q_2 .

3.5. Roof structure – Equivalent Beam Model

In order to model the roof structure in Plaxis 2D, the 3D-model including the recess in the roof structure, had to be converted into the so-called 'Equivalent Beam Model'. The 3D-model of the roof was made in the program Scia Engineer, and this model was used to determine the normal stiffness (EA) and the bending stiffness (EI) of the equivalent beam for calculation in Plaxis 2D. To determine EA and EI of the equivalent beam, a strip of 1 m is considered in the representative mid-section. The roof is schematized as to be supported by hinges along line elements 1 and roller supports along line elements 2 (see Figure 27). It is worth mentioning that along line elements 3 and 4 the roof is supported by springs and roller supports, respectively. If at both sides 3 and 4 the roof is supported by roller supports, the structure becomes unstable.

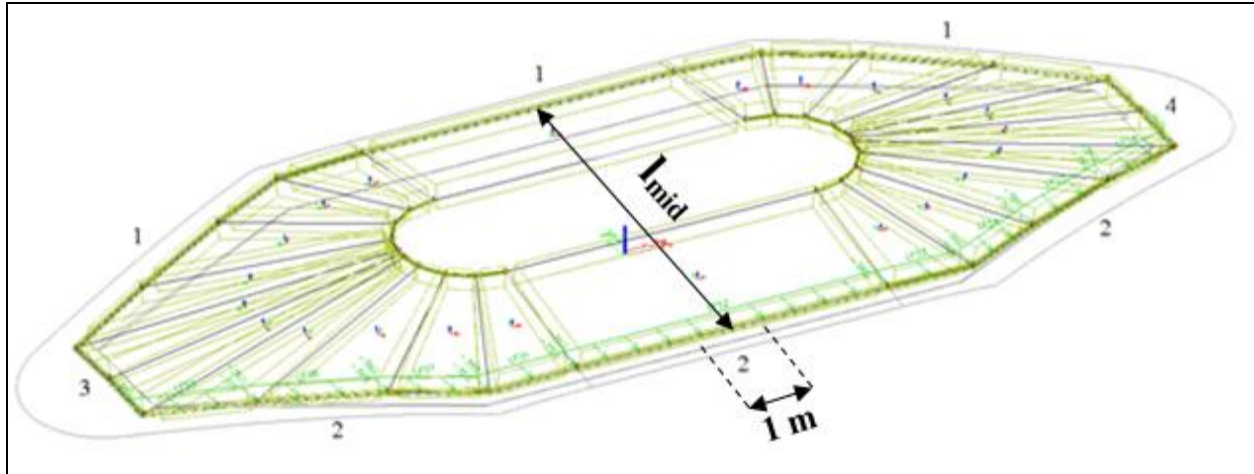


Figure 27: Equivalent beam model using 1 m strip at representative mid-section

▪ Normal stiffness EA

For determination of EA a 'unit force' $F = 360 \text{ kN/m}$ was applied along the circumference of line elements 2 as depicted in Figure 28. This resulted in a horizontal elongation $\Delta l = 1.79 \text{ mm}$. With

$$l_{mid} = 14.232 \text{ m it is found that: } EA = \frac{F \cdot l_{mid}}{\Delta l} = \frac{360 \times 14.232}{1.79 \cdot 10^{-3}} = 2.862 \times 10^6 \text{ kN/m'}$$

▪ Bending stiffness EI

For determination of EI two cases must be considered, in particular:

- 1-sided loading;
- 2-sided loading.

❖ EI: 1-sided loading

Only one diaphragm wall is loaded, represented by a unit moment $M = 1000 \text{ kNm/m'}$ at one side (along line elements 2) of the roof structure as depicted in Figure 29. This results in the angular rotations $\varphi_1 = 0.91 \text{ mrad}$ and $\varphi_2 = 3.79 \text{ mrad}$. For the 1-sided loaded equivalent beam the rotational stiffness

$$c = \frac{3EI}{l_{mid}} \text{ (see Figure 29c) . EI is then found from:}$$

$$c = \frac{3EI}{l_{mid}} \Leftrightarrow \frac{M}{\varphi_2} = \frac{3EI}{l_{mid}} \Leftrightarrow EI = \frac{M \cdot l_{mid}}{3 \cdot \varphi_2} = \frac{1000 \times 14.232}{3 \times 3.79 \cdot 10^{-3}} \Leftrightarrow EI = 1.252 \times 10^6 \text{ kNm}^2/\text{m'}$$
, with:

- An equivalent thickness of the roof structure of: $d_{eq} = \sqrt{\frac{12EI}{EA}} = 2.29 \text{ m}$ and;
- A rotational stiffness: $c = 2.64 \times 10^5 \text{ kNm/rad/m'}$.

❖ EI: 2-sided loading

Both diaphragm walls are loaded simultaneously, represented by a unit moment $M = 1000 \text{ kNm/m'}$ at both sides (along line elements 1 and 2) of the roof structure as depicted in Figure 30. This results in the angular rotations $\varphi_1 = 4.25 \text{ mrad}$ and $\varphi_2 = 4.71 \text{ mrad}$. For the 2-sided loaded equivalent beam the

rotational stiffness $c = \frac{2EI}{l_{mid}}$ (see Figure 30c). EI is then found from:

$$c = \frac{2EI}{l_{mid}} \Leftrightarrow \frac{M}{\varphi_2} = \frac{2EI}{l_{mid}} \Leftrightarrow EI = \frac{M \cdot l_{mid}}{2 \cdot \varphi_2} = \frac{1000 \times 14.232}{2 \times 4.71 \cdot 10^{-3}} \Leftrightarrow EI = 1.511 \times 10^6 \text{ kNm}^2/\text{m}', \text{ with:}$$

- An equivalent thickness of the roof structure of: $d_{eq} = \sqrt{\frac{12EI}{EA}} = 2.52 \text{ m}$ and;
- A rotational stiffness: $c = 2.12 \times 10^5 \text{ kNm/rad/m'}$.

For this research the 2-sided loaded structure is applicable, since both walls deform outwards simultaneously. Due to the loads on both walls, an extra deformation of the structure is obtained compared to the 1-sided loaded structure (Figure 29b vs. Figure 30b), resulting in a lower rotational stiffness. This is the most representative case, and therefore the EI determination for the equivalent beam model is based on the 2-sided loaded structure. Furthermore, it is found that d_{eq} for the equivalent beam model is higher than the actual thickness of the roof $d_{real} = 0.9 \text{ m}$. The explanation lies in the actual geometry of the roof; because of its upright conical shape it becomes more difficult to bend this than in case of a flat roof.

The EI-calculation for the equivalent beam model is based on a 2-sided loaded structure. This is the most representative, since it results in the lowest rotational stiffness (lowest resistance against deformation of the walls). The equivalent beam model has the following properties:

- $EA = 2.862 \times 10^6 \text{ kN/m'}$;
- $EI = 1.511 \times 10^6 \text{ kNm}^2/\text{m'}$;
- $d_{eq} = 2.52 \text{ m}$

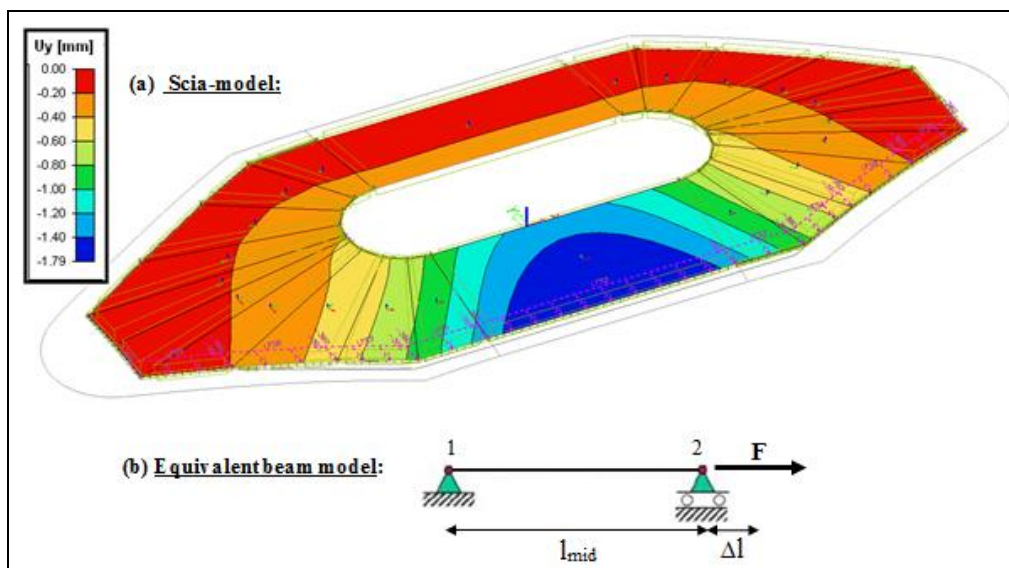


Figure 28: Determining EA

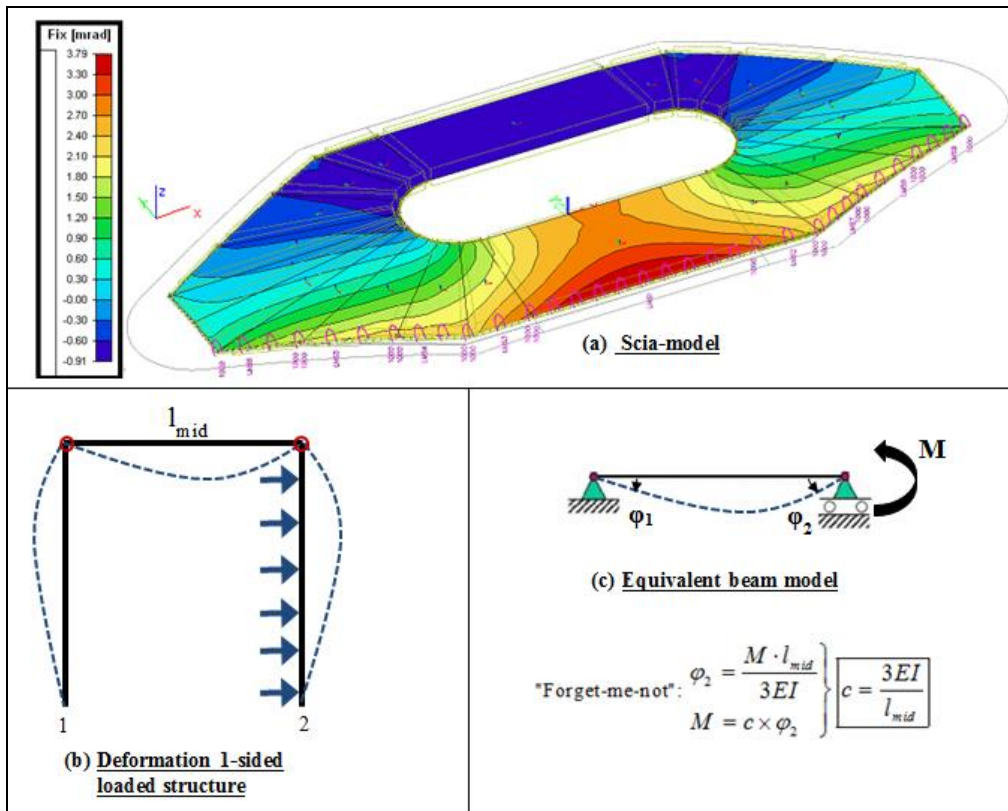


Figure 29: Determining EI for 1-sided loaded structure

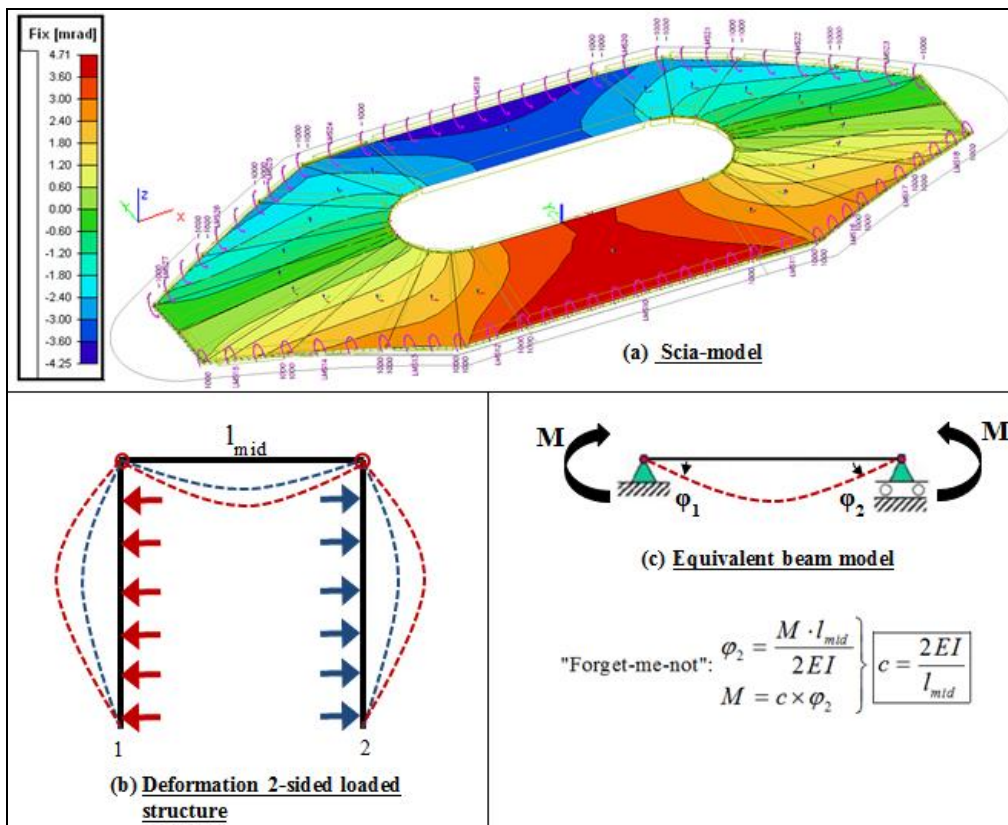


Figure 30: Determining EI for 2-sided loaded structure

3.6. Calculation strategy

The structure will be calculated with the following stiffnesses for the diaphragm wall:

- The totally uncracked stiffness: $EI_0 = 33000 \times I_g$;
- The totally cracked stiffness: $EI_\infty = 11000 \times I_g$;
- The variable stiffness EI_{var} .

The calculations with EI_{var} are required to determine whether or not the results obtained with this stiffness are lying within the results obtained with the outer boundaries EI_0 and EI_∞ . The diaphragm wall properties for EI_0 and EI_∞ are given in Table 16. The EI_{var} must be determined for each case using the M-(N)- κ diagram.

EI	E		EI	EA	$d_{equivalent}$
	[MPa]	[kN/m ²]			
EI_0	33000	3.30E+07	9.28E+06	4.95E+07	1.5
EI_∞	11000	1.10E+07	3.09E+06	1.65E+07	1.5

Table 16: Diaphragm wall properties for EI_0 and EI_∞

In this thesis the structural behaviour is expressed in terms of the bending moment (M_{Ed}), settlement (δ_v) and lateral wall displacement (U_x), which are calculated at the bending stiffnesses EI_0 , EI_∞ and EI_{var} as a function of both $N = 0$ kN and $N \neq 0$ kN. The structural behaviour will be investigated for the following calculation models using the representative loading case LC3:

- Walls only; hinged
- Walls and roof; hinged
- Walls only; clamped
- Walls and roof; clamped.

Calculations based on EI_{var} turned out to be an iterative procedure. In order to obtain the actual EI-distribution of the diaphragm walls, the reinforcement plays a major role in this research. With regard to the wall-roof connection two cases are considered:

- The hinged case, where determination of EI_{var} is based on a basic reinforcement of $\rho_{l,tot} = 0.6\%$ per meter panel width applied over the total wall height of 22.5 m;
- The clamped case, where the determination of EI_{var} will be based on a yet to be defined amount of reinforcement.

It needs to be noted that since the hinged connection was finally chosen for the execution of the “Waalbrug-project” the required amount of reinforcement was only calculated for the hinged case.

In order to reach the aimed results, a certain strategy is applied using the Half Model and Total Model in the calculation programs PCSheetPileWall and Plaxis 2D. The Half Model concerns the left wall with the braking forces on it. The intended purpose of each step of this strategy is as follows:

- PCSheetPileWall – Half Model :Use the EI-distribution (EI_{var}) as input in Plaxis;
- Plaxis 2D – Half Model :Validate EI-distribution (EI_{var}) from PCSheetPileWall by checking the M-line using an approximation for the actual EI-distribution;
- Plaxis 2D – Total Model :Find the EI-distribution for both walls. In the Half Models only the EI-distribution of the left wall is known. The calculations based on EI_{var} turn out to be an iterative procedure. Two iteration procedures are applied, which are explained for each case. By implementation of the final EI-distribution of both walls the aimed results are obtained.

4. RESULTS AND DISCUSSION

4.1. Walls only; hinged

This section deals with the impact of EI_{var} on the diaphragm walls only in case of a hinged wall-roof connection. In order to find a valid iteration procedure for calculations with EI_{var} , different strategies have been employed using the Half Model in PCSheetPileWall and the Half and Total Model in Plaxis 2D. Two cases will be considered for EI_{var} , namely:

- Case a with $EI(\kappa)$, where EI_{var} is determined using the M- κ diagram, and;
- Case b with $EI(\kappa, N)$, where EI_{var} is determined using the M-N- κ diagram.

4.1.1. Case a: EI (κ)

The determination of the calculation strategy for $EI(\kappa)$ will be explained step by step in this section.

4.1.1.1. PCSheetPileWall – Half Model

Consider both walls separately with their corresponding M-line and EI-distribution over the wall height for the representative loading combination - LC3 for the left wall and LC3,R for the right wall - as depicted in Figure 31 and Figure 32, respectively. The left wall (with the braking forces) is partially cracked, while the right wall remains uncracked. The bending stiffness of the left wall is characterized by the “EI-bite” in the cracked zone. According to Table 17, LC3 gives the largest cracked zone for the left wall (7.8 m), thereby distinguishing the following cracking pattern from the top to the bottom of the wall which is also shown in Figure 32: (1) uncracked zone, (2) cracked zone and (3) uncracked zone. For LC3 the cracked zone also starts earlier and ends later compared to LC2. LC1 and LC2 will not be considered further.

	Loading	Zone	Length [m]	
Left wall	LC1	1 Uncracked	22.5	
	LC2	1 Uncracked	3.6	
		2a	Cracked	5.5
		2b		
		2c		
	3 Uncracked	13.4		
	LC3	1 Uncracked	3.1	
		2a	Cracked	7.8
		2b		
		2c		
3 Uncracked	11.6			
Right wall	LC3, R	1 Uncracked	22.5	

Table 17: Cracked and uncracked zones of both walls for the considered loading combinations

The M- κ diagram for both walls, represented in Figure 33, is based on:

- A total reinforcement ratio of $\rho_{l,tot} = 0.6\%$ per meter width ($16\phi 32$ per side/2.8 m panel width);
- $N = 0$ kN ($N_{self\ weight} = 0$, $N_{shear\ force} = 0$)

The cracking moment $M_r = 1150$ kNm.

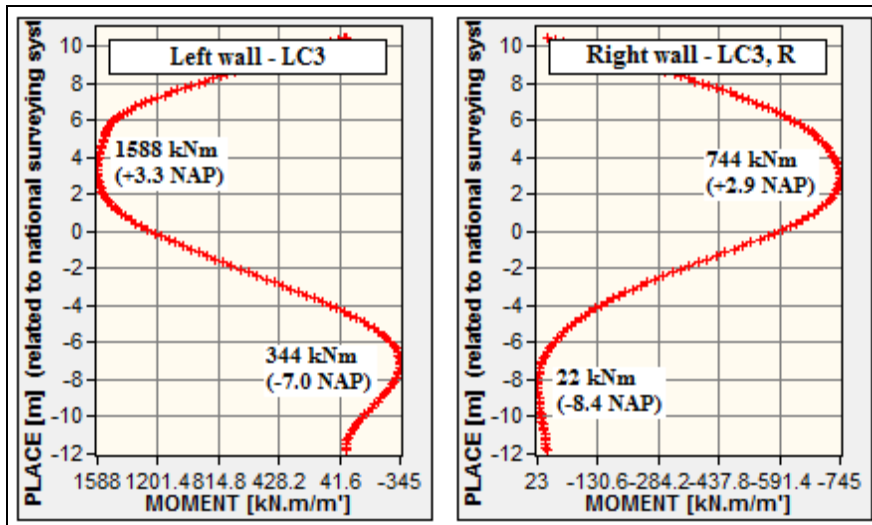


Figure 31: M-line both walls from PCSheetPileWall (hinged connection, N = 0 kN)

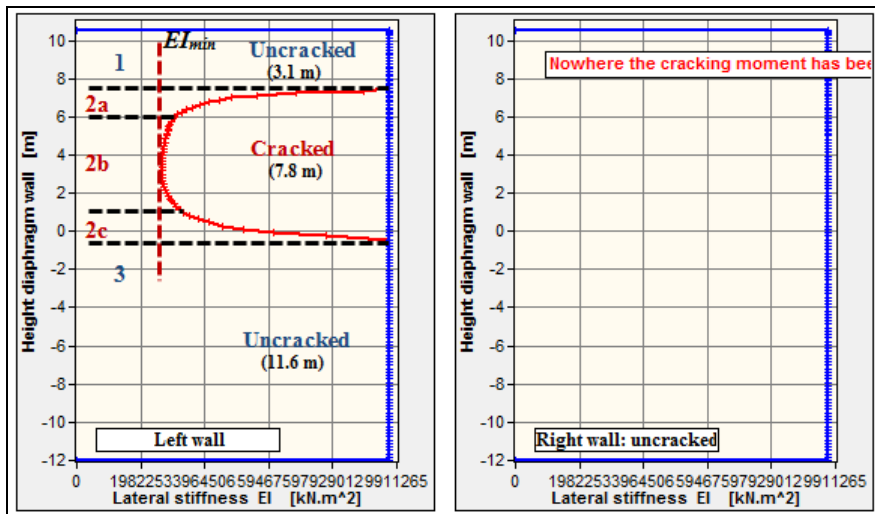


Figure 32: EI-distribution both walls from PCSheetPileWall. Left wall characterized by “EI-bite” in cracked zone.

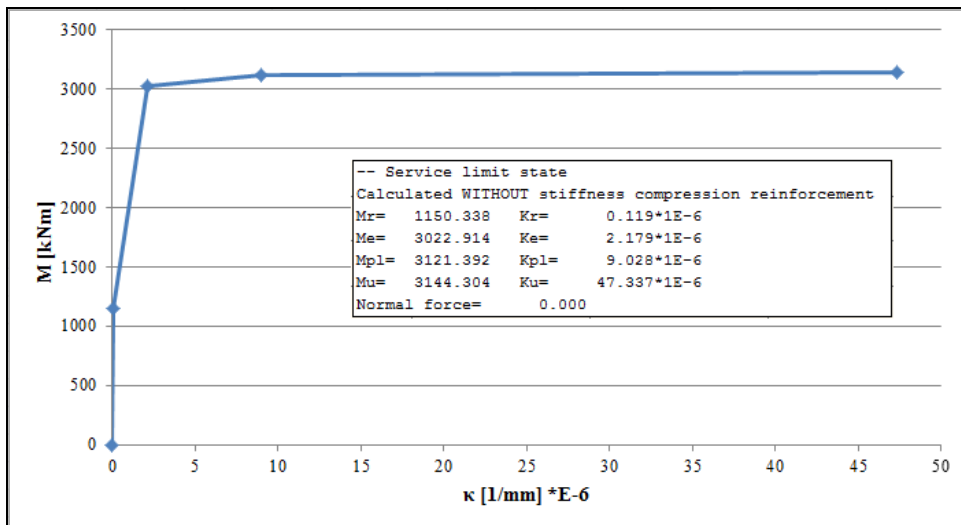


Figure 33: M-κ diagram both walls (hinged connection, N = 0 kN)

The EI-distribution of both walls is given in Table 18. Since it is impossible to implement the exact EI-distribution obtained from PCSheetPileWall into Plaxis 2D, the cracked zone of the left wall is split up into 3 sections (see Figure 32). Here an average EI-value is calculated for the sections 2a and 2c, and a minimum EI-value (EI_{\min}) for section 2b. This was the most reasonable partition for the cracked zone. The reason behind this is explained further in section 4.1.1.2.

In this research it is assumed that $E_{\text{uncracked}} = 33000$ MPa and $E_{\text{cracked}} = 11000$ MPa. From the calculations in PCSheetPileWall it is found that the E-modulus is higher in the uncracked zones (34381 MPa). This can be attributed to the contribution of the reinforcing steel, since $E_{\text{uncracked}} = 33000$ MPa includes only the E-modulus of plain concrete (without the reinforcement). According to PCSheetPileWall the E-modulus in the cracked zone is not always above the assumed $E_{\text{cracked}} = 11000$ MPa. In section 2b one finds a minimum E-modulus of 9407 MPa.

	Zone	Length	From	To	EI	EA	E	d_{eq}
		[m]	[m]	[m]	[kNm ² /m']	[kN/m']	[MPa]	[m]
Left wall	1	3.1	10.5	7.4	9.67E+06	5.16E+07	34381	1.5
	2a	1.4	7.4	6	4.71E+06	2.51E+07	16737	1.5
	2b	4.85	6	1.15	2.65E+06	1.41E+07	9407	1.5
	2c	1.55	1.15	-0.4	4.59E+06	2.45E+07	16316	1.5
	3	11.6	-0.4	-12	9.67E+06	5.16E+07	34381	1.5
Right wall	1	22.5	10.5	-12	9.67E+06	5.16E+07	34381	1.5

Table 18: EI-distribution of both walls obtained from PCSheetPileWall

4.1.1.2. Plaxis 2D – Half Model

The Plaxis 2D – Half Model is used to validate the EI-distribution of the left wall (half model) obtained from PCSheetPileWall. Therefore, the M-line of the Half Models is checked in both programs. The main input in Plaxis 2D consists of:

- The EI-distribution for the left wall according to Table 18;
- $w_{\text{plate}} = 0$ kN/m/m' for the diaphragm wall in order to simulate $N_{\text{self weight}} = 0$ in PCSheetPileWall;
- $R_{\text{inter}} = 1$ (no friction between soil and wall) in order to simulate $N_{\text{shear force}} = 0$ in PCSheetPileWall;
- Fixed-end anchor to simulate the hinged wall-roof connection (see Figure 34a).

In section 4.1.1.1 the cracked zone of the left wall is split up into 3 sections. However, the impact of a minimum EI-value and a weighted average EI-value over the total cracked zone of 7.8 m of the left wall has also been examined. By doing so it is checked which of these 3 approaches, with regard to the EI-distribution for the cracked zone of the left wall, gives the most reasonable results where the results (especially the M-line) with EI_{var} are expected to lie within the results obtained with EI_0 and EI_{∞} . The results are given in Table 19.

EI	δ_v [mm]	M_{max} [kNm/m']		U_x [mm]
		M_1	M_2	
EI_0	72	2190	140	-17
EI_{∞}	80	1780	410	-25
¹⁾ EI_{var} (cracked_3 sections)	79	1780	460	-24
²⁾ EI_{var} (cracked_minimum)	81	1740	510	-25
³⁾ EI_{var} (cracked_weighted average)	79	1850	405	-23

Table 19: Results for Plaxis 2D – Half Model, using 3 different approaches for the EI_{var} of the cracked zone

Clarification Table 19:

¹⁾ EI_{var} (cracked_3sections): The cracked zone of the left wall is split up into sections 2a, 2b and 2c of which the corresponding EI is given in Table 18.

²⁾ EI_{var} (cracked_minimum): A minimum EI-value of $EI_{min} = 2.65E+06 \text{ kNm}^2/\text{m}'$ is applied over the total cracked zone of 7.8 m of the left wall.

³⁾ EI_{var} (cracked_weighted average): A weighted average of $EI_{weighted} = 3.49E+06 \text{ kNm}^2/\text{m}'$ is applied over the total cracked zone of 7.8 m of the left wall.

Although the 3 approaches return results which are not differing a lot from each other, the EI_{var} (cracked_3 sections) is chosen as the safest approach. In case of EI_{var} (cracked_minimum) the total cracked zone is assumed to have a very low bending stiffness, which is not true. For EI_{var} (cracked_weighted average) the results lie perfectly in between the results of EI_0 and EI_{∞} , but this is not representative since there are sections with a lower EI than $EI_{weighted} = 3.49E+06 \text{ kNm}^2/\text{m}'$. The M-line obtained with the EI_{var} (cracked_3 sections) in Plaxis 2D is given in Figure 34b. Compared with PCSheetPileWall the difference in the maximum bending moment is about 12% (1780 vs. 1588 kNm).

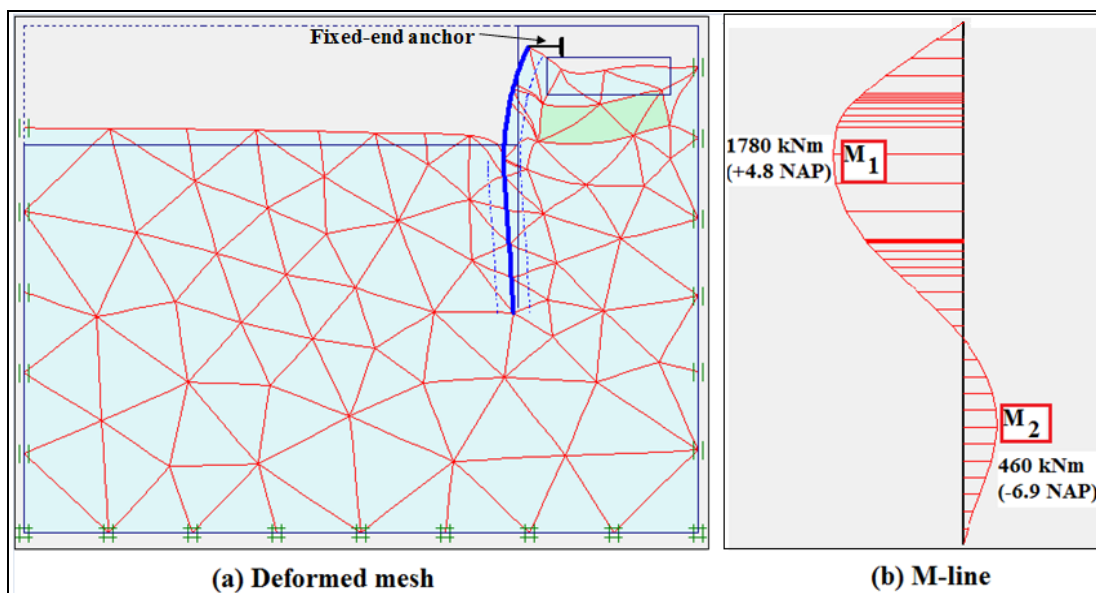


Figure 34: (a) Deformed mesh and (b) M-line of left wall for EI_{var} (cracked_3 zones) in Plaxis 2D – Half Model

Based on the results from the Half Model in PCSheetPileWall and Plaxis 2D, the following is observed:

- The M-line configuration in Plaxis 2D is in accordance with PCSheetPileWall, but there is a difference (12%) in the magnitude of the maximum bending moment for $N = 0 \text{ kN}$;
- This difference can be attributed to:
 - The approximation of the EI-distribution in the cracked zone (3 sections) obtained from PCSheetPileWall;
 - The different soil models: PCSheetPileWall is a discrete model, while Plaxis 2D is a continuous model;
 - No possibility of a 1-on-1 translation of the loading in both programs.

These findings lead to the following statement:

The EI-distribution for the left wall according to PCSheetPileWall is acceptable in Plaxis 2D. The approximation of the EI-distribution in the cracked zone of the left wall by means of 3 sections forms a safe approach.

4.1.1.3. Plaxis 2D – Total Model

With the validation of the EI-distribution for the left wall, the M-line and EI-distribution of the right wall also need to be checked with those according to PCSheetPileWall. This is done by means of the Plaxis 2D – Total Model. The main input in Plaxis 2D consists of:

- The EI-distribution for both walls according to Table 18. Note that the right wall is totally uncracked according to PCSheetPileWall;
- $w_{plate} = 0 \text{ kN/m/m}$ for both diaphragm walls in order to simulate $N_{self\ weight} = 0$;
- $R_{inter} = 1$ (no friction between soil and wall) in order to simulate $N_{shear\ force} = 0$;
- Node-to-node anchor to simulate the hinged wall-roof connection, where the bending stiffness of the roof structure itself has no impact on the diaphragm walls (see Figure 35a).

The M-line obtained from the Plaxis 2D – Total Model is depicted in Figure 35b, showing clearly that the right wall is more heavily loaded than the left wall. This phenomenon can be attributed to the fact that when in Plaxis 2D the left wall (with the braking forces on it) moves sideways, the right wall is pulled along with it, creating an extra load on the right wall. This is not taken into account in PCSheetPileWall. Since both walls have the same M- κ diagram the cracking moment for the right wall is also equal to $M_r = 1150 \text{ kNm}$, implying that in contrast to PCSheetPileWall, the right wall is cracked. Based on these findings it can be stated that:

The EI-distribution for the right wall according to PCSheetPileWall is not valid. In order to find the cracked height and the actual EI-distribution for the right wall an iteration procedure is required.

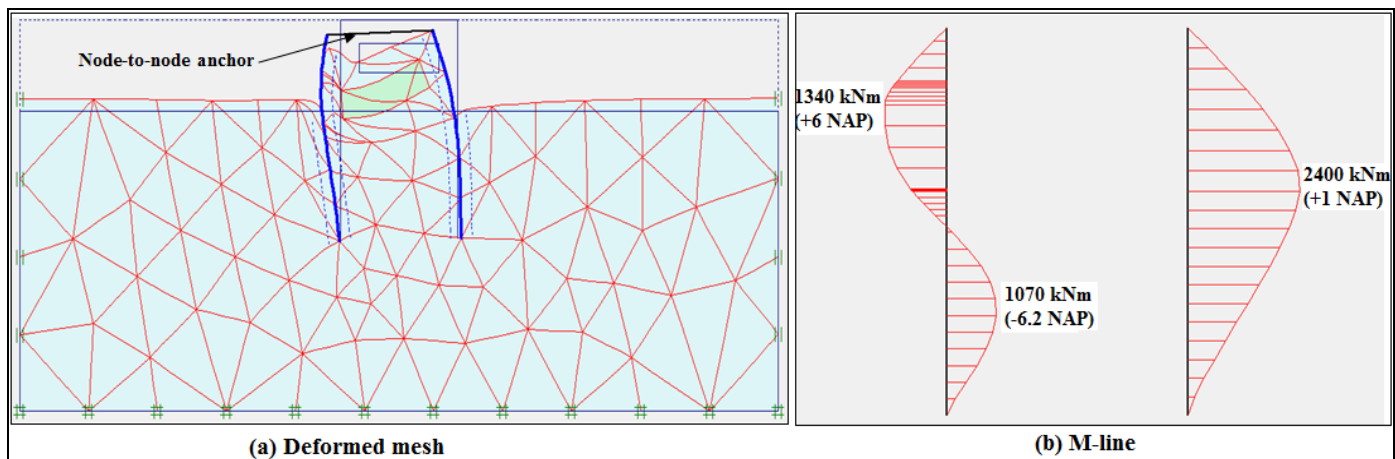


Figure 35: Hinged case - (a) Deformed mesh and (b) M-line for the walls only at $N = 0 \text{ kN}$

4.1.1.4. Iteration procedure 1 – right wall

Iteration procedure 1 is conducted to find the cracked height and the corresponding EI-distribution of the right wall. The following assumptions were made for:

- The left wall: The EI-distribution according to PCSheetPileWall will be maintained with each iteration (see Table 18);
- The right wall: The 1st assumption is that the right wall is totally uncracked, thereby using the uncracked stiffness according to PCSheetPileWall (see Table 18).
- Number of iterations: The iteration process for the right wall will go on until the cracked height remains the same. A difference of 5% is acceptable;

Since the M- κ diagram (from PCSheetPileWall) and the M-line of the right wall (from Plaxis 2D – Total Model) are known, the cracked height and the corresponding EI can be found at every iteration step. For the cracked zone of the right wall the following must be taken into account, with regard to:

- **The height of the cracked zone (l_{cracked}):** This will be obtained from Plaxis 2D. Since the M-line and the M- κ diagram (cracking moment) are known, the cracked height can be determined: if $M_{\text{Ed}} > M_{\text{cr}}$ the section is cracked;
- **The EI of the cracked zone ($(EI)_{\text{Ed,min}}$):** For the EI of the cracked zone the highest occurring moment in the cracked area of the right wall ($M_{\text{Ed,max}}$) is taken as point of departure. Based on $M_{\text{Ed,max}}$ the EI is determined from the M- κ diagram by means of interpolation. It concerns the lowest EI of the cracked area: $(EI)_{\text{Ed,min}}$. Actually, just as for the left wall one should divide the cracked area into more zones for a more reasonable result. Since it was found that refining the cracked area did not influence $M_{\text{Ed,max}}$ that much (2-3%), the $(EI)_{\text{Ed,min}}$ will be applied over the total cracked area. This is a safe approach.

The iteration process for the right wall consists of the following steps:

1. Start with the uncracked stiffness of the right wall. This results in a certain M-line with the corresponding l_{cracked} . Based on $M_{\text{Ed,max}}$ the $(EI)_{\text{Ed,min}}$ is calculated and maintained for the total l_{cracked} ;
2. This l_{cracked} with its corresponding $(EI)_{\text{Ed,min}}$ will be entered in the next iteration, which will result in another M-line. From this new M-line, a new l_{cracked} with its corresponding $(EI)_{\text{Ed,min}}$ (based on the new $M_{\text{Ed,max}}$) can be determined;
3. Repeat step 2 until the l_{cracked} remains constant. For all the iterations, reference is made to Appendix C1.

An overview of the iteration results for the right wall is given in Table 20, observing a jump between the even and uneven iterations with regard to the $M_{\text{Ed,max}}$ and l_{cracked} . For the uneven iterations the l_{cracked} decreases, while for the even iterations the l_{cracked} increases. But at a certain point the iteration procedure cannot go on and the results of one iteration step are equal to another. In this case iteration # 11 and 12 are equal to iteration # 13 and 14, respectively. The l_{cracked} lingers between 7.9 m and 10.9 m. For both the even and uneven iterations the $M_{\text{Ed,max}}$ is plotted against the l_{cracked} in Figure 36. Failed attempts to generate the actual value for $M_{\text{Ed,max}}$ and l_{cracked} with the computer lead to the following assumption:

If the 'average result' in the middle of both graphs (average of l_{cracked} and $M_{\text{Ed,max}}$) in Figure 36 is chosen as input in Plaxis 2D, the result obtained for the right wall in Plaxis 2D must be equal to the 'average result'.

	$M_{\text{Ed,max}}$	$(EI)_{\text{Ed,min}}$	EA	l_{cracked}
Iteration #	[kNm]	[kNm ² /m']	[kN/m']	[m]
1	2400	1.61E+06	8.57E+06	12.2
2	1390	3.63E+06	1.94E+07	6
3	2050	1.85E+06	9.86E+06	11.9
4	1470	3.12E+06	1.67E+07	6.9
5	1930	1.98E+06	1.05E+07	11.6
6	1520	2.89E+06	1.54E+07	7.4
7	1850	2.08E+06	1.11E+07	11
8	1560	2.74E+06	1.46E+07	7.8
9	1820	2.13E+06	1.13E+07	10.8
10	1570	2.70E+06	1.44E+07	8
11	1830	2.11E+06	1.13E+07	10.9
12	1560	2.74E+06	1.46E+07	7.9
13	1830	2.11E+06	1.13E+07	10.9
14	1560	2.74E+06	1.46E+07	7.9
FINAL	1695	2.36E+06	1.26E+07	9.4

Table 20: Results iteration process right wall for N = 0 kN - hinged connection

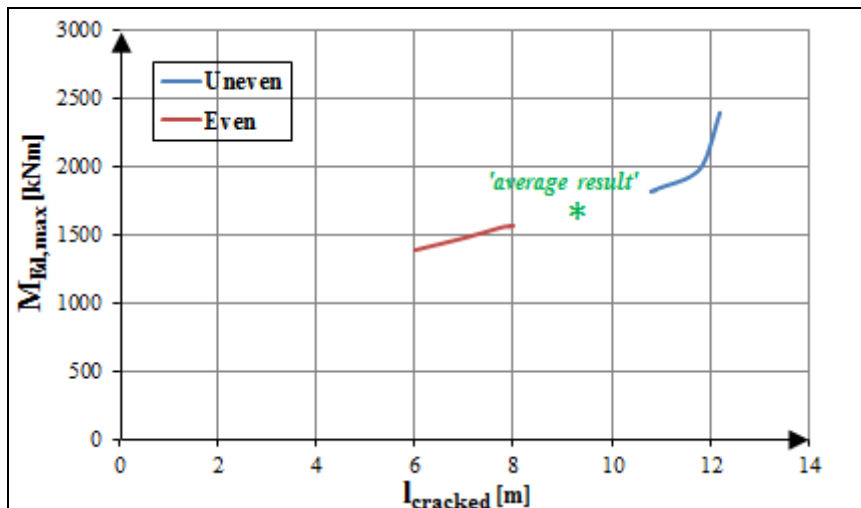


Figure 36: Results for even and uneven iterations of right wall for $N = 0$ kN

▪ Validity 'average result' assumption for right wall

In order to check the validity of the 'average result' assumption the next steps are taken, considering the last even and uneven iteration step where the iteration process stops.

1. Determine the average and the course of $l_{cracked}$;
2. Determine the average of $M_{Ed,max}$ and the corresponding EI and EA;
3. Use the above-mentioned input ($l_{cracked}$, EI and EA) for the right wall in the Plaxis 2D - Total Model and check the result.

Step 1:

Figure 37 shows the M-line and the cracked height of the right wall belonging to the iterations #13 and #14. From this one can determine the:

- Average cracked height: $l_{cr,av} = 0.5 \times (10.9 + 7.9) = 9.4$ m;
- Course of cracked height: starting at $0.5 \times (6.5 + 6) = 6.2$ m and ending at $0.5 \times (-4.4 + -1.9) = -3.2$ m with regard to NAP-level.

Step 2:

The average $M_{Ed,max}$ is equal to: $0.5 \times (1830 + 1560) = 1695$ kNm. From interpolation in the M- κ diagram it is found that $(EI)_{Ed,min} = 2.36E+06$ kNm²/m' with a corresponding $EA = 1.26E+07$ kN/m'.

The average calculated values at step 1 and step 2 have also been given in Table 20 for the final iteration. These values will now be used as input for the right wall in the Plaxis 2D – Total Model.

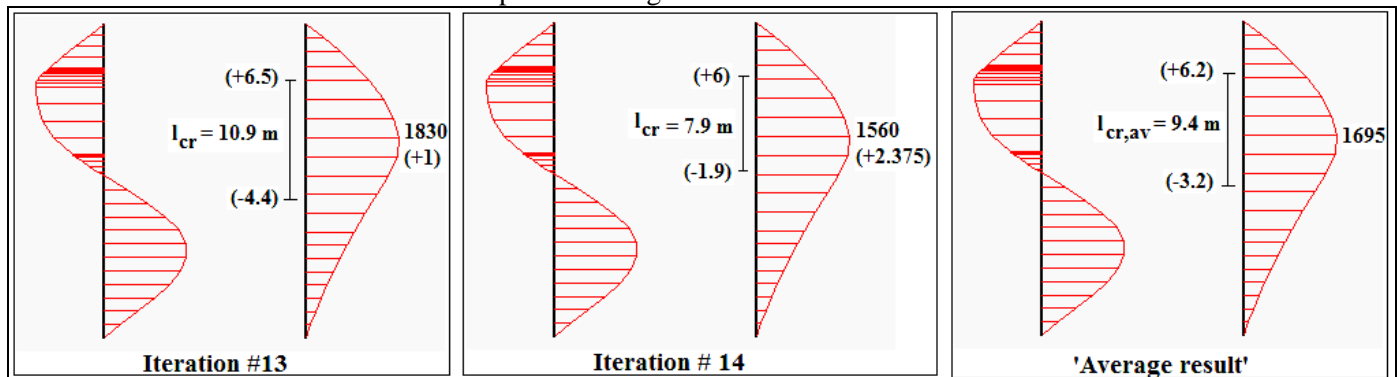


Figure 37: The assumed 'average result' for the right wall based on iteration #13 and #14.

(Note: Bending moment values in kNm and levels with regard to NAP are placed between brackets)

Step 3:

For a good overview, the input in the Plaxis 2D – Total Model for both walls is given in Table 21. Note that the EI-distribution for the left wall is according to PCSheetPileWall, while the EI-distribution for the right wall is based on the assumed ‘average result’ following from the even and uneven iterations. This input results in Figure 38. On comparison of the assumed ‘average result’ in Figure 37 and the Plaxis-result in Figure 38 there appears to be hardly any difference (see Table 22). Based on these findings it can be concluded that:

For an iteration procedure which comes to a standstill after a number of iterations: By implementing the assumed ‘average result’ from the last even and uneven iteration as input in the Plaxis 2D – Total Model, one finds a method which converges for the right wall.

	Zone	Cracked/ uncracked	Length	From	To	EI	EA
			[m]	[m]	[m]	[kNm ² /m']	[kN/m']
Left wall <i>(from PCSheet-PileWall)</i>	1	uncracked	3.1	10.5	7.4	9.67E+06	5.16E+07
	2a	cracked	1.4	7.4	6	4.71E+06	2.51E+07
	2b		4.85	6	1.15	2.65E+06	1.41E+07
	2c	uncracked	1.55	1.15	-0.4	4.59E+06	2.45E+07
	3		11.6	-0.4	-12	9.67E+06	5.16E+07
Right wall <i>(from 'average result' iterations)</i>	1	uncracked	4.3	10.5	6.2	9.67E+06	5.16E+07
	2	cracked	9.4	6.2	-3.2	2.36E+06	1.26E+07
	3	uncracked	8.8	-3.2	-12	9.67E+06	5.16E+07

Table 21: EI-distribution for both walls used as input in Plaxis 2D – Total Model for iteration procedure 1

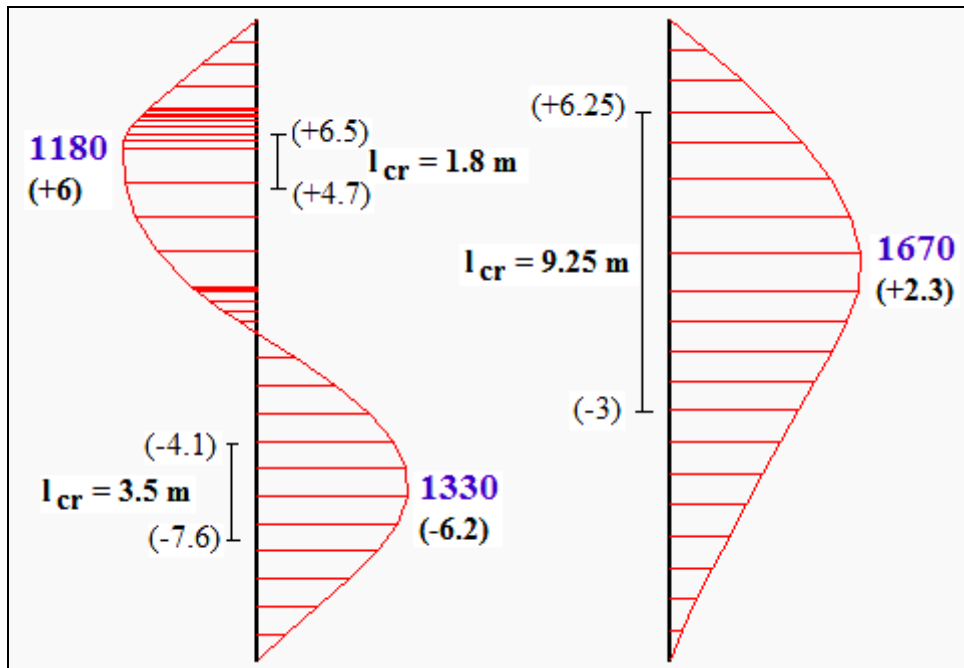


Figure 38: Final result EI_{var} according to iteration procedure 1 in Plaxis 2D – Total Model. (Note: Bending moment values in kNm and levels with regard to NAP are placed between brackets)

	Assumed 'average result'	Plaxis- result	Difference	Check
l_{cracked} [m]	9.4	9.25	-2%	OK!
$M_{\text{right wall}}$ [kNm/m']	1695	1670	-1%	OK!

Table 22: Comparison of the assumed 'average result' and the Plaxis-result for the right wall

4.1.1.5. Problem left wall

Summarizing the process from the beginning till this point, the following steps have been taken:

- Maintain the EI-distribution according to PCSheetPileWall of the cracked left wall ("EI-bite") and the uncracked right wall for further calculations in Plaxis 2D;
- When from the Plaxis 2D – Total Model it turns out that the right wall is also cracked, the iteration procedure 1 is set up to find the actual EI-distribution and cracked zones of the right wall. The EI-distribution of the left wall according to PCSheetPileWall is maintained here;
- After finding the l_{cracked} and M-line of the right wall with the converging iteration procedure 1, it is now found that the left wall cracks differently than initially assumed.

According to Figure 38 the left wall is found to be cracked over 2 different sections at the top (1.8 m) and the bottom (3.5 m) of the wall after an intensive iteration procedure for the right wall. This is in contradiction with the result from PCSheetPileWall where the left wall is cracked over 1 section (7.8 m). Because of these different cracked zones (see Figure 39) it can be concluded that the EI-distribution of the left wall in Plaxis 2D is not in accordance with the 1st assumed EI-distribution of the left wall from PCSheetPileWall. As a result of the wall movement, the EI-distribution of the left wall has also changed. Based on these findings it can be stated that:

In all probability it concerns a back-and-forth iteration process between the left and right wall.

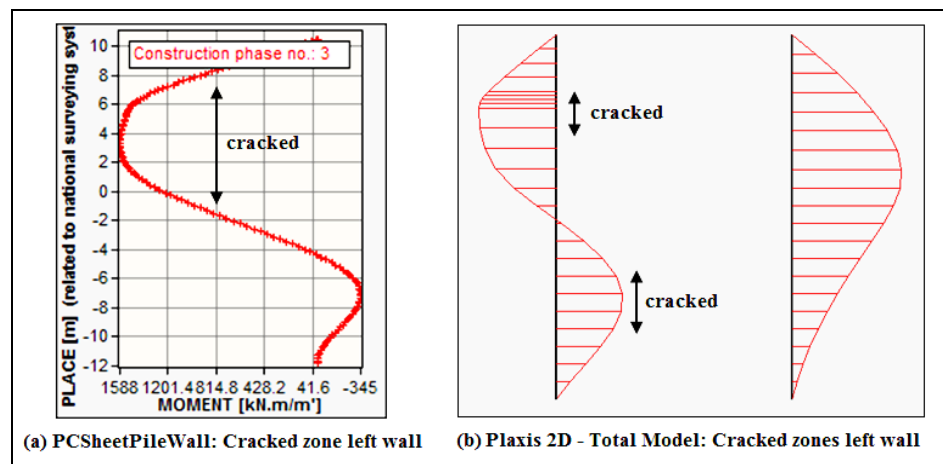


Figure 39: Contradicting cracked zones for the left wall

The research question arising at this point is:

Are the results following from iteration procedure 1 valid for EI_{var} ?

In order to investigate this matter further a new strategy, the so-called iteration procedure 2, is devised. This is dealt with in section 4.1.1.6.

4.1.1.6. Iteration procedure 2 – both walls

Iteration procedure 2 is set up to verify the final result of iteration procedure 1. The applied strategy here is as follows:

- Do not use the EI-distribution from PCSheetPileWall as input;
- Estimate the M-line and cracked zones of both walls based on the results with EI_0 and EI_∞ . The behaviour at the outer boundaries is a known fact and the actual behaviour of the structure is assumed to lie in between;
- Check the results with those of iteration procedure 1, for whether or not the same pattern for the M-line and $l_{cracked}$ have been obtained.

Iteration procedure 2, steps (for both walls):

1. Determine the average M-line and the average $l_{cracked}$ from EI_0 and EI_∞ . This is depicted as the ‘average result’ in Figure 40.
2. Based on the average bending moment, the EI and EA are determined for the average $l_{cracked}$. The EI is determined by means of interpolation in the M- κ diagram ($M_{cr} = 1150$ kNm). The input in the Plaxis 2D – Total Model for the left and the right wall are given in Table 23. This input results in Figure 41.

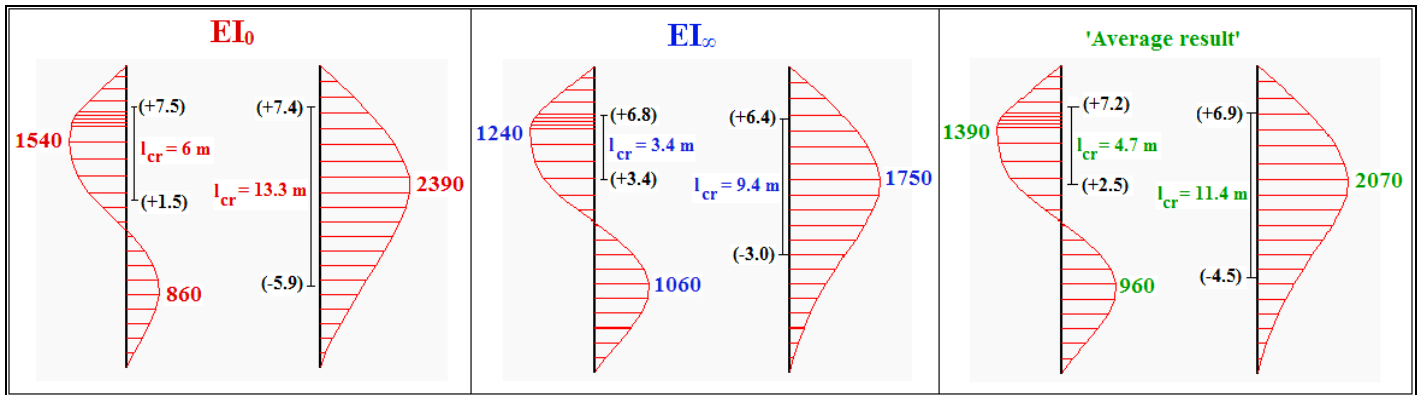


Figure 40: The ‘average result’ based on EI_0 and EI_∞ .
 (Note: Bending moment values in kNm and levels with regard to NAP are placed between brackets)

	Zone	Cracked/ uncracked	Length	From	To	$M_{Ed,average}$ [kNm/m']	EI [kNm ² /m']	EA [kN/m']
			[m]	[m]	[m]			
Left wall	1	uncracked	3.3	10.5	7.2	-	9.67E+06	5.16E+07
	2	cracked	4.7	7.2	2.5	1390	3.63E+06	1.94E+07
	3	uncracked	14.5	2.5	-12	-	9.67E+06	5.16E+07
Right wall	1	uncracked	3.6	10.5	6.9	-	9.67E+06	5.16E+07
	2	cracked	11.4	6.9	-4.5	2070	1.83E+06	9.76E+06
	3	uncracked	7.5	-4.5	-12	-	9.67E+06	5.16E+07

Table 23: EI-distribution for both walls used as input in Plaxis 2D – Total Model for iteration procedure 2

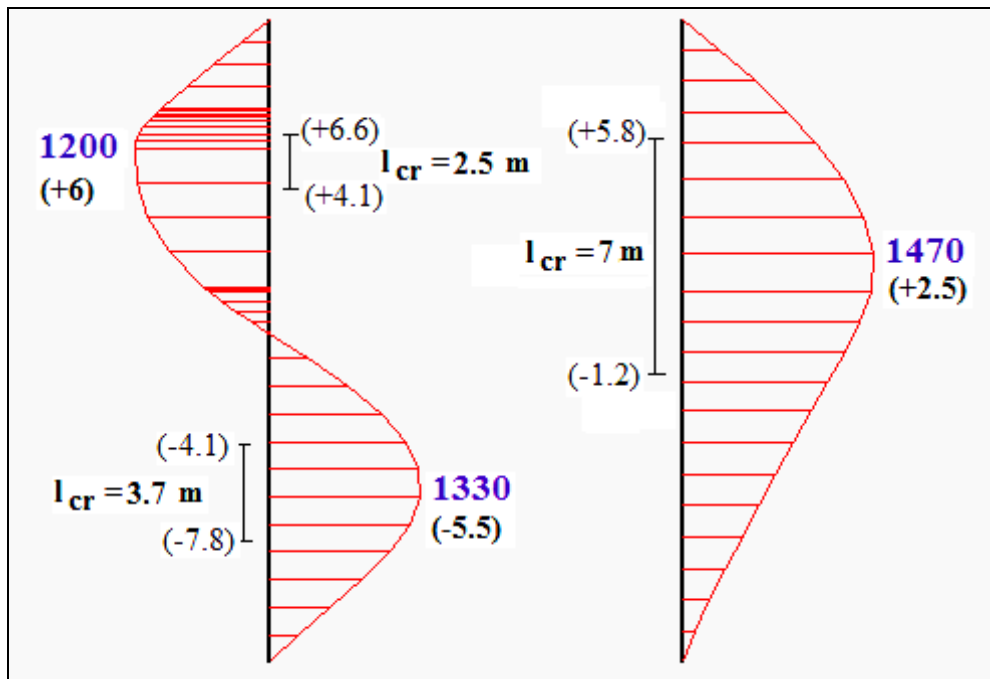


Figure 41: Final result EI_{var} according to iteration procedure 2 in Plaxis 2D – Total Model.
(Note: Bending moment values in kNm and levels with regard to NAP are placed between brackets)

Results iteration procedure 1 vs. iteration procedure 2:

On comparison of the final result according to iteration procedure 1 and iteration procedure 2 (Figure 38 vs. Figure 41) it can be stated that the points of departure for procedure 2 with regard to the *cracked zones* are obviously more reliable compared to procedure 1. For iteration procedure 2 only one iteration is required for both walls to get the same cracking pattern and M-line configuration as with iteration procedure 1. With iteration procedure 1 an intensive iteration process was required for the right wall only, after which the EI-distribution of the left wall was still not ensured. In all probability, many more iterations are required to reach the same result as of iteration procedure 2. Based on these findings it can be stated that:

The results of iteration procedure 2 are valid for EI_{var} .

4.1.1.7. Final results EI (κ)

The M-line of both walls for EI_0 , EI_∞ and EI_{var} is given in Figure 42. The reported values in Table 24 concern the maximum values for the occurring bending moment (M_{Ed}), the settlement (δ_v) and the lateral wall displacement (U_x). Based on these results the following conclusions can be drawn:

- The right wall (without braking forces on it) is the most heavily loaded wall for EI_0 , EI_∞ and EI_{var} . In all 3 cases the representative bending moment is the field moment of the right wall;
- The right wall has the largest lateral displacement (in the direction of the braking force) for EI_0 , EI_∞ and EI_{var} ;
- The results with EI_{var} are not lying within the results of the outer boundaries EI_0 and EI_∞ :
 - δ_v and U_x are higher than expected;
 - The M_{Ed} -values are even lower than expected, except for the bottom part of the left wall where $M_{Ed} = 1330$ kNm.

Explanation more heavily loaded bottom part of left wall for EI_{var} :

Large displacements cause large shear stresses in the soil, by which the soil comes into action and takes over the load. For both EI_0 and EI_∞ the left wall is more heavily loaded at the top, while for EI_{var} the wall is more heavily loaded at the bottom. For EI_0 a smaller wall displacement will occur due to the relatively high EI, resulting in smaller shear stresses in the soil and thus a smaller contribution of the soil in taking up the load. For EI_0 the load is mainly carried by the wall. The opposite holds for EI_∞ . Due to the relatively low EI, a higher wall displacement will occur, resulting in higher shear stresses in the soil and thus a higher contribution of the soil in taking up the load. For EI_∞ the wall is less loaded, while the soil carries a greater part of the load. *The reason for the more heavily loaded bottom part of the left wall for EI_{var} lies in the mutual relationship between the wall stiffness (EI) and the soil stiffness:*

- *Low stiffness at the top:* Due to the cracked zone (lower EI) and the lower stress-level in the soil (lower soil stiffness) at the top part of the wall, less load can be carried at the top of the wall. As a result, the load will have to be transferred to a more rigid part of the wall;
- *High stiffness at the bottom:* Because of the increased depth, a higher soil stiffness is present at the bottom part of the wall. Therefore, in spite of the cracked zone in the wall at the bottom part, the combination soil-wall in its entirety behaves more rigid which makes it possible to take up more load at the bottom of the wall.

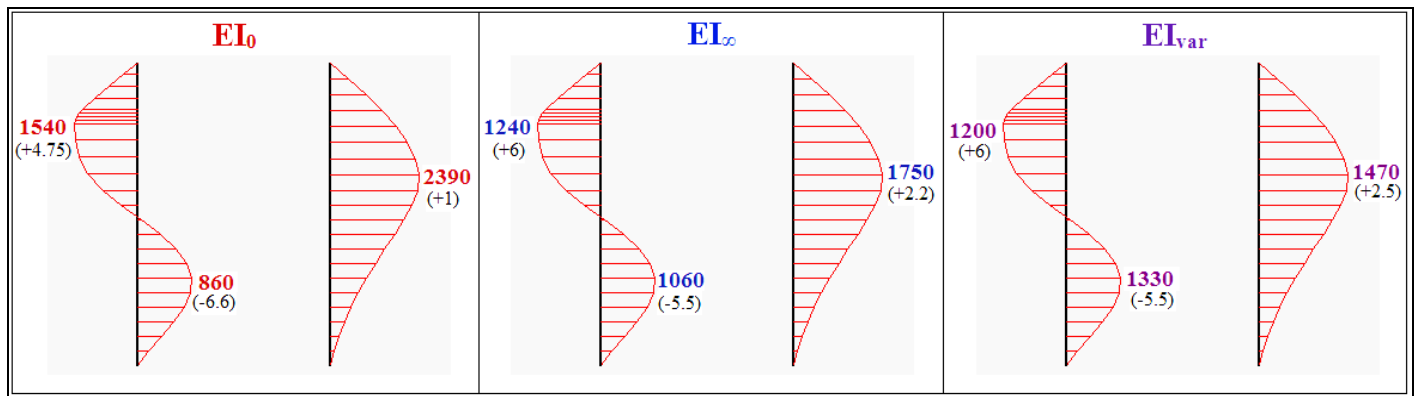


Figure 42: Hinged case – The M-line for EI_0 , EI_∞ and EI_{var} for $N= 0$ kN
(Note: Bending moment values in kNm and levels with regard to NAP are placed between brackets)

	M_{Ed} [kNm/m']	δ_v [mm]	U_x [mm]	
			Left wall	Right wall
EI_0	2390	91	-44	-62
EI_∞	1750	112	-64	-85
EI_{var}	1470	118	-69	-92

Table 24: Hinged case - Final results for EI_0 , EI_∞ and EI_{var} for $N= 0$ kN

4.1.2. Case b: EI (κ , N)

The determination of the calculation strategy for EI (κ , N) is found to be similar as for EI (κ). The only difference now is that an axial force is included in determining the bending stiffness of the diaphragm wall. Therefore, this section presents the relevant results without going into too much detail. If necessary, reference will be made to section 4.1.1 for detailed explanation.

4.1.2.1. PCSheetPileWall – Half Model

Consider both walls separately with their corresponding M-line and EI-distribution over the wall height as depicted in Figure 43 and Figure 44, respectively. The left wall (with the braking forces) is partially cracked, while the right wall remains uncracked. According to Table 25, LC3 gives the largest cracked zone for the left wall (7.3 m), thereby distinguishing the following cracking pattern from the top to the bottom of the wall which is also shown in Figure 44: (1) uncracked zone, (2) cracked zone and (3) uncracked zone.

	Loading	Zone	Length [m]	
Left wall	LC1	1 Uncracked	22.5	
	LC2	1 Uncracked	3.6	
		2a	Cracked	5.0
		2b		
		2c		
	3 Uncracked	13.9		
	LC3	1 Uncracked	3.25	
		2a	Cracked	7.3
		2b		
		2c		
3 Uncracked	11.95			
Right wall	LC3, R	1 Uncracked	22.5	

Table 25: Cracked and uncracked zones of both walls for the considered loading combinations

The M-N- κ diagram for both walls, represented in Figure 45, is based on:

- A total reinforcement ratio of $\rho_{l,tot} = 0.6\%$ per meter width (16 ϕ 32 per side/2.8 m panel width);
- $N = N_{self\ weight} = -810\text{ kN/m}'$ ($b \times d \times \gamma_{concrete} = 1 \times 1.5 \times 24$)
- $N_{shear\ force} = 0$

The cracking moment $M_r = 1351\text{ kNm}$.

Since it is impossible to implement the exact EI-distribution obtained from PCSheetPileWall into Plaxis 2D, the cracked zone of the left wall in Figure 44 is split up into 3 sections similarly as for EI (κ). For the mid-section of the cracked zone (section 2b) a minimum EI-value (EI_{min}) is applied with a corresponding E-modulus of 10539 MPa which is below the assumed $E_{cracked} = 11000\text{ MPa}$. An average EI-value is calculated for the sections 2a and 2c. The EI-distribution of both walls is given in Table 26.

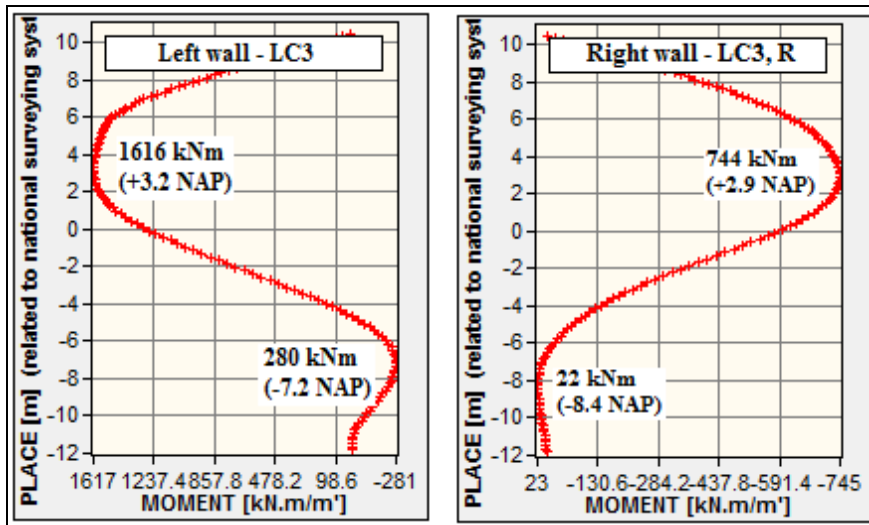


Figure 43: M-line both walls from PCSheetPileWall (hinged connection, $N \neq 0$ kN)

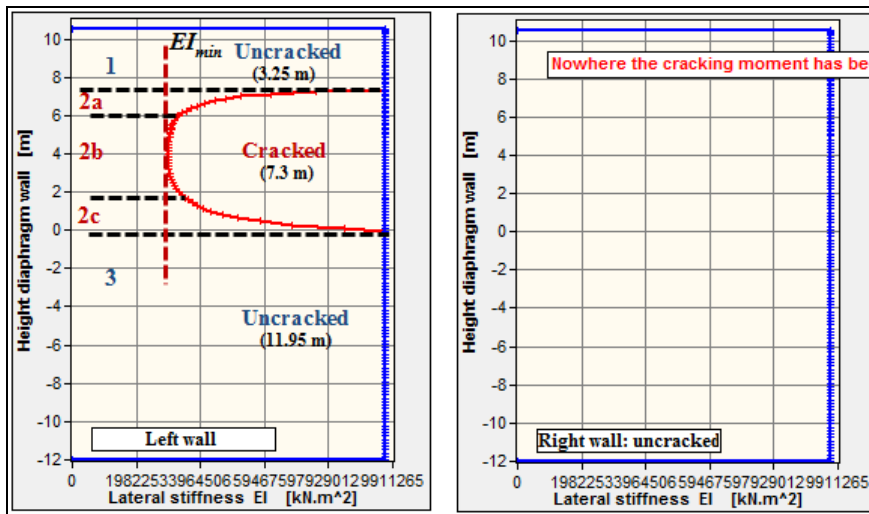


Figure 44: EI-distribution both walls from PCSheetPileWall. Left wall characterized by “EI-bite” in cracked zone.

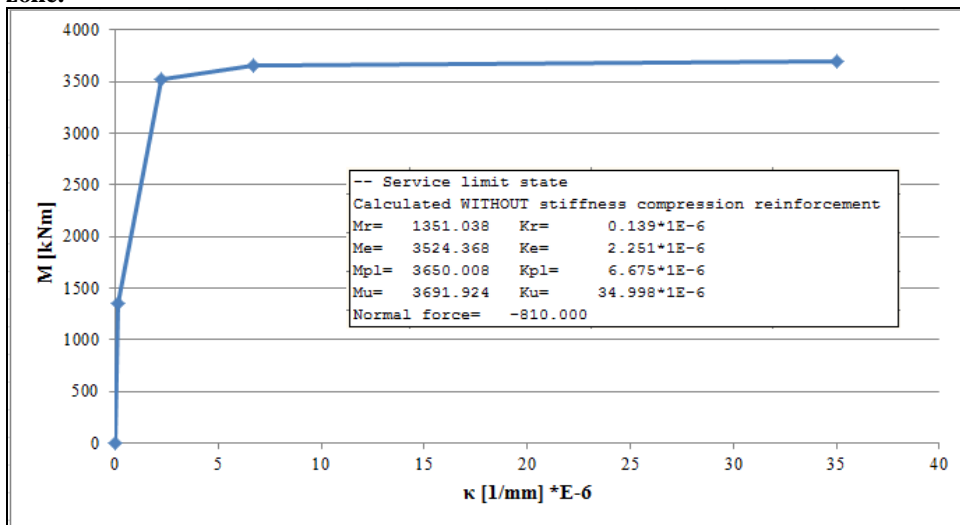


Figure 45: M-N- κ diagram both walls (hinged connection, $N \neq 0$ kN)

	Zone	Length	From	To	EI	EA	E	d _{eq}
		[m]	[m]	[m]	[kNm ² /m']	[kN/m']	[MPa]	[m]
Left wall	1	3.25	10.5	7.25	9.67E+06	5.16E+07	34381	1.5
	2a	1.25	7.25	6	4.66E+06	2.49E+07	16580	1.5
	2b	4	6	2	2.96E+06	1.58E+07	10539	1.5
	2c	2.05	2	-0.05	4.65E+06	2.48E+07	16517	1.5
	3	11.95	-0.05	-12	9.67E+06	5.16E+07	34381	1.5
Right wall	1	22.5	10.5	-12	9.67E+06	5.16E+07	34381	1.5

Table 26: EI-distribution of both walls obtained from PCSheetPileWall

4.1.2.2. Plaxis 2D – Half Model

The Plaxis 2D – Half Model is used to validate the EI-distribution of the left wall (half model) obtained from PCSheetPileWall. Therefore, the M-line of the Half Models is checked in both programs. The main input in Plaxis 2D consists of:

- The EI-distribution for the left wall according to Table 26;
- $w_{plate} = 23 \text{ kN/m/m'}$ for the diaphragm wall in order to simulate $N_{self\ weight} \neq 0$ in PCSheetPileWall;
- $R_{inter} = 1$ (no friction between soil and wall) in order to simulate $N_{shear\ force} = 0$ in PCSheetPileWall;
- Fixed-end anchor to simulate the hinged wall-roof connection (see Figure 46a).

In section 4.1.2.1 the cracked zone of the left wall is split up into 3 sections. Just like in the former case with $EI(\kappa)$, the impact of a minimum EI-value and a weighted average EI-value over the total cracked zone of 7.3 m of the left wall has also been examined. The results obtained with these 3 approaches for EI_{var} are given in Table 27. The results (especially the M-line) are expected to lie within the results obtained with EI_0 and EI_{∞} .

EI	δ_v [mm]	M_{max} [kNm/m']		U_x [mm]
		M_1	M_2	
EI_0	77	2300	60	-18
EI_{∞}	85	1810	330	-25
¹⁾ EI_{var} (cracked_3 sections)	84	1950	270	-24
²⁾ EI_{var} (cracked_minimum)	85	1880	350	-25
³⁾ EI_{var} (cracked_weighted average)	82	1940	270	-22

Table 27: Results for Plaxis 2D – Half Model, using 3 different approaches for the EI_{var} of the cracked zone

Clarification Table 27:

¹⁾ EI_{var} (cracked_3sections): The cracked zone of the left wall is split up into sections 2a, 2b and 2c of which the corresponding EI is given in Table 26.

²⁾ EI_{var} (cracked_minimum): A minimum EI-value of $EI_{min} = 2.96E+06 \text{ kNm}^2/\text{m'}$ is applied over the total cracked zone of 7.3 m of the left wall.

³⁾ EI_{var} (cracked_weighted average): A weighted average of $EI_{weighted} = 3.81E+06 \text{ kNm}^2/\text{m'}$ is applied over the total cracked zone of 7.3 m of the left wall.

Based on the same reasoning as given in case of $EI(\kappa)$ in section 4.1.1.2, the EI_{var} (cracked_3 sections) is chosen as the safest approach. The deformed mesh and the M-line for the left wall obtained with EI_{var} (cracked_3 sections) in Plaxis 2D are given in Figure 46. Compared with PCSheetPileWall the M-line

configuration is the same but then with a difference in the maximum bending moment of about 21% (1950 vs. 1616 kNm). The difference can be attributed to the same reasons listed in section 4.1.1.2.

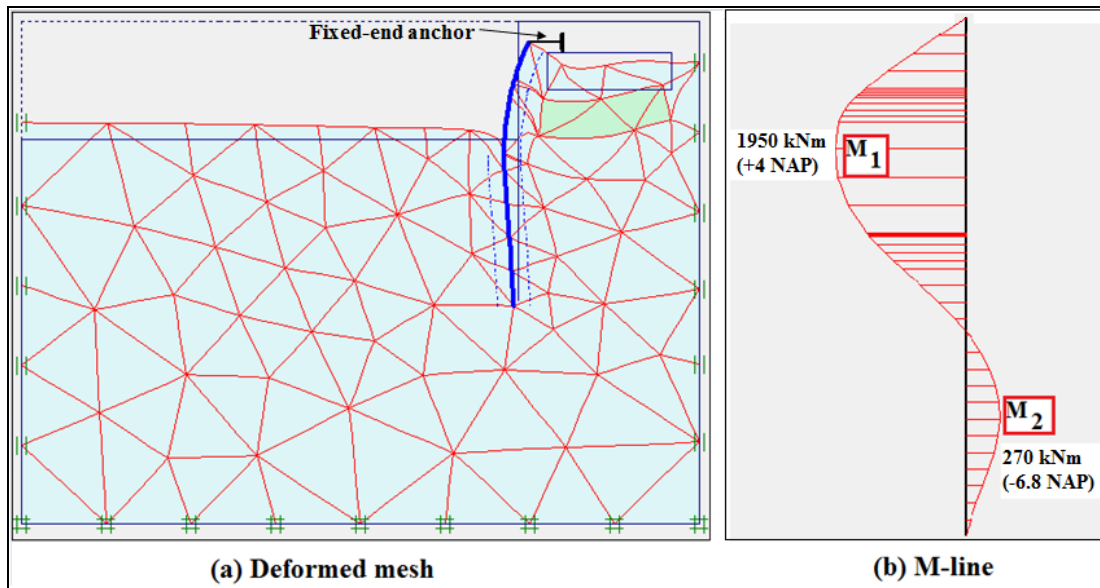


Figure 46: (a) Deformed mesh and (b) M-line of left wall for EI_{var} (cracked_3 zones) in Plaxis 2D – Half Model

4.1.2.3. Plaxis 2D – Total Model

With the Plaxis 2D – Total Model the M-line and EI-distribution of the right wall are checked with those according to PCSheetPileWall. The main input in Plaxis 2D consists of:

- The EI-distribution for both walls according to Table 26. Note that the right wall is totally uncracked according to PCSheetPileWall;
- $w_{plate} = 23 \text{ kN/m/m}'$ for both diaphragm walls in order to simulate $N_{self\ weight} \neq 0$;
- $R_{inter} = 1$ (no friction between soil and wall) in order to simulate $N_{shear\ force} = 0$;
- Node-to-node anchor to simulate the hinged wall-roof connection, where the bending stiffness of the roof structure itself has no impact on the diaphragm walls (see Figure 47a).

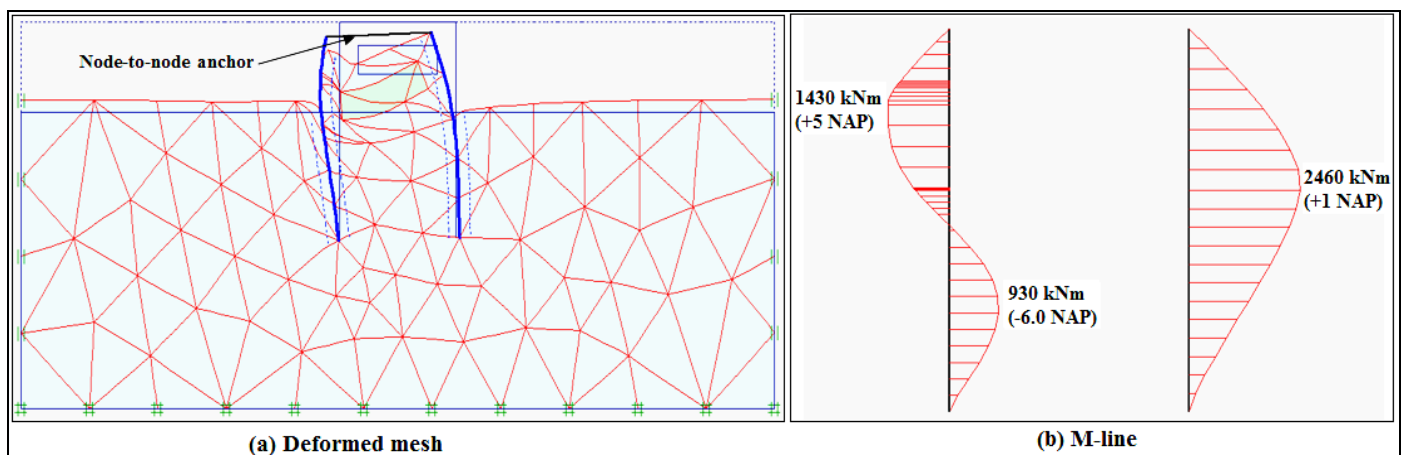


Figure 47: Hinged case - (a) Deformed mesh and (b) M-line for the walls only at $N \neq 0 \text{ kN}$

The deformed mesh and the M-line of both walls are depicted in Figure 47. Similarly as for $EI(\kappa)$ it is obvious that the right wall, in contrast to PCSheetPileWall, must be cracked. For the right wall the field moment has exceeded the cracking moment $M_r = 1351 \text{ kNm}$. Since the EI-distribution for the right wall

according to PCSheetPileWall is not valid anymore, iteration procedure 1 is set up to find the cracked height and the actual EI-distribution for this wall.

4.1.2.4. Iteration procedure 1 – right wall

Iteration procedure 1 is conducted to find the cracked height and the corresponding EI-distribution of the right wall. The following assumptions were made for:

- The left wall: The EI-distribution according to PCSheetPileWall will be maintained with each iteration (see Table 26);
- The right wall: The 1st assumption is that the right wall is totally uncracked, thereby using the uncracked stiffness according to PCSheetPileWall (see Table 26).
- Number of iterations: The iteration process for the right wall will go on until the cracked height remains the same. A difference of 5% is acceptable;

The determination of the cracked height (l_{cracked}) and its corresponding EI ($(EI)_{\text{Ed,min}}$) will take place in the same way as explained in section 4.1.1.4. The steps to be taken in the iteration process for the right wall have also been explained thoroughly in this section. For all the iterations in case of EI (κ , N) reference is made to Appendix C2.

An overview of the iteration results for the right wall is given in Table 28. Similarly as for EI(κ) a jump is observed between the even and uneven iterations with regard to the $M_{\text{Ed,max}}$ and l_{cracked} , where at a certain point the iteration procedure cannot go on and the results of one iteration step are equal to another. In this case iteration # 10 and 11 are equal to iteration # 12 and 13, respectively. The l_{cracked} lingers between 7.1 m and 9.9 m. For both the even and uneven iterations the $M_{\text{Ed,max}}$ is plotted against the l_{cracked} in Figure 48. Failed attempts to generate the actual value for $M_{\text{Ed,max}}$ and l_{cracked} with the computer lead to application of the ‘average result’ assumption for the right wall just like in case of EI(κ):

If the ‘average result’ in the middle of both graphs (average of l_{cracked} and $M_{\text{Ed,max}}$) in Figure 48 is chosen as input in Plaxis 2D, the result obtained for the right wall in Plaxis 2D must be equal to the ‘average result’.

	$M_{\text{Ed,max}}$	$(EI)_{\text{Ed,min}}$	EA	l_{cracked}
Iteration #	[kNm]	[kNm ² /m']	[kN/m']	[m]
1	2460	2.02E+06	1.08E+07	13
2	1540	4.77E+06	2.55E+07	5
3	2200	2.28E+06	1.22E+07	10.9
4	1630	3.97E+06	2.12E+07	6.1
5	2110	2.41E+06	1.28E+07	10.5
6	1650	3.84E+06	2.05E+07	6.4
7	2060	2.49E+06	1.33E+07	10.1
8	1690	3.61E+06	1.92E+07	6.8
9	2020	2.56E+06	1.37E+07	10
10	1720	3.46E+06	1.84E+07	7.1
11	2020	2.56E+06	1.37E+07	9.9
12	1720	3.46E+06	1.84E+07	7.1
13	2020	2.56E+06	1.37E+07	9.9
FINAL	1870	2.91E+06	1.55E+07	8.5

Table 28: Results iteration process right wall for $N \neq 0$ kN – hinged connection

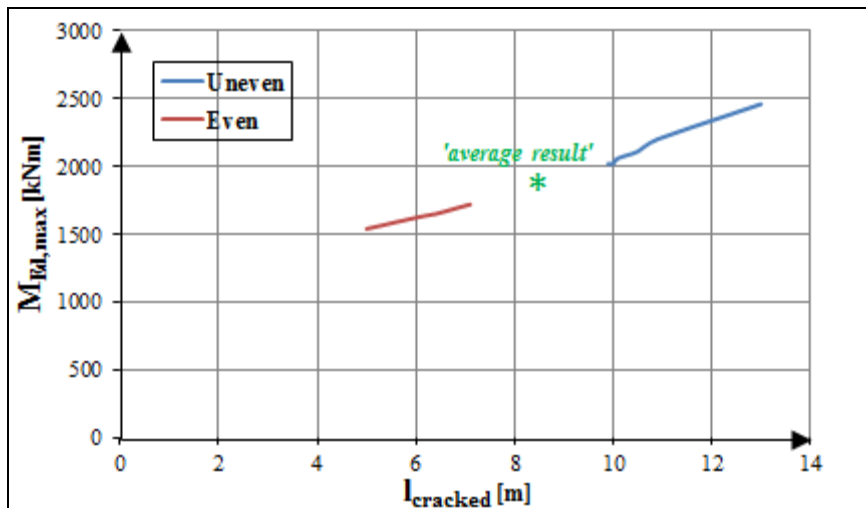


Figure 48: Results for even and uneven iterations of right wall for $N \neq 0$ kN

▪ *Validity 'average result' assumption for right wall*

In order to check the validity of the 'average result' assumption, the same procedure given in section 4.1.1.4 is applied in case of $EI(\kappa, N)$, considering the last even and uneven iteration step where the iteration process stops.

Step 1:

Figure 49 shows the M-line and the cracked height of the right wall belonging to the iterations #12 and #13. From this one can determine the:

- Average cracked height: $l_{cr,av} = 0.5 \times (9.9 + 7.1) = 8.5$ m;
- Course of cracked height: starting at $0.5 \times (5.5 + 6.1) = 5.8$ m and ending at $0.5 \times (-1.6 + -3.8) = -2.7$ m with regard to NAP-level.

Step 2:

The average $M_{Ed,max}$ is equal to: $0.5 \times (1720 + 2020) = 1870$ kNm. From interpolation in the M-N- κ diagram it is found that $(EI)_{Ed,min} = 2.91E+06$ kNm²/m' with a corresponding $EA = 1.55E+07$ kN/m'.

The average calculated values at step 1 and step 2 have also been given in Table 28 for the final iteration. These values will now be used as input for the right wall in the Plaxis 2D – Total Model.

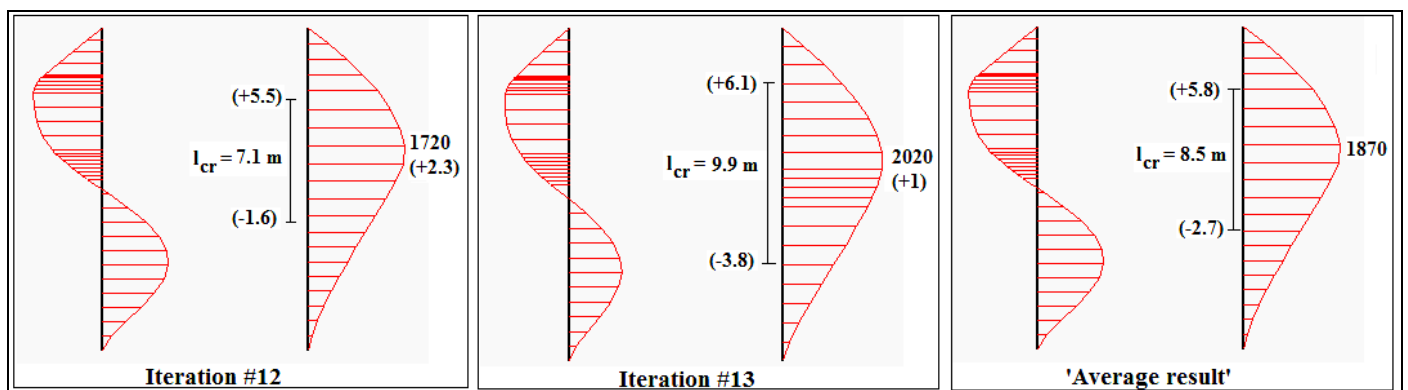


Figure 49: The assumed 'average result' for the right wall based on iteration #12 and #13.

(Note: Bending moment values in kNm and levels with regard to NAP are placed between brackets)

Step 3:

For a good overview, the input in the Plaxis 2D – Total Model for both walls is given in Table 29. Note that the EI-distribution for the left wall is according to PCSheetPileWall, while the EI-distribution for the right wall is based on the assumed ‘average result’ following from the even an uneven iterations. This input results in Figure 50. On comparison of the assumed ‘average result’ in Figure 49 and the Plaxis-result in Figure 50 there appears to be hardly any difference (see Table 30). Based on these findings it can be concluded that with iteration procedure 1 a method has been found which converges for the right wall.

	Zone	Cracked/ uncracked	Length	From	To	EI	EA
			[m]	[m]	[m]	[kNm ² /m']	[kN/m']
Left wall <i>(from PCSheet-PileWall)</i>	1	uncracked	3.25	10.5	7.25	9.67E+06	5.16E+07
	2a	cracked	1.25	7.25	6	4.66E+06	2.49E+07
	2b		4	6	2	2.96E+06	1.58E+07
	2c		2.05	2	-0.05	4.65E+06	2.48E+07
	3	uncracked	11.95	-0.05	-12	9.67E+06	5.16E+07
Right wall <i>(from 'average result' iterations)</i>	1	uncracked	4.7	10.5	5.8	9.67E+06	5.16E+07
	2	cracked	8.5	5.8	-2.7	2.91E+06	1.55E+07
	3	uncracked	9.3	-2.7	-12	9.67E+06	5.16E+07

Table 29: EI-distribution for both walls used as input in Plaxis 2D – Total Model for iteration procedure 1

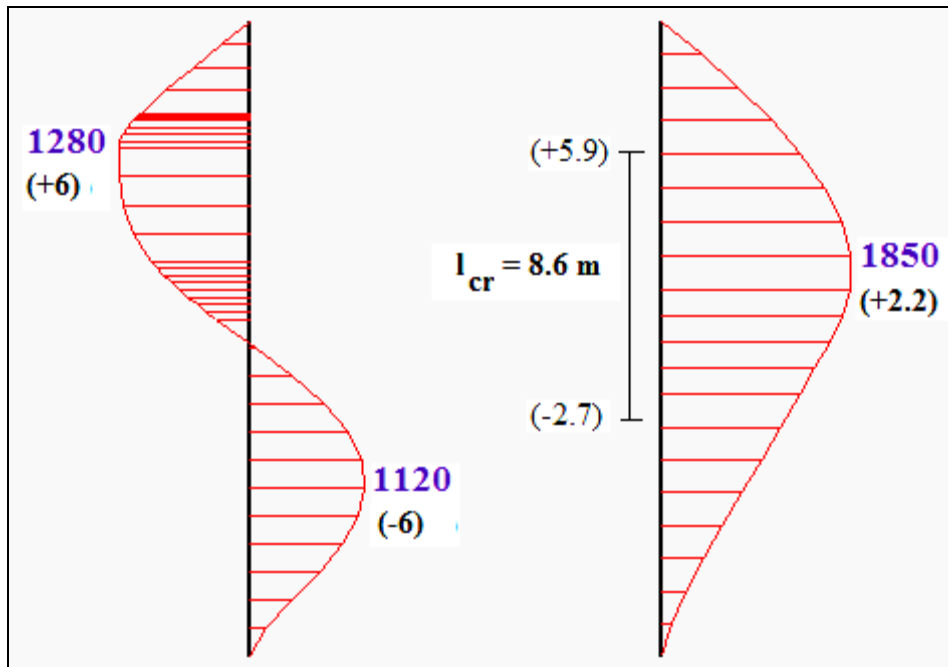


Figure 50: Final result EI_{var} according to iteration procedure 1 in Plaxis 2D – Total Model. (Note: Bending moment values in kNm and levels with regard to NAP are placed between brackets)

	Assumed 'average result'	Plaxis- result	Difference	Check
l_{cracked} [m]	8.5	8.6	1%	OK!
$M_{\text{right wall}}$ [kNm/m']	1870	1850	-1%	OK!

Table 30: Comparison of the assumed 'average result' and the Plaxis-result for the right wall

4.1.2.5. Problem left wall

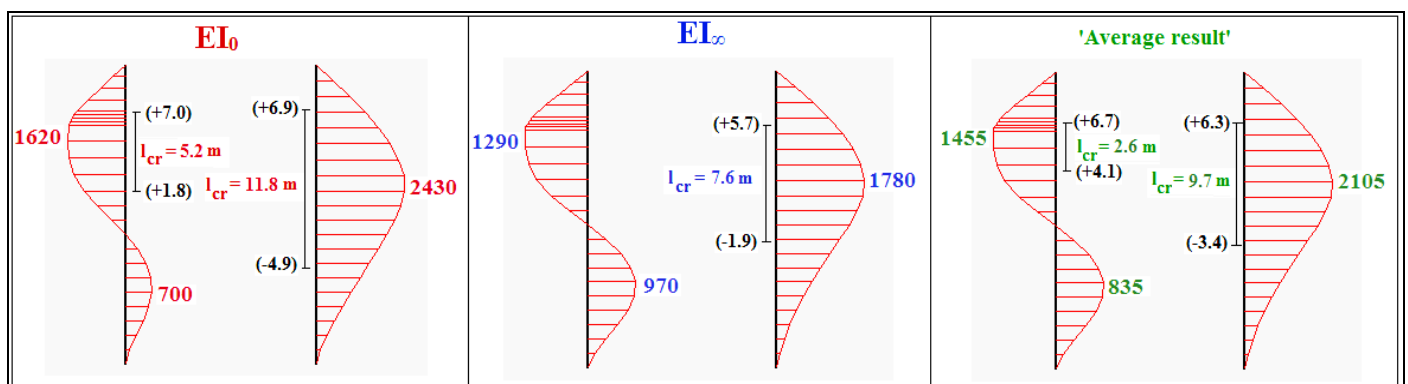
After an intensive iteration procedure 1 for the right wall, the left wall is now found to be totally uncracked according to Figure 50. This is in contradiction with the result from PCSheetPileWall where the left wall is cracked over a section of 7.3 m (see Figure 44). From this it can be concluded that the EI-distribution of the left wall in Plaxis 2D is not in accordance with the 1st assumed EI-distribution of the left wall from PCSheetPileWall. In all probability, just like in case of $EI(\kappa)$, it also concerns a back-and-forth iteration process between the left and the right wall for $EI(\kappa, N)$. Therefore, iteration procedure 2 will also be conducted for the case $EI(\kappa, N)$ without using the EI-distribution from PCSheetPileWall.

4.1.2.6. Iteration procedure 2 – both walls

Iteration procedure 2 is set up to verify the final result of iteration procedure 1. The applied strategy has already been explained in section 4.1.1.6.

Iteration procedure 2, steps:

1. Determine the average M-line and the average l_{cracked} from EI_0 and EI_{∞} . This is depicted as the 'average result' in Figure 51.
2. Based on the average bending moment, the EI and EA are determined for the average l_{cracked} . The EI is determined by means of interpolation in the M-N- κ diagram ($M_{\text{cr}} = 1351$ kNm). The input in the Plaxis 2D – Total Model for the left and the right wall are given in Table 31. This input results in Figure 52.

Figure 51: The 'average result' based on EI_0 and EI_{∞} .

(Note: Bending moment values in kNm and levels with regard to NAP are placed between brackets)

	Zone	Cracked/ uncracked	Length	From	To	$M_{Ed,average}$	EI	EA
			[m]	[m]	[m]	[kNm/m']	[kNm ² /m']	[kN/m']
Left wall	1	uncracked	3.8	10.5	6.7	-	9.67E+06	5.16E+07
	2	cracked	2.6	6.7	4.1	1455	6.06E+06	3.23E+07
	3	uncracked	16.1	4.1	-12	-	9.67E+06	5.16E+07
Right wall	1	uncracked	4.2	10.5	6.3	-	9.67E+06	5.16E+07
	2	cracked	9.7	6.3	-3.4	2105	2.41E+06	1.29E+07
	3	uncracked	8.6	-3.4	-12	-	9.67E+06	5.16E+07

Table 31: EI-distribution for both walls used as input in Plaxis 2D – Total Model for iteration procedure 2

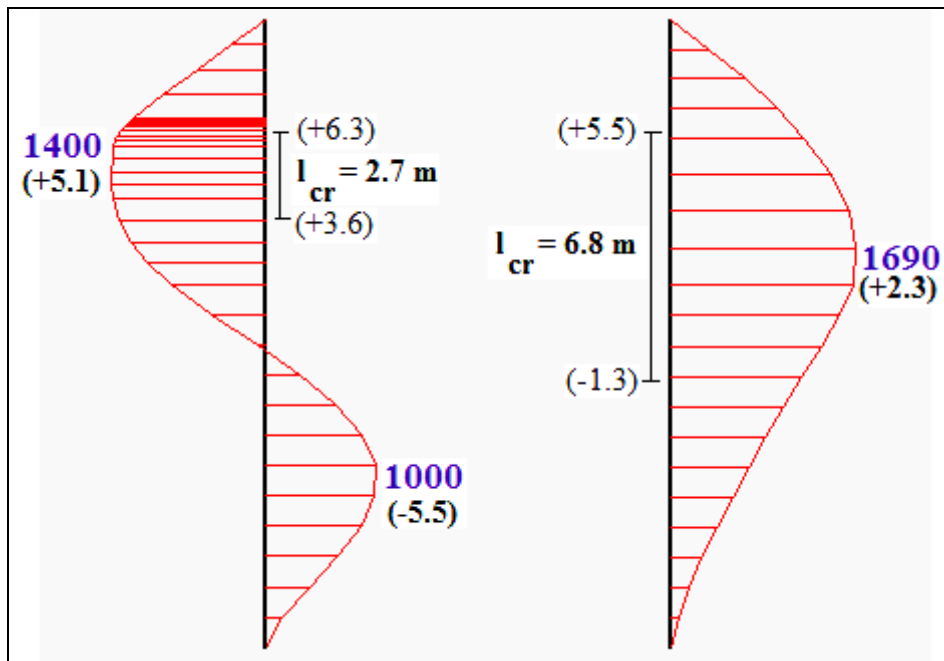


Figure 52: Final result EI_{var} according to iteration procedure 2 in Plaxis 2D – Total Model.
(Note: Bending moment values in kNm and levels with regard to NAP are placed between brackets)

Results iteration procedure 1 vs. iteration procedure 2:

On comparison of the final result according to iteration procedure 1 and iteration procedure 2 (Figure 50 vs. Figure 52) it can be stated that both procedures result in a cracking pattern and M-line configuration for EI_{var} which are comparable with the cracking pattern and M-line configuration from the outer boundaries (EI_0 and EI_∞ in Figure 51). Similarly as for the case of $EI(\kappa)$, with iteration procedure 2 only one iteration is required for both walls to get a reliable cracking pattern and M-line configuration. This in contrast to procedure 1, which required an intensive iteration process for the right wall, after which the EI-distribution of the left wall was still not ensured. In all probability, many more iterations are required to reach the same result as of iteration procedure 2.

It is found that the points of departure for iteration procedure 2 are obviously still more reliable compared to iteration procedure 1, regardless of the presence of an axial force $N \neq 0$ kN. Based on these findings it can be stated that:

The results of iteration procedure 2 are still valid for EI_{var} , irrespective of the presence of an axial force.

4.1.2.7. Final results EI (κ , N)

The M-line of both walls for EI_0 , EI_∞ and EI_{var} is given in Figure 53. The reported values in Table 32 concern the maximum values for the occurring bending moment (M_{Ed}), the settlement (δ_v) and the lateral wall displacement (U_x). Based on these results the following conclusions can be drawn:

- The right wall (without braking forces on it) is the most heavily loaded wall for EI_0 , EI_∞ and EI_{var} . In all 3 cases the representative bending moment is the field moment of the right wall;
- The right wall has the largest lateral displacement (in the direction of the braking force) for EI_0 , EI_∞ and EI_{var} ;
- The maximum occurring moment obtained with EI_{var} does not lie within the outer boundaries; it is lower than expected.
- The δ_v and U_x obtained with EI_{var} lie within the results of the outer boundaries EI_0 and EI_∞ .

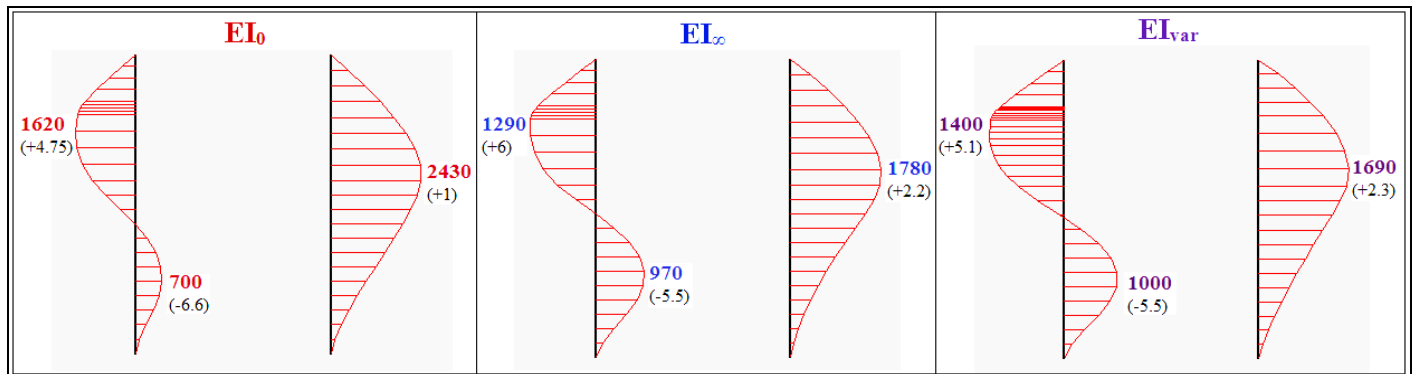


Figure 53: Hinged case - The M-line for EI_0 , EI_∞ and EI_{var} for $N \neq 0$ kN
(Note: Bending moment values in kNm and levels with regard to NAP are placed between brackets)

	M_{Ed} [kNm/m']	δ_v [mm]	U_x [mm]	
			Left wall	Right wall
EI_0	2430	101	-45	-63
EI_∞	1780	121	-65	-84
EI_{var}	1690	115	-59	-82

Table 32: Hinged case - Final results for EI_0 , EI_∞ and EI_{var} for $N \neq 0$ kN

4.2. Walls only; clamped

This section deals with the impact of EI_{var} on the diaphragm walls only in case of a clamped wall-roof connection. The clamped connection concerns a design case for which the amount of reinforcement over the wall height has to be determined first. After this a valid iteration procedure is defined for calculations with EI_{var} . For the hinged case the iteration procedure 2 was found to be valid for calculations with EI_{var} . For the clamped case it needs yet to be proven whether this iteration procedure is also applicable. Therefore, the same strategy as applied for the hinged case will also be applied for the clamped case. The Half Model in PCSheetPileWall and the Half and Total Model in Plaxis 2D will be employed. Two cases will be considered for EI_{var} , namely:

- Case a with $EI(\kappa)$, where EI_{var} is determined using the $M-\kappa$ diagram, and;
- Case b with $EI(\kappa, N)$, where EI_{var} is determined using the $M-N-\kappa$ diagram.

4.2.1. The clamped connection: A design case

Since the hinged connection was chosen above the clamped connection for the execution of the “Waalbrug-project” the required amount of reinforcement was only calculated for the hinged case. For the hinged case the EI_{var} was determined based on a basic reinforcement of $\rho_{l,tot} = 0.6\%$ per meter panel width. This has already been dealt with in section 4.1. For the clamped case there is no input with regard to the reinforcement. This implies that the clamped case is a fictitious case requiring an own interpretation, or in other words:

“The clamped case is a design case.”

4.2.2. Defining the reinforcement for the clamped case

In order to find the amount of reinforcement for the clamped case, both the PCSheetPileWall – Half Model and the Plaxis 2D – Half Model were applied considering the following basic assumption:

“Create a sufficiently large clamped moment at the top of the diaphragm wall which lies in between the clamped moment obtained with the outer boundaries EI_0 and EI_∞ .”

❖ Plaxis 2D – Half Model:

First of all, the clamped moment at the top of the diaphragm wall was calculated for the outer boundaries EI_0 and EI_∞ using the Plaxis 2D – Half Model. For $w_{plate} = 0 \text{ kN/m/m'}$ and $R_{inter} = 1$ (to simulate $N = 0 \text{ kN}$) a clamped moment of 2560 kNm/m' and 2190 kNm/m' is found for EI_0 and EI_∞ , respectively.

❖ PCSheetPileWall – Half Model:

The next step was to design a reinforcement pattern in the PCSheetPileWall – Half Model such that the obtained clamped moment in PCSheetPileWall ($M_{clamped}$) lies in between the calculated moments from the Plaxis 2D – Half Model. In order to reach this goal, the following steps had to be made in PCSheetPileWall:

- **Introduce the “Fictitious Rigid Plate” above the real wall.** Since the clamped connection was insufficiently present in PCSheetPileWall, a fictitious rigid plate was applied above the real wall creating a beam on 3 supports. Now a fully clamped connection was created at the top of the wall.
- **Introduce the “Stiffened Region” with a high reinforcement ratio.** This region, just beneath the top of the wall, was necessary in order to create a sufficiently large clamped moment at the top of the wall which lies in between the outer boundaries. According to EC2, clause 9.6.2 a maximum reinforcement ratio of $\rho_{l,max} = 4\%$ is allowed for a diaphragm wall.

The created model in PCSheetPileWall with the fictitious rigid plate (I_{rigid}), the stiffened region (I_{stiff}) and the remaining part of the wall (I_{field}) is depicted in Figure 54. The corresponding reinforcement ratios in

each of these regions are also denoted in this figure together with the requirement for the clamped moment.

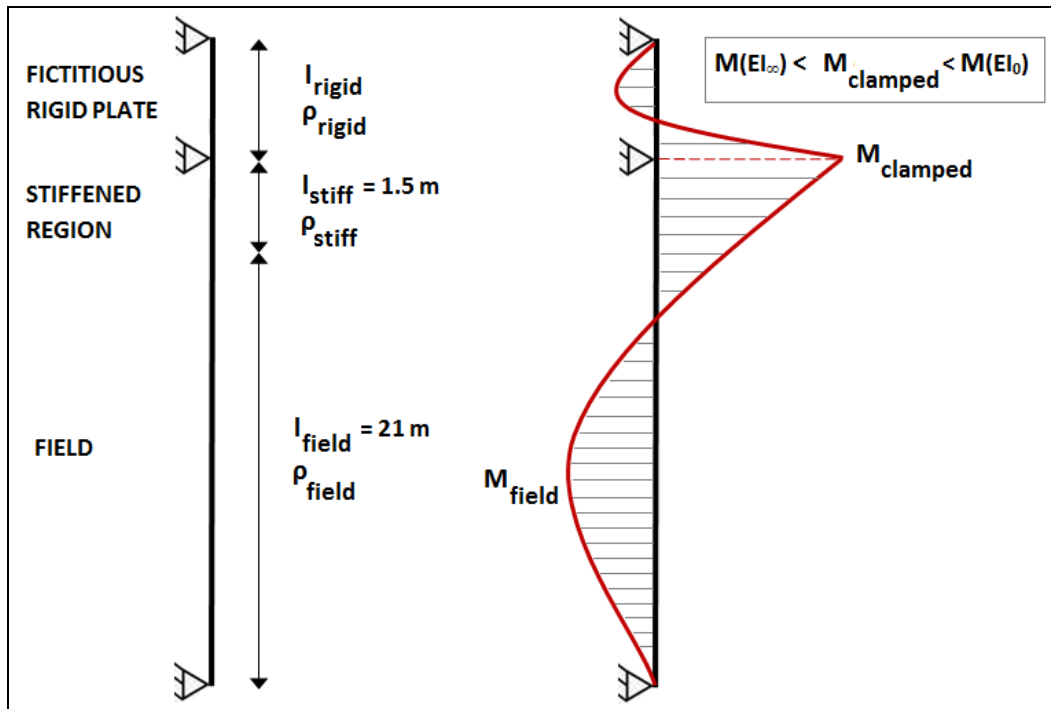


Figure 54: Model in PCSheetPileWall

The Fictitious Rigid Plate

For calculation purposes the following properties are assigned to the rigid plate in PCSheetPileWall:

- A height of $l_{rigid} = 3.5$ m;
- A wall thickness $d_{rigid} = 3.5$ m;
- A reinforcement of $A_{s,total} = 60.000$ mm².

The Stiffened Region

Applying a fictitious rigid plate above the real wall is not enough to create a sufficiently large clamped moment. In order to take up the clamped moment a relatively high reinforcement ratio is required just beneath the top of the wall. Therefore, the stiffened region was introduced. In case of insufficient reinforcement in this region, the diaphragm wall becomes unstable regardless of the properties of the fictitious rigid plate; the occurring moment is then larger than the ultimate moment capacity and no M-(N)- κ diagram can be generated. It turns out that the stiffened region is the determining factor in attaining a sufficiently large clamped moment at the top of the wall. Moreover, implementing a very high reinforcement ratio over the full wall height for the purpose of the clamped connection at the top is not economical. It is better to apply the high reinforcement ratio (ρ_{stiff}) only over a part of the upper side of the diaphragm wall. The research question arising at this point is:

How much reinforcement can be allowed in the stiffened region and how large can l_{stiff} be?

In order to answer this research question, the following strategy is applied:

- Investigate the influence of l_{stiff} , ρ_{stiff} and ρ_{field} on $M_{clamped}$. This is done by varying one of these three parameters and keeping the others constant. The influence is observed for:
 - l_{stiff} : 0.5 – 1 – 1.5 – 2 – 5 m
 - ρ_{stiff} : 0.6 – 1 – 2 – 3 – 4 %

- ρ_{field} : 0.6 – 1 – 2 – 3 – 4 %

It should be noted that for the clamped connection the minimum reinforcement ratio for the stiffened region and the field are kept at 0.6%. This value corresponds with the reinforcement ratio used in the hinged case. For $\rho_{\text{stiff}} < 0.6\%$ the wall becomes unstable.

In general, 4 cases have been investigated for LC3 with $N = 0$ kN, from which the most reasonable reinforcement pattern is chosen for the clamped connection.

Case 1:

The first attempt is to find a reasonable l_{stiff} . For $\rho_{\text{stiff}} = 4\%$ and $\rho_{\text{field}} = 0.6\%$ the results are given in Table 33. For both $l_{\text{stiff}} = 1.5$ m and $l_{\text{stiff}} = 2.0$ m an M_{clamped} is reached which lies in between the calculated moments from the Plaxis 2D – Half Model ($2190 < M_{\text{clamped}} < 2560$ kNm). For the next calculations it is chosen to maintain:

$$l_{\text{stiff}} = 1.5 \text{ m}$$

l_{stiff} [m]	M_{clamped} [kNm/m']
0.5	1908
1.0	2110
1.5	2247
2.0	2319

Table 33: The clamped moment at different lengths for the stiffened region

Case 2:

In this case the following holds:

- $l_{\text{stiff}} = 1.5$ m (constant)
- $\rho_{\text{stiff}} = 4\%$ (constant)
- $\rho_{\text{field}} = 0.6$ to 4% (variable)

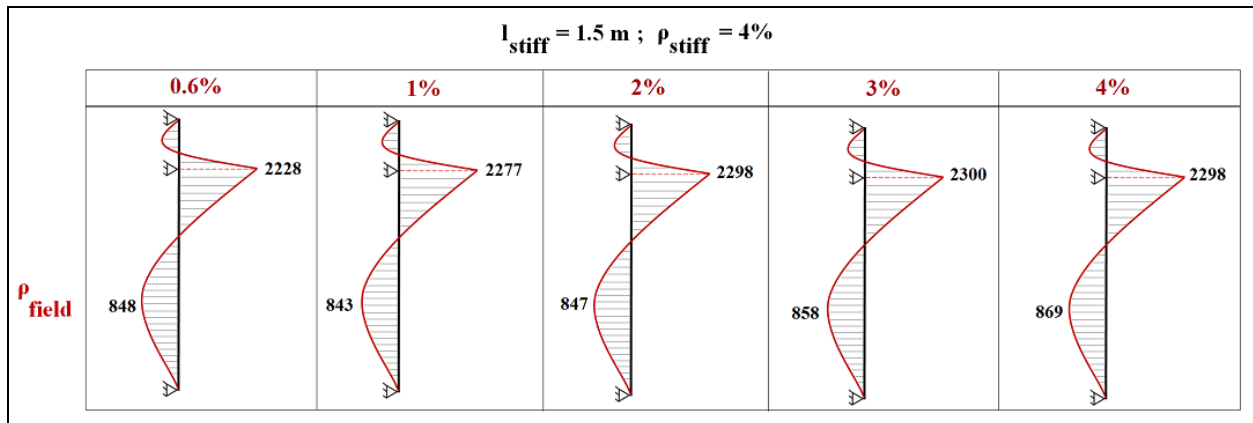


Figure 55: Results case 2

The results for case 2 are depicted in Figure 55. The following is observed:

- Regardless of the reinforcement ratio in the field it is found that the $M_{\text{clamped}} \approx 2300$ kNm and the $M_{\text{field}} \approx 850$ kNm;
- Apparently, M_{clamped} can only be influenced by ρ_{stiff} and l_{stiff} ;
- From the last case with a reinforcement ratio of 4% over the total wall height it is obvious that to reach a certain M_{clamped} , it is not necessary to apply a high reinforcement ratio over the total wall height;
- M_{clamped} is (almost) not to be influenced by ρ_{field} .

Case 3:

In this case the following holds:

- $l_{\text{stiff}} = 1.5 \text{ m}$ (constant)
- $\rho_{\text{stiff}} = 0.6 \text{ to } 4\%$ (variable)
- $\rho_{\text{field}} = 0.6\%$ (constant)

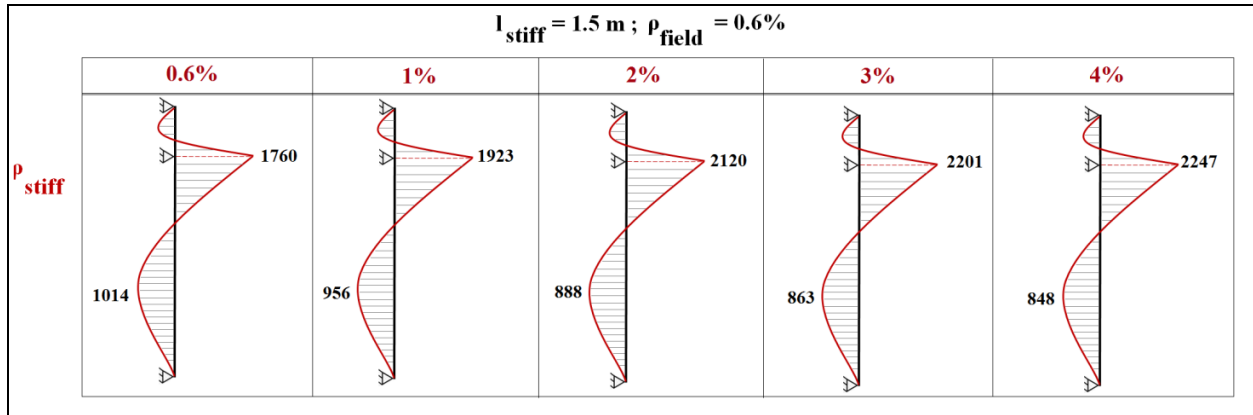


Figure 56: Results case 3

The results for case 3 are depicted in Figure 56. The following is observed:

- M_{clamped} depends mainly on ρ_{stiff} (M_{clamped} increases with ρ_{stiff}).

Case 4:

In order to examine the influence of l_{stiff} in combination with the determining factor ρ_{stiff} , as observed from case 3, the l_{stiff} is increased. In this case the following holds:

- $l_{\text{stiff}} = 5 \text{ m}$ (constant)
- $\rho_{\text{stiff}} = 0.6 \text{ to } 4\%$ (variable)
- $\rho_{\text{field}} = 0.6\%$ (constant)

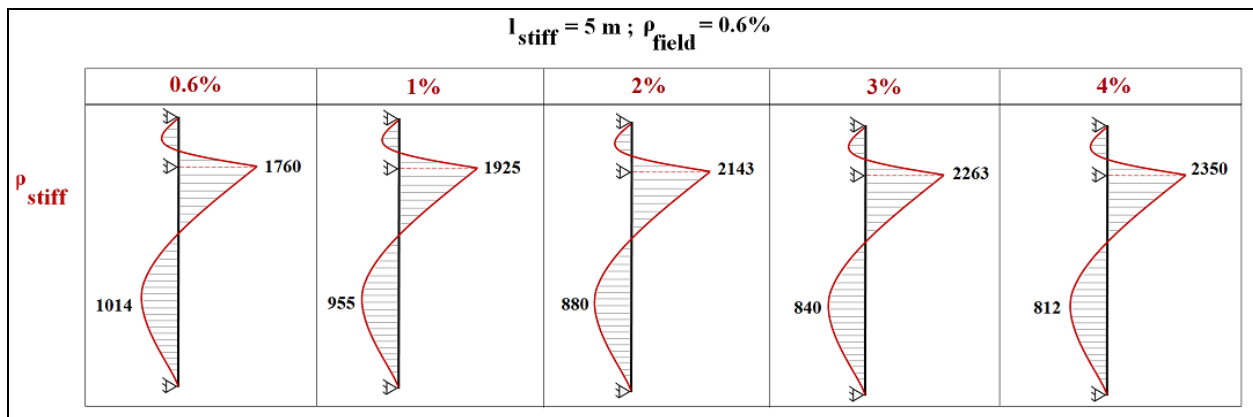


Figure 57: Results case 4

The results for case 4 are depicted in Figure 57. When compared to case 3, the following is observed:

- Despite the large increase of l_{stiff} this does not result in an appreciable increase in the M_{clamped} .

The parameters that influence the M_{clamped} are:

- l_{stiff} : An l_{stiff} of 1.5 m is determining. A further increase of l_{stiff} has almost no impact on M_{clamped} ;
- ρ_{stiff} : The M_{clamped} depends mainly on the ρ_{stiff} , while it is hardly influenced by the ρ_{field} . Therefore, ρ_{field} will be kept at a minimum of 0.6%. Considering the intended M_{clamped} ($2190 < M_{\text{clamped}} < 2560$ kNm) at $l_{\text{stiff}} = 1.5$ m and $\rho_{\text{field}} = 0.6\%$ a ρ_{stiff} of 3 - 4% can be chosen (see Figure 56). However, the problem is that a reinforcement ratio of 3 - 4% in the stiffened region is too high, because in that case concrete crushing (M_{pl}) occurs before yielding of the reinforcement (M_{e}). This is not desirable. For this research a $\rho_{\text{stiff}} = 2\%$ is acceptable with a difference of 3% in the M_{clamped} with regard to the lower boundary obtained in Plaxis 2D – Half Model (2120 vs. 2190 kNm)

It needs to be noted that the phenomenon of the occurrence of concrete crushing before yielding of the steel is observed from M- κ diagrams based on $N = 0$ kN and no influence of the reinforcement holes and compression reinforcement on the bending stiffness of the wall. In case one considers the influence of the compression reinforcement, the stiffness is increased where in case of $\rho_{\text{stiff}} = 2 - 3\%$ the more desirable situation $M_{\text{e}} < M_{\text{pl}}$ is obtained. This does not hold for $\rho_{\text{stiff}} = 4\%$;

- A local thickening of the cross-section at the top side of the wall. This will increase the M_{clamped} , but it is practically irrelevant.

Based on these findings it can be stated that:

For the clamped connection a sufficiently large clamped moment is attained for $l_{\text{stiff}} = 1.5$ m, $\rho_{\text{stiff}} = 2\%$ and $\rho_{\text{field}} = 0.6\%$. The EI_{var} in the clamped case will be determined based on these parameters.

4.2.3. Case a: EI (κ)

The calculation strategy for EI (κ) and the obtained results with the iteration procedures 1 and 2 are presented in this section.

4.2.3.1. PCSheetPileWall – Half Model

Consider both walls separately with their corresponding M-line for the representative loading combination - LC3 for the left wall and LC3,R for the right wall - as depicted in Figure 58. The left wall (with the braking forces) is cracked over 1.7 m just beneath the top of the wall, while the rest remains uncracked. The right wall is totally uncracked. Since two different reinforcement ratios are applied, $\rho_{\text{stiff}} = 2\%$ over the 1.5 m stiffened region and $\rho_{\text{field}} = 0.6\%$ over the remaining part of the wall, it is obvious that two M- κ diagrams must be considered for both walls. The stiffened region and the field are denoted as region I and region II in Figure 58, respectively. The M- κ diagrams for both regions are represented in Figure 59 and Figure 60, and are based on $N = 0$ kN. The cracking moment for:

- Region I : $M_{\text{r}}(\text{I}) = 1291$ kNm;
- Region II: $M_{\text{r}}(\text{II}) = 1150$ kNm.

The EI-distribution of both walls is given in Table 34. It should be noted that an average EI-value is considered for the cracked zone of the left wall. Furthermore, it can be noted that the E-moduli in the uncracked zones of the walls are found to be higher than the considered $E_{\text{uncracked}} = 33000$ MPa.

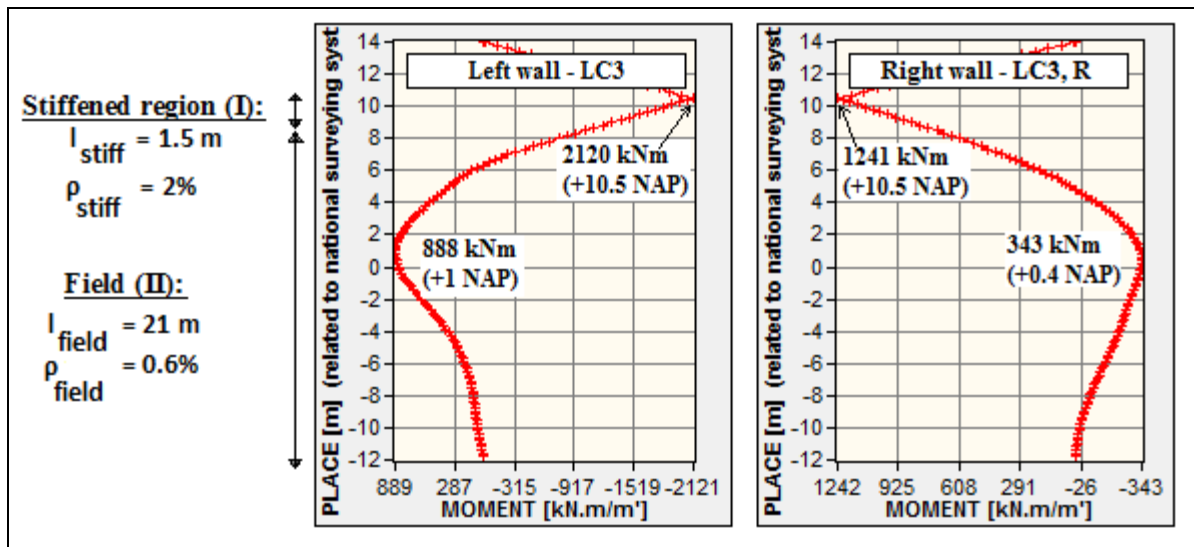


Figure 58: M-line both walls from PCSheetPileWall (clamped connection, N = 0 kN)

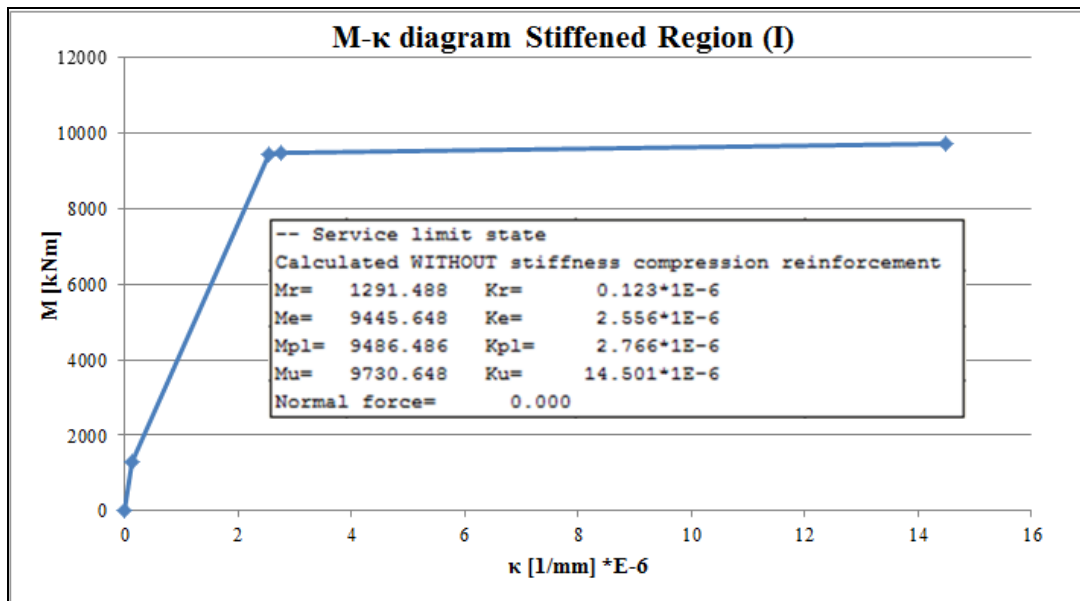


Figure 59: M-κ diagram both walls for the Stiffened Region (I)

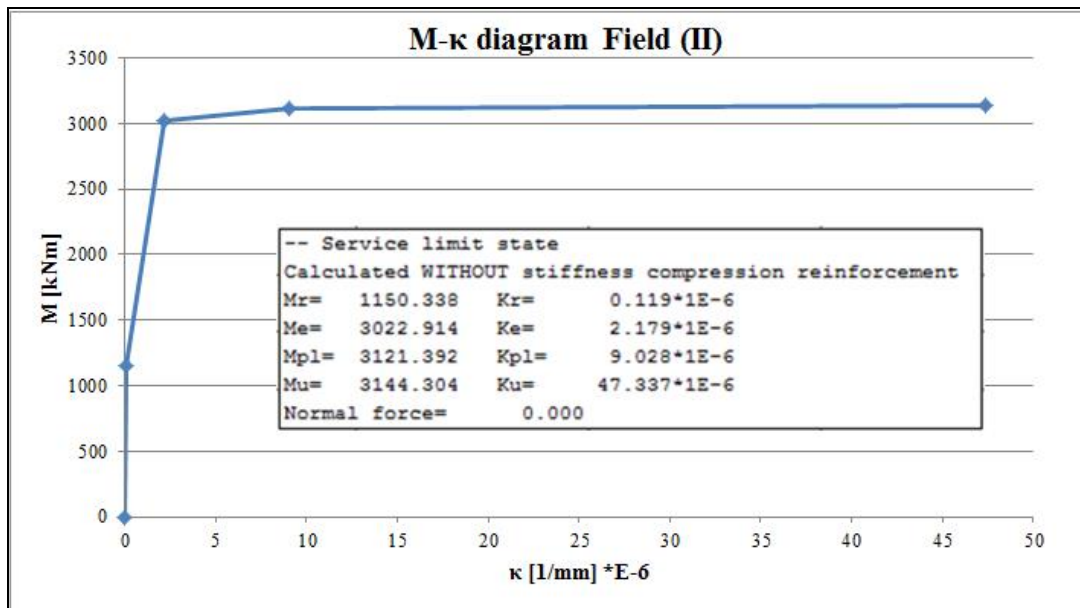


Figure 60: M-κ diagram both walls for the Field (II)

	Zone	Cracked/ uncracked	Length	From	To	EI	EA	E	d _{eq}
			[m]	[m]	[m]	[kNm ² /m']	[kN/m']	[MPa]	[m]
Left wall	1	cracked	1.7	10.5	8.8	7.34E+06	3.91E+07	26089	1.5
	2	uncracked	20.8	8.8	-12	9.67E+06	5.16E+07	34381	1.5
Right wall	1	uncracked	1.5	10.5	9	1.05E+07	5.63E+07	37507	1.5
	2	uncracked	21	9	-12	9.67E+06	5.16E+07	34381	1.5

Table 34: EI-distribution of both walls obtained from PCSheetPileWall

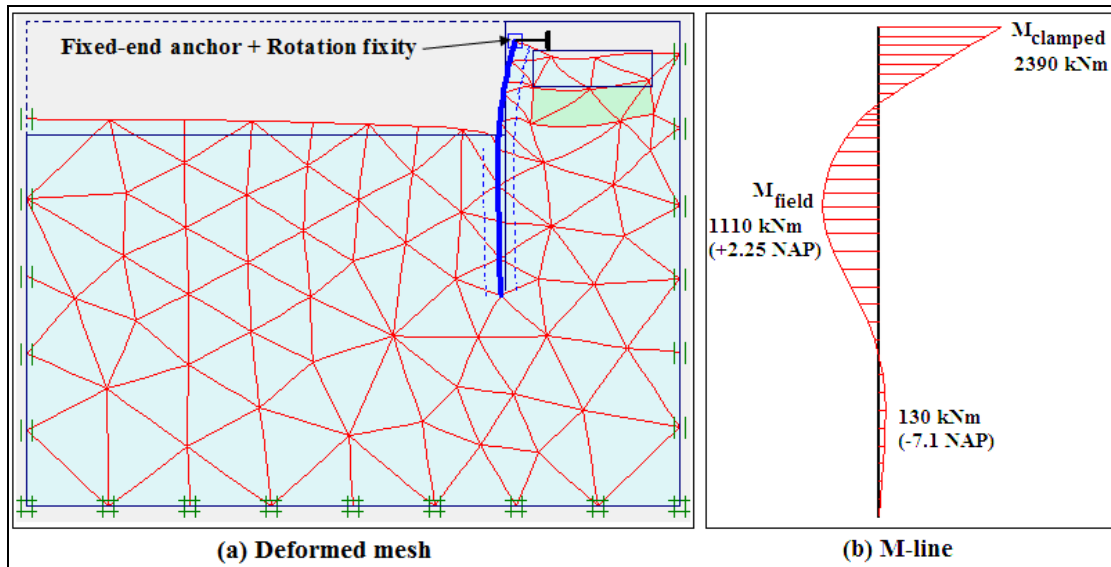
4.2.3.2. Plaxis 2D – Half Model

The Plaxis 2D – Half Model is used to validate the EI-distribution of the left wall (half model) obtained from PCSheetPileWall. Therefore, the M-line of the Half Models is checked in both programs. The main input in Plaxis 2D consists of:

- The EI-distribution for the left wall according to Table 34;
- $w_{plate} = 0$ kN/m/m' for the diaphragm wall in order to simulate $N_{self\ weight} = 0$ in PCSheetPileWall;
- $R_{inter} = 1$ (no friction between soil and wall) in order to simulate $N_{shear\ force} = 0$ in PCSheetPileWall;
- Fixed-end anchor plus rotation fixity (beams) to simulate the clamped wall-roof connection (see Figure 61a).

The deformed mesh and the M-line for the left wall obtained in Plaxis 2D for EI_{var} are given in Figure 61. The results obtained with EI_0 , EI_{∞} and EI_{var} are given in Table 35. It is obvious that the $M_{clamped}$ with EI_{var} lies within the outer boundaries. Compared with PCSheetPileWall the $M_{clamped}$ for EI_{var} differs with about 13% from the Plaxis 2D – Half Model (2390 vs. 2120 kNm). With this difference the EI-distribution of the left wall according to PCSheetPileWall is accepted for the Plaxis 2D – Total Model.

EI	δ_v [mm]	M_{clamped} [kNm/m']	M_{field} [kNm/m']	U_x [mm]
EI_0	67	2560	1040	16
EI_∞	70	2190	930	16
EI_{var}	67	2390	1110	16

Table 35: Results in Plaxis 2D – Half Model for EI_0 , EI_∞ and EI_{var} Figure 61: (a) Deformed mesh and (b) M-line of left wall for EI_{var} in Plaxis 2D – Half Model

4.2.3.3. Plaxis 2D – Total Model

With the Plaxis 2D – Total Model the M-line and EI-distribution of the right wall are checked with those according to PCSheetPileWall. The main input in Plaxis 2D consists of:

- The EI-distribution for both walls according to Table 34. Note that the right wall is totally uncracked according to PCSheetPileWall;
- $w_{\text{plate}} = 0$ kN/m/m' for both diaphragm walls in order to simulate $N_{\text{self weight}} = 0$;
- $w_{\text{fict.plate}} = 0$ kN/m/m' for the fictitious rigid plate, because in PCSheetPileWall the axial force of the fictitious rigid plate is also ignored;
- $R_{\text{inter}} = 1$ (no friction between soil and wall) in order to simulate $N_{\text{shear force}} = 0$;
- Stiff structure above the diaphragm walls to simulate the clamped connection in the Plaxis 2D –Total Model. The stiff structure consists of rigid plates connected by struts (see Figure 62a). For the properties of the rigid plates and the struts reference is made to Appendix D.

The M-line obtained from the Plaxis 2D – Total Model is depicted in Figure 62b, showing clearly that the right wall is more heavily loaded in the field than the left wall. It is obvious that the right wall, in contrast to PCSheetPileWall, must be cracked in both the stiffened region and the field. It is found that:

- In the stiffened region: $M_{\text{clamped}} > M_r$ (I) and;
- In the field $M_{\text{field}} > M_r$ (II).

Since the EI-distribution for the right wall according to PCSheetPileWall is not valid anymore, iteration procedure 1 is set up to find the cracked height and the actual EI-distribution for this wall.

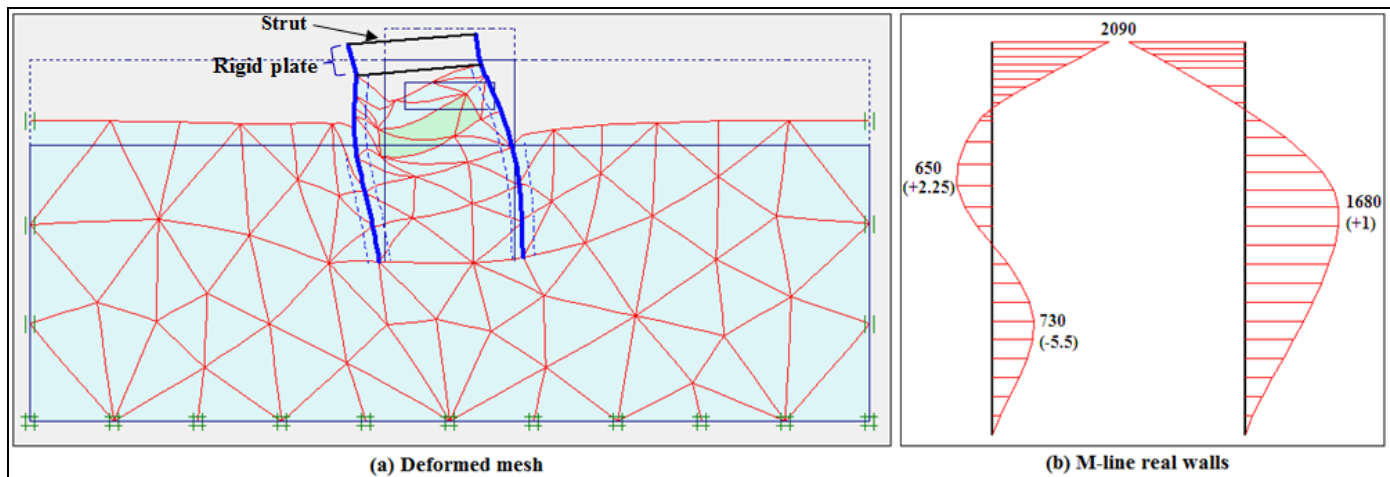


Figure 62: Clamped case - (a) Deformed mesh and (b) M-line for the walls only at $N = 0$ kN

4.2.3.4. Iteration procedure 1 – right wall

Iteration procedure 1 is conducted to find the cracked height and the corresponding EI-distribution of the right wall. The following assumptions were made for:

- The left wall: The EI-distribution according to PCSheetPileWall will be maintained with each iteration (see Table 34);
- The right wall: The 1st assumption is that the right wall is totally uncracked, thereby using the uncracked stiffness according to PCSheetPileWall (see Table 34).

Since the M - κ diagrams of both regions (region I and region II) and the M -line of the right wall (from Plaxis 2D – Total Model) are known, the cracked heights with their corresponding EI can be found at every iteration step. For the cracked zone of the right wall the following must be taken into account, with regard to:

- **The height of the cracked zones ($l_{cr,I}$ and $l_{cr,II}$):** This will be obtained from Plaxis 2D. Two cracked zones are to be distinguished over the wall height:
 - For the stiffened region: $l_{cr,I}$, where $M_{Ed} > M_{cr}(I)$;
 - For the field: $l_{cr,II}$, where $M_{Ed} > M_{cr}(II)$.
- **The EI of the cracked zones ($(EI)_{Ed,min,I}$ and $(EI)_{Ed,min,II}$):** For both $l_{cr,I}$ and $l_{cr,II}$ the highest occurring moment ($M_{Ed,max}$) in these cracked zones is taken as point of departure for the calculation of the corresponding EI. The EI is determined from the M - κ diagrams by means of interpolation. It concerns the lowest EI which is applied over the cracked region. One distinguishes:
 - For the stiffened region: $(EI)_{Ed,min,I}$ applied over $l_{cr,I}$, where the bending stiffness is determined from $M_{Ed,max} = M_{clamped}$;
 - For the field: $(EI)_{Ed,min,II}$ applied over $l_{cr,II}$, where the bending stiffness is determined from $M_{Ed,max}$ present over $l_{cr,II}$.

The iteration process for the right wall consists of the following steps:

1. Start with the uncracked stiffness of the right wall. This results in a certain M -line with $l_{cr,I}$ and $l_{cr,II}$ for which the corresponding $(EI)_{Ed,min,I}$ and $(EI)_{Ed,min,II}$ are calculated, respectively;
2. Both cracked zones with their corresponding EI will be entered in the next iteration, which will result in another M -line. From this new M -line, a new set of $l_{cr,I}$ and $l_{cr,II}$ with their corresponding EI can be determined;
3. Repeat step 2 until $l_{cr,I}$ and $l_{cr,II}$ remain constant. For all the iterations, reference is made to Appendix C3.

An overview of the iteration results for the right wall is given in Table 36, observing a jump between the even and uneven iterations with regard to the cracked zones $l_{cr,I}$ and $l_{cr,II}$. The observed cracking pattern for the even and uneven iteration is as depicted in Figure 63.

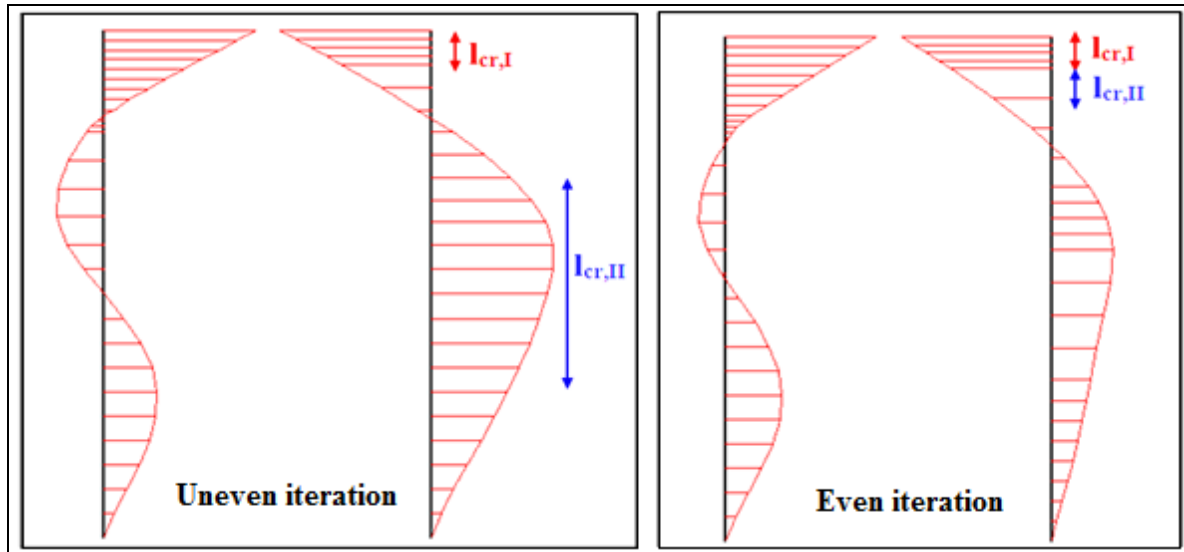


Figure 63: Cracking pattern at an uneven and even iteration step

Iteration #	$l_{cr,I}$ [m]	$l_{cr,II}$ [m]
1	1.4	8.6
2	1.5	0.8
3	1	9.3
4	1.5	0.9
5	0.9	9.2
6	1.5	0.9
7	0.3	13.3
8	1.5	1.2
9	0.9	9.6
10	1.5	1
11	0.9	9.4
12	1.5	0.9
13	0.9	9.3

Table 36: Results iteration process right wall for $N = 0$ kN – clamped connection

The iteration procedure for the right wall is very laborious, without noticing significant differences in the cracked zones for the even and uneven iterations. At a certain point the iteration procedure comes to a standstill, where it is found that the cracked zones of one iteration step are equal to another. Similarly as in the hinged case the average result of the last even and uneven iteration step, where the iteration process stops, is considered as input in the Plaxis 2D –Total Model. In this case the average result of iteration # 10 and 11 are considered as input for the right wall. The obtained result will then be compared with the result obtained with iteration procedure 2.

Iteration procedure 1, steps (right wall only):

Points of departure:

1. The EI-distribution of the left wall is according to PCSheetPileWall;
2. The EI-distribution of the right wall is based on the average result of iteration #10 and 11, as depicted in Figure 74. The average cracked zones and the average M-line are determined for the right wall. From the average M-line the EI and EA are derived;
3. The above is used as input for the Plaxis 2D – Total Model, see Table 37. This input results in Figure 65, showing the final result for EI_{var} according to iteration procedure 1.

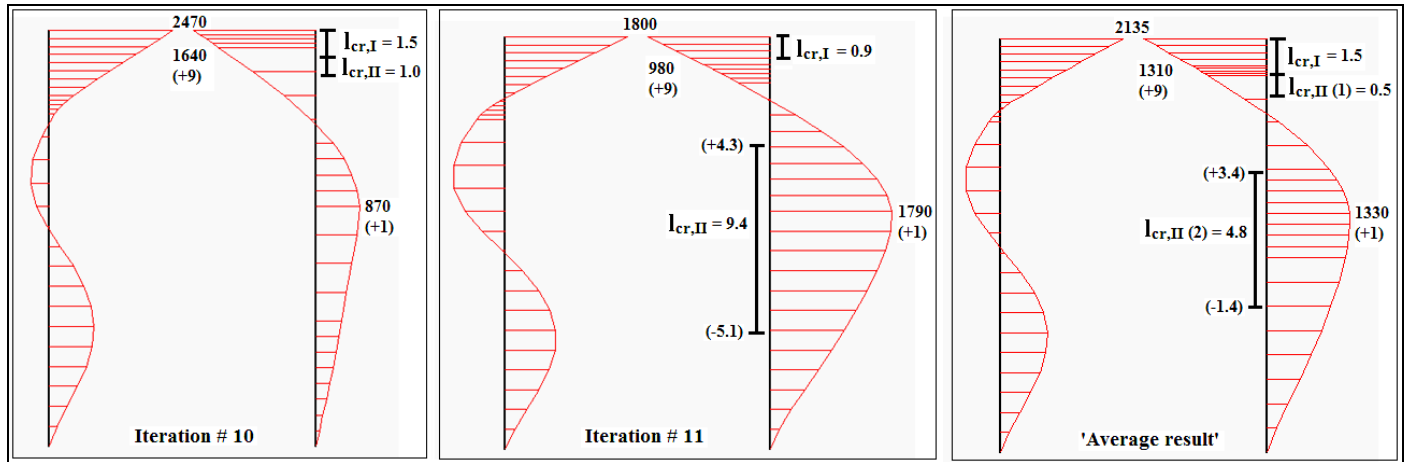


Figure 64: The assumed ‘average result’ for the right wall based on iteration #10 and #11.

(Note: Bending moment values in kNm, cracked zones in m, and levels with regard to NAP are placed between brackets)

	Zone	Cracked/ uncracked	Length	From	To	$M_{Ed,average}$ [kNm/m']	EI [kNm ² /m']	EA [kN/m']
			[m]	[m]	[m]			
Left wall <i>(from PCSheet-PileWall)</i>	1	cracked	1.7	10.5	8.8	-	7.34E+06	3.91E+07
	2	uncracked	20.8	8.8	-12	-	9.67E+06	5.16E+07
Right wall <i>(from 'average result' iterations)</i>	1	cracked	¹⁾ 1.5	10.5	9	2135	5.70E+06	3.04E+07
	2	cracked	0.5	9	8.5	1310	4.45E+06	2.37E+07
	3	uncracked	5.1	8.5	3.4	-	9.67E+06	5.16E+07
	4	cracked	4.8	3.4	-1.4	1330	4.20E+06	2.24E+07
	5	uncracked	10.6	-1.4	-12	-	9.67E+06	5.16E+07

Table 37: EI-distribution for both walls used as input in Plaxis 2D – Total Model for iteration procedure 1

Clarification Table 37:

¹⁾ Actually, the average $l_{cr,I} = 1.2$ m from the top. Since the introduction of an extra uncracked zone of 0.3 m in the stiffened region has no effect on the load distribution, the total cracked stiffened region of 1.5 m is considered as basic input in Plaxis 2D.

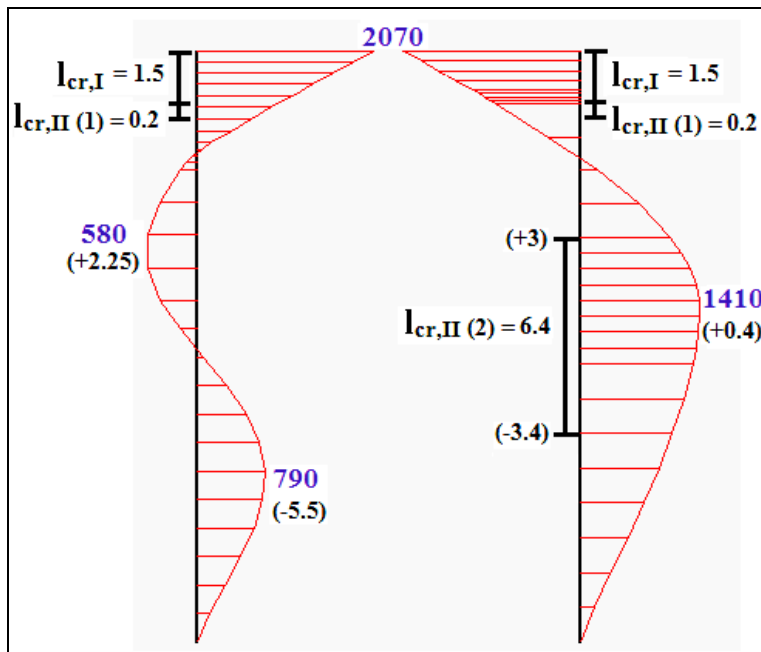


Figure 65: Final result EI_{var} according to iteration procedure 1 in Plaxis 2D – Total Model. (Note: Bending moment values in kNm, cracked zones in m, and levels with regard to NAP are placed between brackets)

4.2.3.5. Iteration procedure 2 – both walls

Iteration procedure 2 is set up to verify the final result of iteration procedure 1. The applied strategy has already been explained in section 4.1.1.6.

Iteration procedure 2, steps:

1. Determine the average M-line and the average cracked zones from EI_0 and EI_{∞} for both walls. This is depicted as the ‘average result’ in Figure 51;
2. Based on the average bending moment, the EI and EA are determined for the average cracked zones. The input in the Plaxis 2D – Total Model for the left and the right wall are given in Table 38. This input results in Figure 77, showing the final result for EI_{var} according to iteration procedure 2.

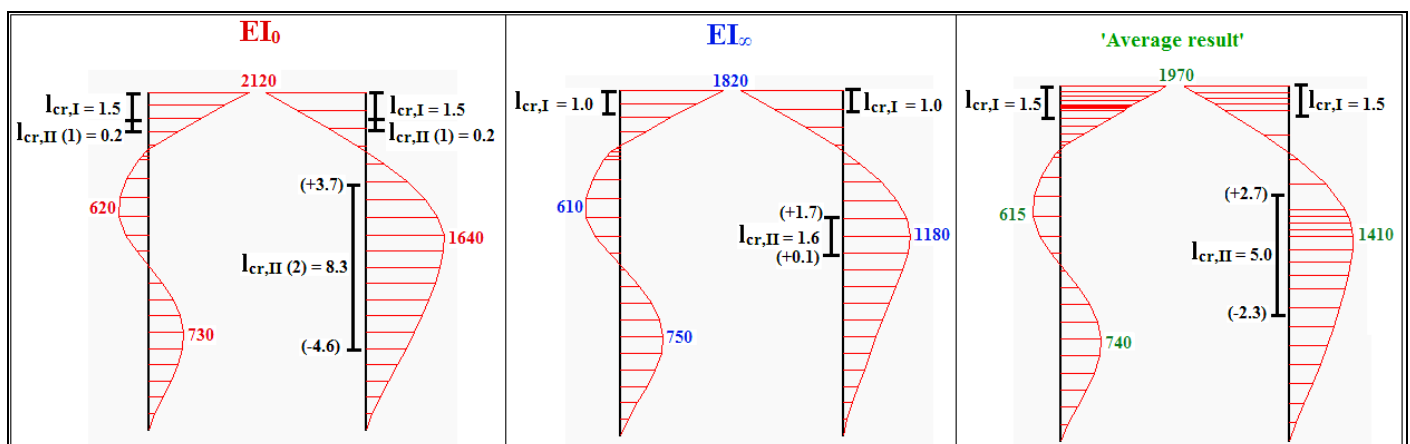
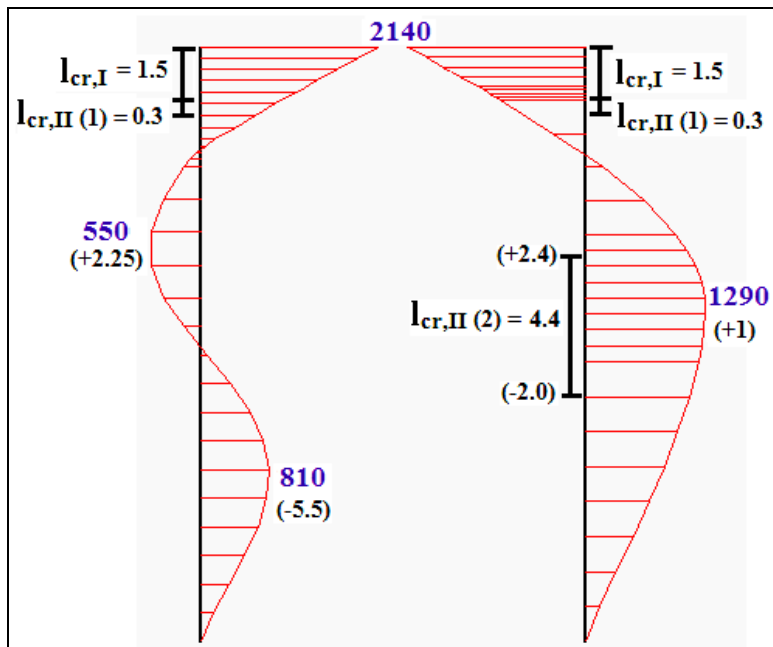


Figure 66: The ‘average result’ based on EI_0 and EI_{∞} . (Note: Bending moment values in kNm, cracked zones in m, and levels with regard to NAP are placed between brackets)

	Zone	Cracked/ uncracked	Length [m]	From [m]	To [m]	$M_{Ed,average}$ [kNm/m']	EI [kNm ² /m']	EA [kN/m']
Left wall	1	cracked	1.3	10.5	9.2	1970	6.05E+06	3.23E+07
	2	uncracked	0.2	9.2	9	-	1.05E+07	5.63E+07
	3	uncracked	21	9	-12	-	9.67E+06	5.16E+07
Right wall	1	cracked	1.5	10.5	9	1970	6.05E+06	3.23E+07
	2	uncracked	6.3	9	2.7	-	9.67E+06	5.16E+07
	3	cracked	5	2.7	-2.3	1410	3.48E+06	1.86E+07
	4	uncracked	9.7	-2.3	-12	-	9.67E+06	5.16E+07

Table 38: EI-distribution for both walls used as input in Plaxis 2D – Total Model for iteration procedure 2

Figure 67: Final result EI_{var} according to iteration procedure 2 in Plaxis 2D – Total Model.

(Note: Bending moment values in kNm, cracked zones in m, and levels with regard to NAP are placed between brackets)

Results iteration procedure 1 vs. iteration procedure 2:

On comparison of the final result according to iteration procedure 1 and iteration procedure 2 (Figure 75 vs. Figure 77) it can be observed that the cracking pattern and the M-line configuration are similar. While iteration procedure 2 requires only one iteration for both walls, an intensive iteration process is performed according to iteration procedure 1. This phenomenon is comparable with the hinged case. Noteworthy is that according to both procedures the stiffened region appears to be totally cracked. Based on these findings it can be stated that:

The results of iteration procedure 2 are valid for EI_{var} , both for a hinged and a clamped wall-roof connection.

4.2.3.6. Final results EI (κ)

The M-line of both walls for EI_0 , EI_∞ and EI_{var} is given in Figure 78. The reported values in Table 39 concern the maximum values for the occurring bending moment (M_{Ed}), the settlement (δ_v) and the lateral wall displacement (U_x). Based on these results the following conclusions can be drawn:

- In the field the right wall (without braking forces on it) appears to be more heavily loaded than the left wall. This is the case for EI_0 , EI_∞ and EI_{var} . The governing bending moments are the clamped moments ($M_{clamped}$), which are equal for both walls;
- The right wall has the largest lateral displacement (in the direction of the braking force) for EI_0 , EI_∞ and EI_{var} ;
- The $M_{clamped}$ obtained with EI_{var} does not lie within the outer boundaries; it is higher than expected;
- The δ_v and U_x obtained with EI_{var} lie within the results of the outer boundaries EI_0 and EI_∞ ;
- For EI_{var} it is obvious that both walls crack over the total stiffened region ($l_{stiff} = 1.5\text{m}$, $\rho_{stiff} = 2\%$). The occurring $M_{clamped}$ makes it impossible to keep the stiffened region uncracked, despite the high reinforcement ratio. Based on this finding it can be stated that:

The clamped connection is an academic case which is not realizable/ practicable, because the total stiffened region cracks. Therefore, do not connect the roof rigidly to the diaphragm wall. Otherwise, perform the analysis in accordance with a hinged/ 'cracked' connection.

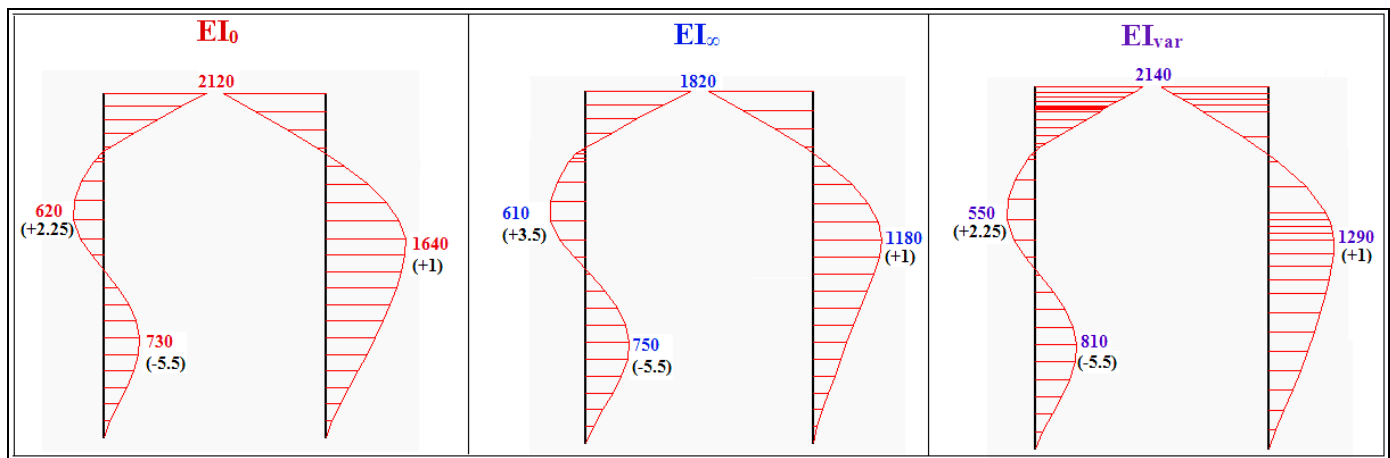


Figure 68: Clamped case – The M-line for EI_0 , EI_∞ and EI_{var} for $N = 0$ kN

(Note: Bending moment values in kNm and levels with regard to NAP are placed between brackets)

	M_{Ed} [kNm/m']	δ_v [mm]	U_x [mm]	
			Left wall	Right wall
EI_0	2120	54	-35	-37
EI_∞	1820	64	-45	-50
EI_{var}	2140	57	-38	-42

Table 39: Clamped case - Final results for EI_0 , EI_∞ and EI_{var} for $N = 0$ kN

4.2.4. Case b: EI (κ , N)

The calculation strategy for EI (κ , N) and the obtained results with the iteration procedures 1 and 2 are presented in this section.

4.2.4.1. PCSheetPileWall – Half Model

Consider both walls separately with their corresponding M-line for the representative loading combination - LC3 for the left wall and LC3,R for the right wall - as depicted in Figure 69. The left wall (with the braking forces) is cracked over 2 different sections in the stiffened region and the field. The right wall is totally uncracked. Since two different reinforcement ratios are applied, $\rho_{\text{stiff}} = 2\%$ over the 1.5 m stiffened region and $\rho_{\text{field}} = 0.6\%$ over the remaining part of the wall, it is obvious that two M-N- κ diagrams must be considered for both walls. The stiffened region and the field are denoted as region I and region II in Figure 69, respectively. The M-N- κ diagrams for both regions are represented in Figure 70 and Figure 71, and are based on $N = N_{\text{self weight}} = -810 \text{ kN/m}^2$. The cracking moment for:

- Region I : $M_r \text{ (I)} = 1488 \text{ kNm}$;
- Region II: $M_r \text{ (II)} = 1351 \text{ kNm}$.

From the M-N- κ diagram of the stiffened region it is noted that due to $N \neq 0$, concrete crushing occurs before yielding of the steel ($M_{\text{pl}} < M_c$). When defining the reinforcement for the clamped case, this situation was not desirable. However, a ductile failure is still guaranteed since the reinforcement yields before the concrete compression zone fails, thus before reaching M_u . The EI-distribution of both walls is given in Table 40. The uncracked zone in the field of the left wall has an E-modulus of 34381 MPa, as a result of the combined stiffness of the concrete and the tensile reinforcement (the compression reinforcement is not taken into account for the stiffness determination, which would otherwise result in a higher E-modulus). The uncracked zone in the stiffened region of the left wall has an even higher E-modulus of 37507 MPa, which can be attributed to the higher reinforcement ratio in the stiffened region. The E-moduli in the uncracked zones of the walls are found to be higher than the considered $E_{\text{uncracked}} = 33000 \text{ MPa}$.

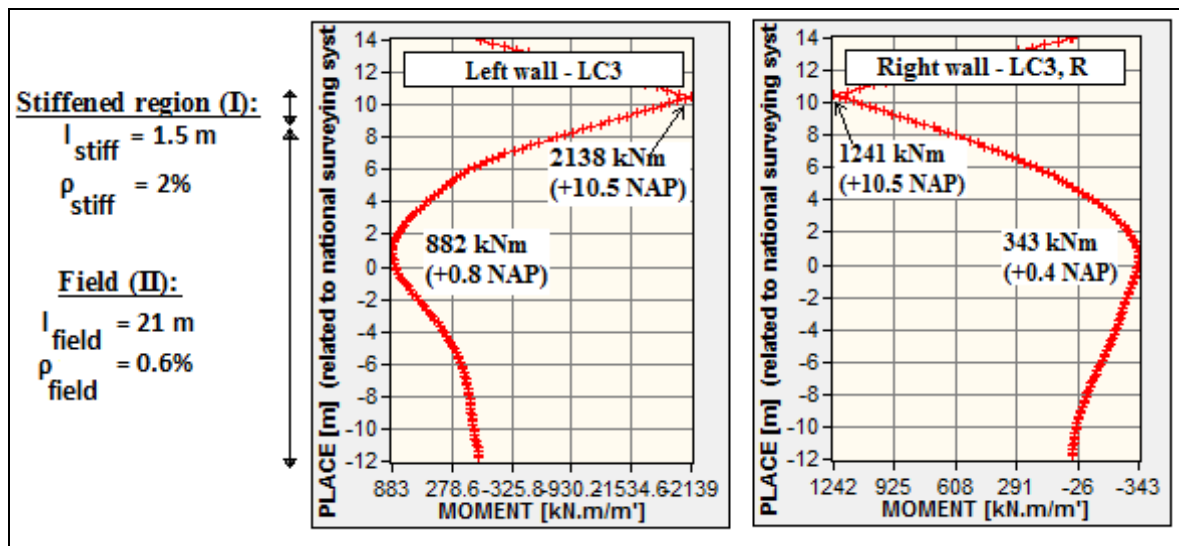


Figure 69: M-line both walls from PCSheetPileWall (clamped connection, $N \neq 0 \text{ kN}$)

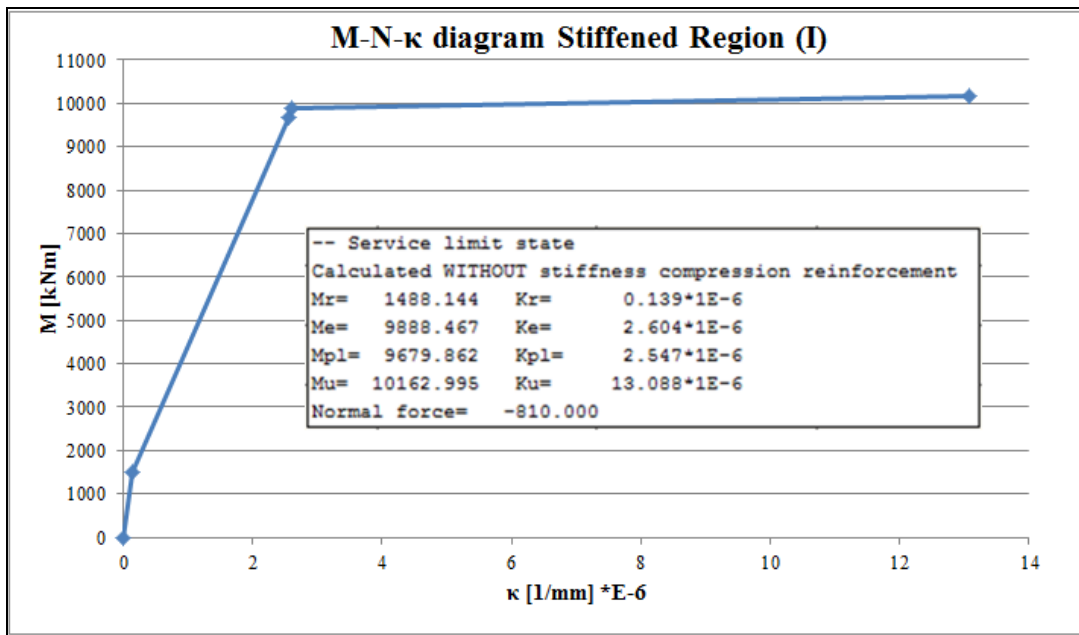


Figure 70: M-N-κ diagram both walls for the Stiffened Region (I)

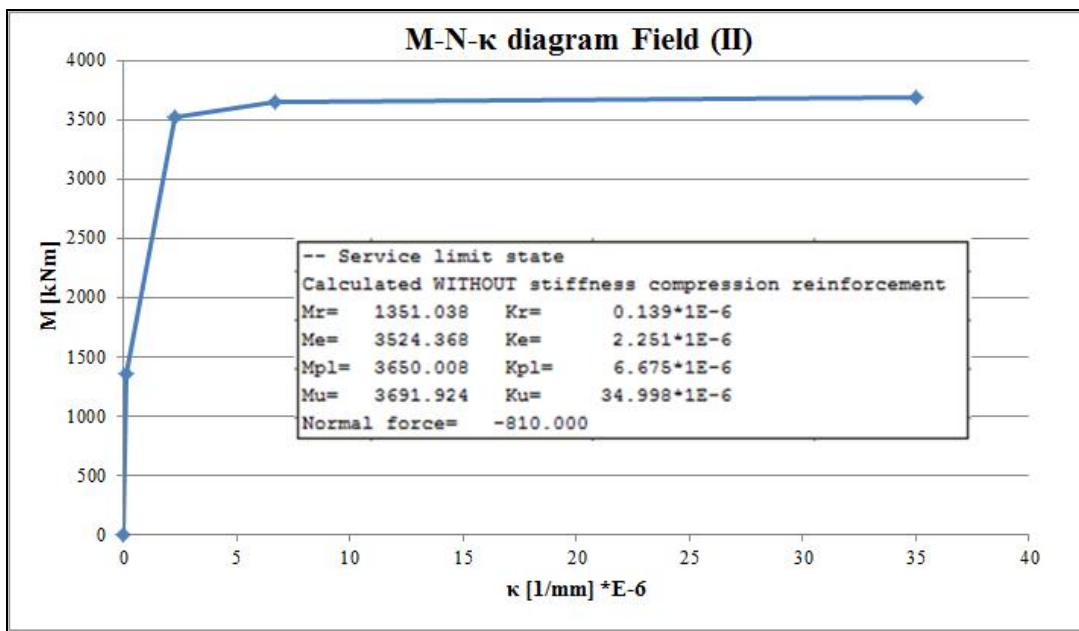


Figure 71: M-N-κ diagram both walls for the Field (II)

	Zone	Cracked/ uncracked	Length	From	To	EI	EA	E	d_{eq}
			[m]	[m]	[m]	[kNm ² /m']	[kN/m']	[MPa]	[m]
Left wall	1	cracked	1.3	10.5	9.2	7.22E+06	3.85E+07	25669	1.5
	2	uncracked	0.3	9.2	8.9	1.05E+07	5.63E+07	37507	1.5
	3	cracked	0.2	8.9	8.7	8.11E+06	4.33E+07	28837	1.5
	4	uncracked	20.7	8.7	-12	9.67E+06	5.16E+07	34381	1.5
Right wall	1	uncracked	1.5	10.5	9	1.05E+07	5.63E+07	37507	1.5
	2	uncracked	21	9	-12	9.67E+06	5.16E+07	34381	1.5

Table 40: EI-distribution of both walls obtained from PCSheetPileWall

4.2.4.2. Plaxis 2D – Half Model

The Plaxis 2D – Half Model is used to validate the EI-distribution of the left wall (half model) obtained from PCSheetPileWall. Therefore, the M-line of the Half Models is checked in both programs. The main input in Plaxis 2D consists of:

- The EI-distribution for the left wall according to Table 40;
- $w_{plate} = 23$ kN/m/m' for the diaphragm wall in order to simulate $N_{self\ weight} \neq 0$ in PCSheetPileWall;
- $R_{inter} = 1$ (no friction between soil and wall) in order to simulate $N_{shear\ force} = 0$ in PCSheetPileWall;
- Fixed-end anchor plus rotation fixity (beams) to simulate the clamped wall-roof connection (see Figure 72a).

The deformed mesh and the M-line for the left wall obtained in Plaxis 2D for EI_{var} are given in Figure 72. The results obtained with EI_0 , EI_{∞} and EI_{var} are given in Table 41. It is obvious that the $M_{clamped}$ with EI_{var} lies within the outer boundaries. Compared with PCSheetPileWall the $M_{clamped}$ for EI_{var} differs with about 19% from the Plaxis 2D – Half Model (2540 vs. 2138 kNm).

EI	δ_v [mm]	$M_{clamped}$ [kNm/m']	M_{field} [kNm/m']	U_x [mm]
EI_0	72	2630	1020	16
EI_{∞}	76	2340	1000	-16
EI_{var}	73	2540	1190	16

Table 41: Results in Plaxis 2D – Half Model for EI_0 , EI_{∞} and EI_{var}

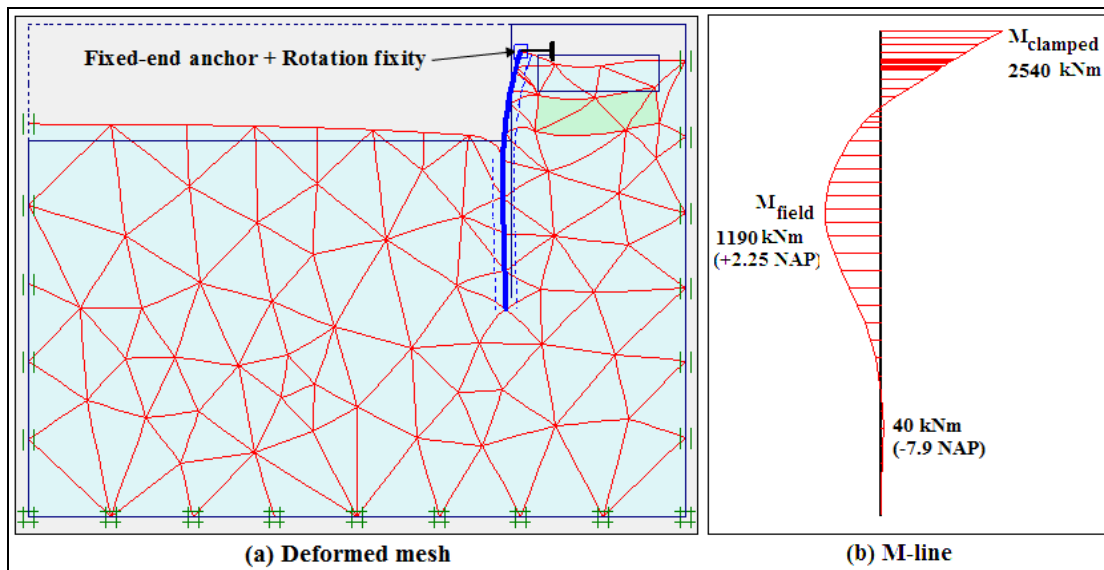


Figure 72: (a) Deformed mesh and (b) M-line of left wall for EI_{var} in Plaxis 2D – Half Model

4.2.4.3. Plaxis 2D – Total Model

With the Plaxis 2D – Total Model the M-line and EI-distribution of the right wall are checked with those according to PCSheetPileWall. The main input in Plaxis 2D consists of:

- The EI-distribution for both walls according to Table 40. Note that the right wall is totally uncracked according to PCSheetPileWall;
- $w_{plate} = 23 \text{ kN/m/m}^2$ for both diaphragm walls in order to simulate $N_{self\ weight} \neq 0$;
- $w_{fict.plate} = 84 \text{ kN/m/m}^2$ for the fictitious rigid plate, because in PCSheetPileWall the axial force of the fictitious rigid plate due to its self weight is also included;
- $R_{inter} = 1$ (no friction between soil and wall) in order to simulate $N_{shear\ force} = 0$;
- Stiff structure above the diaphragm walls to simulate the clamped connection in the Plaxis 2D –Total Model. The stiff structure consists of rigid plates connected by struts (see Figure 73a).

The M-line obtained from the Plaxis 2D – Total Model is depicted in Figure 73b, showing clearly that the right wall is more heavily loaded in the field than the left wall. It is obvious that the right wall, in contrast to PCSheetPileWall, must be cracked in both the stiffened region and the field. It is found that:

- In the stiffened region: $M_{clamped} > M_r$ (I) and;
- In the field $M_{field} > M_r$ (II).

Since the EI-distribution for the right wall according to PCSheetPileWall is not valid anymore, iteration procedure 1 is set up to find the cracked height and the actual EI-distribution for this wall.

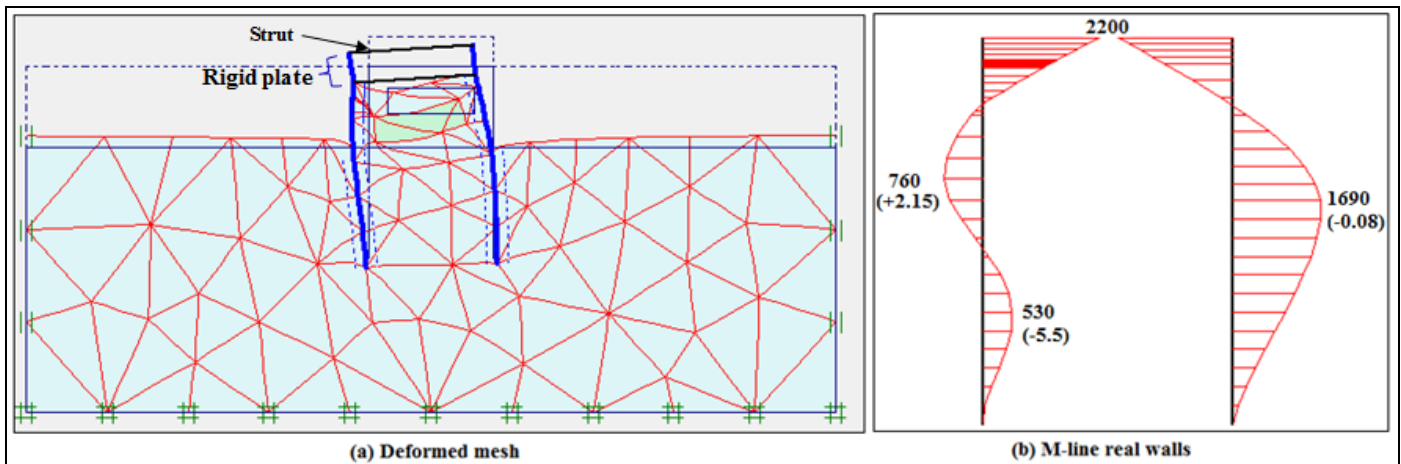


Figure 73: Clamped case - (a) Deformed mesh and (b) M-line for the walls only at $N \neq 0$ kN

4.2.4.4. Iteration procedure 1 – right wall

Iteration procedure 1 is conducted to find the cracked height and the corresponding EI-distribution of the right wall. The following assumptions were made for:

- The left wall: The EI-distribution according to PCSheetPileWall will be maintained with each iteration (see Table 40);
- The right wall: The 1st assumption is that the right wall is totally uncracked, thereby using the uncracked stiffness according to PCSheetPileWall (see Table 40).

The determination of the cracked height ($l_{cr,I}$ and $l_{cr,II}$) and their corresponding EI ($(EI)_{Ed,min,I}$ and $(EI)_{Ed,min,II}$) will take place in the same way as explained in section 4.2.3.4. The steps to be taken in the iteration process for the right wall have also been explained thoroughly in this section. For all the iterations in case of EI (κ , N) reference is made to Appendix C4.

An overview of the iteration results for the right wall is given in Table 42, observing a jump between the even and uneven iterations with regard to the cracked zones $l_{cr,I}$ and $l_{cr,II}$. The observed cracking pattern for the even and uneven iteration is similarly as depicted in Figure 63.

Iteration #	$l_{cr,I}$ [m]	$l_{cr,II}$ [m]
1	1.2	6.5
2	1.5	0
3	1	6.8
4	1.5	0.3
5	1	6.9
6	1.5	0.4

Table 42: Results iteration process right wall for $N \neq 0$ kN – clamped connection

Similarly as observed in section 4.2.3.4, where $N = 0$ kN, the iteration procedure for the right wall comes to a standstill. In this case the average result of iteration # 5 and 6 are considered as input for the right wall. The obtained result will then be compared with the result obtained with iteration procedure 2.

Iteration procedure 1, steps (right wall only):

Points of departure:

1. The EI-distribution of the left wall is according to PCSheetPileWall;
2. The EI-distribution of the right wall is based on the average result of iteration #5 and 6, as depicted in Figure 74. The average cracked zones and the average M-line are determined for the right wall. From the average M-line the EI and EA are derived;
3. The above is used as input for the Plaxis 2D – Total Model, see Table 43. This input results in Figure 75, showing the final result for EI_{var} according to iteration procedure 1.

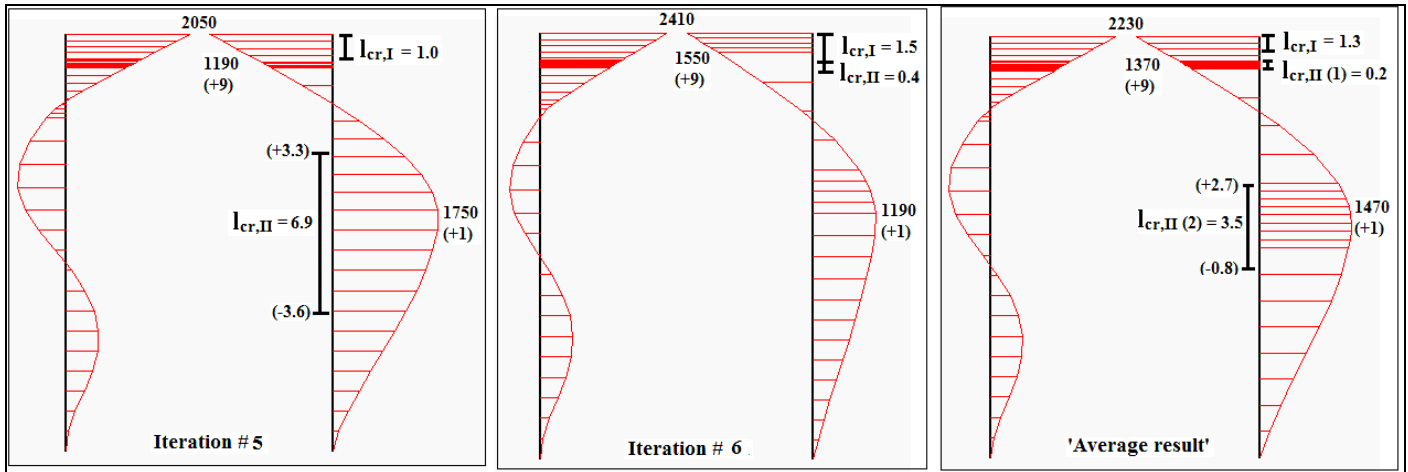


Figure 74: The assumed ‘average result’ for the right wall based on iteration #5 and #6. (Note: Bending moment values in kNm, cracked zones in m, and levels with regard to NAP are placed between brackets)

	Zone	Cracked/ uncracked	Length	From	To	$M_{Ed,average}$	EI	EA
			[m]	[m]	[m]	[kNm/m']	[kNm ² /m']	[kN/m']
Left wall <i>(from PCSheet-PileWall)</i>	1	cracked	1.3	10.5	9.2	-	7.22E+06	3.85E+07
	2	uncracked	0.3	9.2	8.9	-	1.05E+07	5.63E+07
	3	cracked	0.2	8.9	8.7	-	8.11E+06	4.33E+07
	4	uncracked	20.7	8.7	-12	-	9.67E+06	5.16E+07
Right wall <i>(from 'average result' iterations)</i>	1	cracked	1.3	10.5	9.2	2230	6.25E+06	3.33E+07
	2	uncracked	0.2	9.2	9	-	1.05E+07	5.63E+07
	3	cracked	0.2	9	8.8	1370	8.70E+06	4.64E+07
	4	uncracked	6.1	8.8	2.7	-	9.67E+06	5.16E+07
	5	cracked	3.5	2.7	-0.8	1470	5.77E+06	3.08E+07
	6	uncracked	11.2	-0.8	-12	-	9.67E+06	5.16E+07

Table 43: EI-distribution for both walls used as input in Plaxis 2D – Total Model for iteration procedure 1

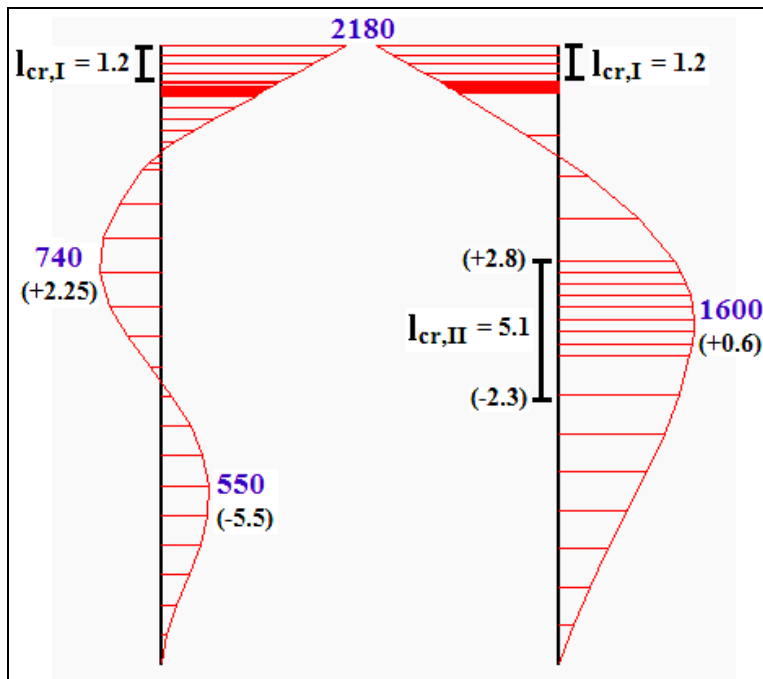


Figure 75: Final result EI_{var} according to iteration procedure 1 in Plaxis 2D – Total Model. (Note: Bending moment values in kNm, cracked zones in m, and levels with regard to NAP are placed between brackets)

4.2.4.5. Iteration procedure 2 – both walls

Iteration procedure 2 is set up to verify the final result of iteration procedure 1. The applied strategy has already been explained in section 4.1.1.6.

Iteration procedure 2, steps:

1. Determine the average M-line and the average cracked zones from EI_0 and EI_∞ for both walls. This is depicted as the ‘average result’ in Figure 76.
2. Based on the average bending moment, the EI and EA are determined for the average cracked zones. The input in the Plaxis 2D – Total Model for the left and the right wall are given in Table 44. This input results in Figure 77, showing the final result for EI_{var} according to iteration procedure 2.

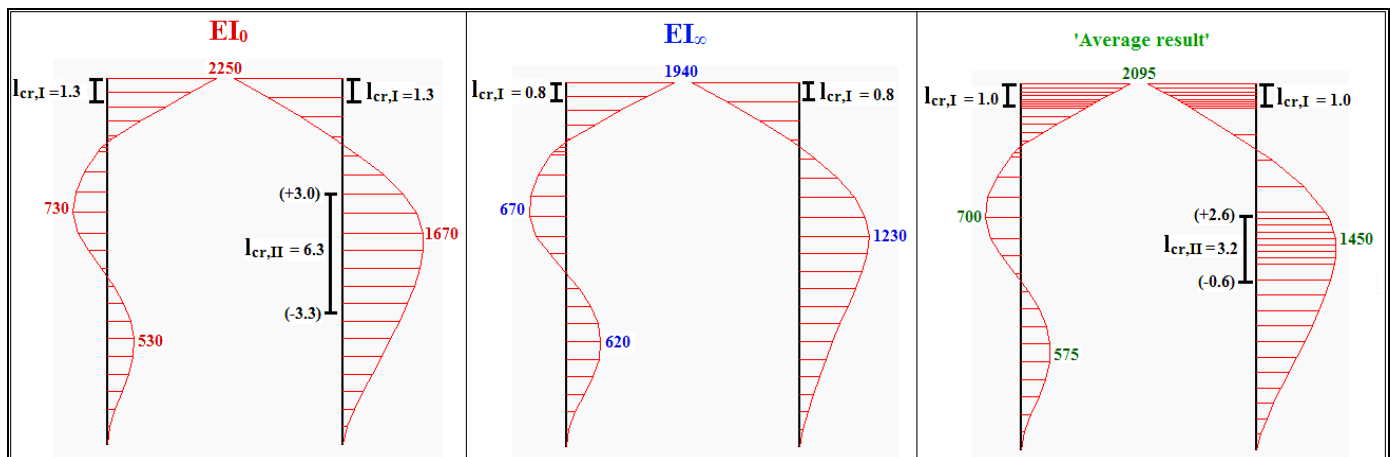


Figure 76: The ‘average result’ based on EI_0 and EI_∞ . (Note: Bending moment values in kNm, cracked zones in m, and levels with regard to NAP are placed between brackets)

	Zone	Cracked/ uncracked	Length	From	To	$M_{Ed,average}$	EI	EA
			[m]	[m]	[m]	[kNm/m']	[kNm ² /m']	[kN/m']
Left wall	1	cracked	1	10.5	9.5	2095	6.60E+06	3.52E+07
	2	uncracked	0.5	9.5	9	-	1.05E+07	5.63E+07
	3	uncracked	21	9	-12	-	9.67E+06	5.16E+07
Right wall	1	cracked	1	10.5	9.5	2095	6.60E+06	3.52E+07
	2	uncracked	0.5	9.5	9	-	1.05E+07	5.63E+07
	3	uncracked	6.4	9	2.6	-	9.67E+06	5.16E+07
	4	cracked	3.2	2.6	-0.6	1450	6.17E+06	3.29E+07
	5	uncracked	11.4	-0.6	-12	-	9.67E+06	5.16E+07

Table 44: EI-distribution for both walls used as input in Plaxis 2D – Total Model for iteration procedure 2

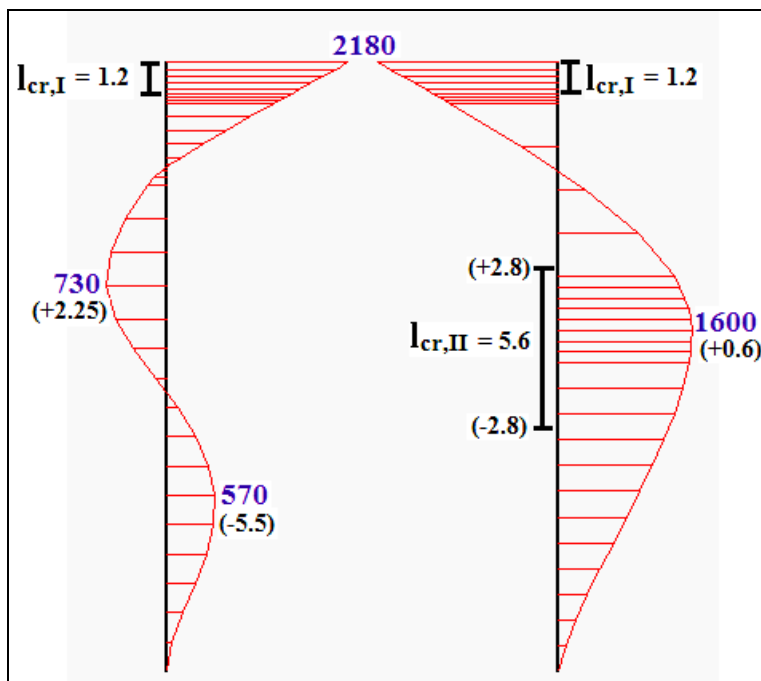


Figure 77: Final result EI_{var} according to iteration procedure 2 in Plaxis 2D – Total Model. (Note: Bending moment values in kNm, cracked zones in m, and levels with regard to NAP are placed between brackets)

Results iteration procedure 1 vs. iteration procedure 2:

On comparison of the final result according to iteration procedure 1 and iteration procedure 2 (Figure 75 vs. Figure 77) it can be observed that the cracking pattern and the M-line configuration are similar. Noteworthy is that according to both procedures the stiffened region appears to be cracked for 80% (1.2 m). While iteration procedure 2 requires only one iteration for both walls, an intensive iteration process is performed according to iteration procedure 1. With this last case it has been proven that:

The results of iteration procedure 2 are valid for EI_{var} for every case. It is independent of the connection type between wall-roof and the inclusion of the axial force in the determination of the bending stiffness.

4.2.4.6. Final results EI (κ , N)

The M-line of both walls for EI₀, EI_∞ and EI_{var} is given in Figure 78. The reported values in Table 45 concern the maximum values for the occurring bending moment (M_{Ed}), the settlement (δ_v) and the lateral wall displacement (U_x). Based on these results the following conclusions can be drawn:

- In the field the right wall (without braking forces on it) appears to be more heavily loaded than the left wall. This is the case for EI₀, EI_∞ and EI_{var}. The governing bending moments are the clamped moments (M_{clamped}), which are equal for both walls;
- The right wall has the largest lateral displacement (in the direction of the braking force) for EI₀, EI_∞ and EI_{var};
- The results obtained with EI_{var} lie within the results obtained for the outer boundaries EI₀ and EI_∞. The results with EI_{var} are just about the same as with EI₀;
- For EI_{var} both walls crack over 80% of the stiffened region (l_{stiff} = 1.5m, ρ_{stiff} = 2%) in case the axial force of the wall (N_{self weight}) is included. In case N = 0 kN the stiffened region cracked over its full height. Nevertheless, it can be concluded that the clamped connection is not practicable.

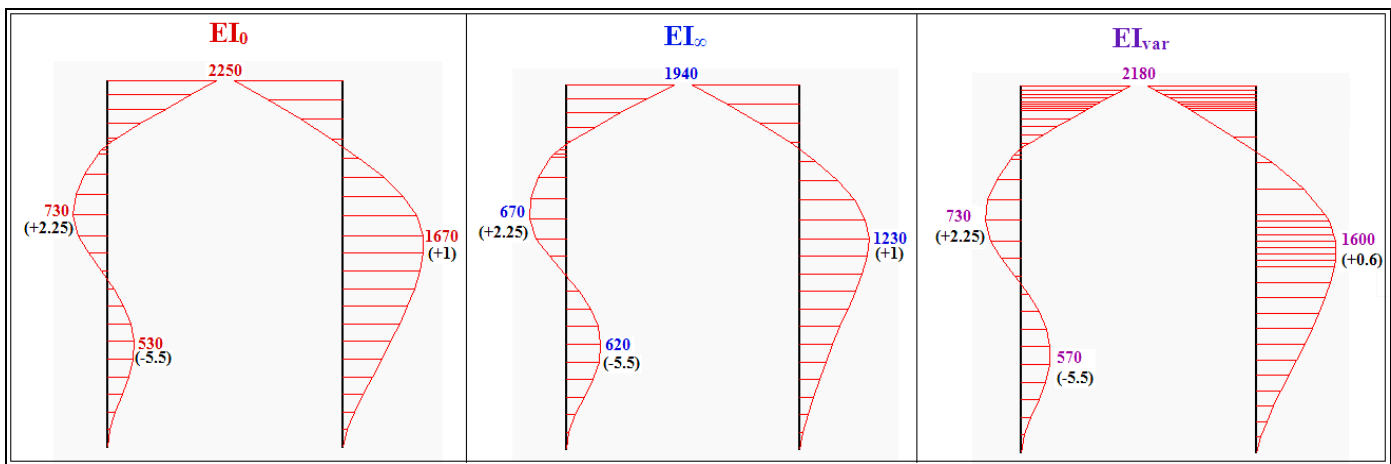


Figure 78: M-line for EI₀, EI_∞ and EI_{var} for N ≠ 0 kN
(Note: Bending moment values in kNm and levels with regard to NAP are placed between brackets)

	M _{Ed} [kNm/m']	δ _v [mm]	U _x [mm]	
			Left wall	Right wall
EI ₀	2250	69	-38	-42
EI _∞	1940	81	-49	-54
EI _{var}	2180	70	-38	-42

Table 45: Clamped case - Final results for EI₀, EI_∞ and EI_{var} for N ≠ 0 kN

4.3. Evaluation iteration procedure EI_{var}

Calculations based on EI_{var} concern an iterative procedure. In finding the actual EI-distribution of the walls for a hinged and a clamped wall-roof connection two different iteration procedures were developed. The points of departure for both iteration procedures are summarized in the following.

Iteration procedure 1:

- Maintain the EI-distribution of the left wall according to PCSheetPileWall;
- Perform an iterative process for the right wall to find its actual EI-distribution. This is obtained by using the Plaxis 2D –Total Model;
- Many iterations are required for the right wall.

Iteration procedure 2:

- For both walls the average M-line and the average cracked zone are determined based on the results for EI_0 and EI_{∞} ;
- The average M-line is used to determine the EI-distribution of both walls;
- Only 1 iteration is required for both walls to reach a similar cracking pattern as obtained with iteration procedure 1.

In all the studied cases of the “walls only” the points of departure for iteration procedure 2 with regard to the cracked zones were found to be more reliable compared to iteration procedure 1. The results of iteration procedure 2 have proven to be valid for EI_{var} in all the previous studied cases. Therefore, the results of all the remaining cases to be investigated yet are also based on iteration procedure 2.

4.4. Walls and roof; hinged

By adding the roof, which is approached by the equivalent beam model, to the walls in Plaxis 2D it is found that the results for the case "Walls and roof; hinged" are nearly the same as for the case "Walls only; hinged". Because of the hinged connection there is no bending moment transfer between the walls and the roof. The roof stiffness is irrelevant for the moment distribution of the walls, the obtained settlements and the lateral wall displacements. Therefore, the results of the case "Walls and roof; hinged" are not reported and will also not be dealt with further.

4.5. Walls and roof; clamped

In the Plaxis 2D – Total Model the roof, which is approached by the equivalent beam model, is added to the walls for EI_0 , EI_{∞} and EI_{var} . The behaviour of the total packing structure and the M-line configuration are depicted in Figure 79.

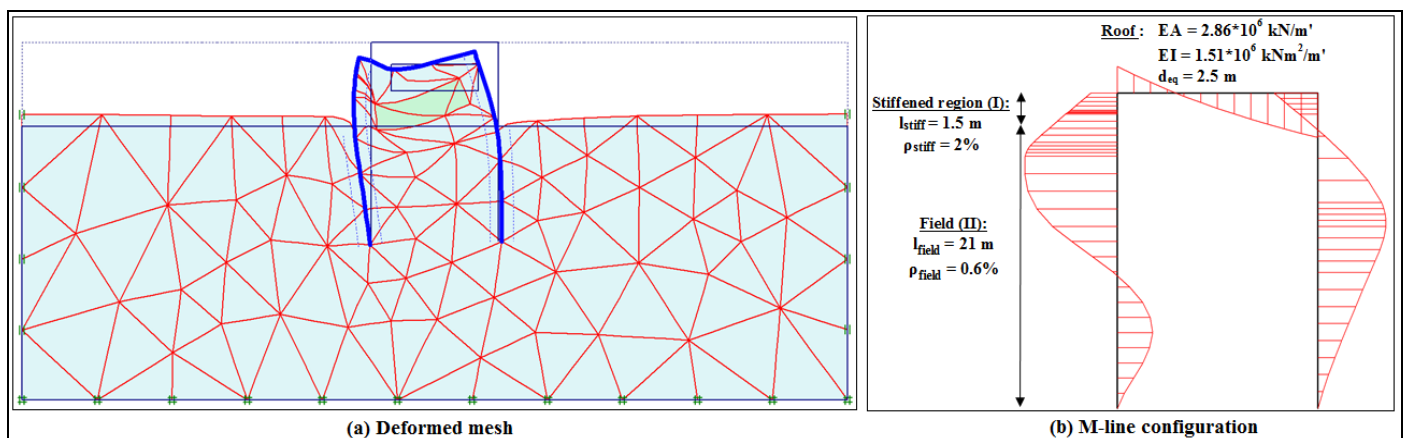


Figure 79: Clamped case – (a) Behaviour of the total packing structure and (b) the corresponding M-line configuration

4.5.1. Case a: EI (κ)

The M-line and the cracked zones of both walls for EI_0 , EI_∞ and EI_{var} at $N = 0$ kN are given in Figure 80. Note that the cracked zones for EI_0 and EI_∞ are imaginary and are only used to determine the cracked zones for EI_{var} . From this figure it can be observed that the cracked zones obtained with EI_{var} lie within the imaginary cracked zones obtained at the outer boundaries. The reported values in Table 46 concern the maximum values for M_{Ed} , δ_v and U_x obtained at the 3 stiffnesses in the Plaxis 2D – Total Model. The right wall has the largest lateral displacement (in the direction of the braking force) for EI_0 , EI_∞ and EI_{var} . The δ_v and U_x obtained with EI_{var} are found to be lying within the outer boundaries, while this is not the case for M_{Ed} .

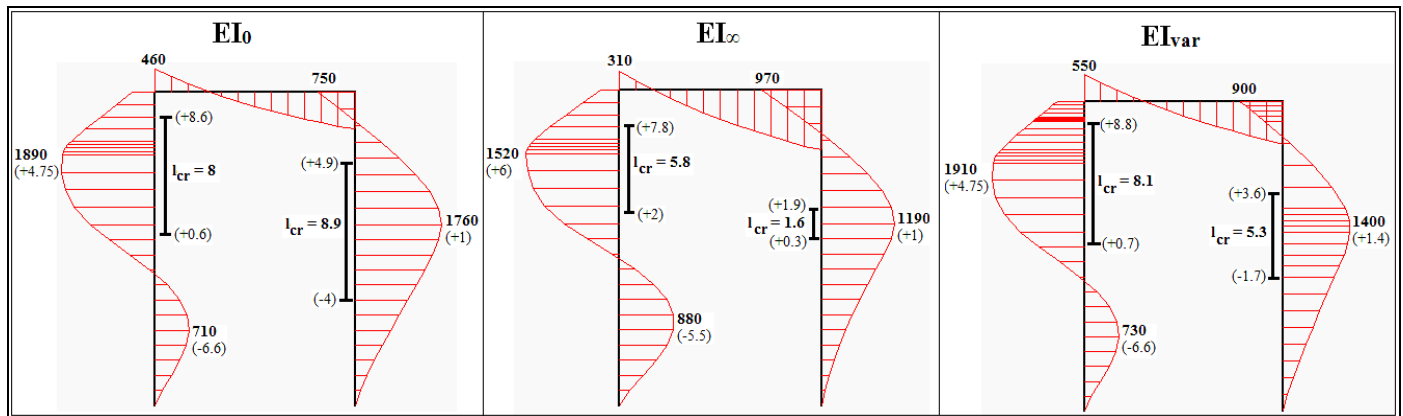


Figure 80: Clamped case – The M-line and cracked zones of the total structure for EI_0 , EI_∞ and EI_{var} at $N = 0$ kN

	M_{Ed} [kNm/m']	δ_v [mm]	U_x [mm]	
			Left wall	Right wall
EI_0	1890	86	-38	-51
EI_∞	1520	101	-51	-63
EI_{var}	1910	89	-41	-55

Table 46: Clamped case - Final results for the total structure for EI_0 , EI_∞ and EI_{var} at $N = 0$ kN

4.5.2. Case b: EI (κ , N)

The M-line and the cracked zones of both walls for EI_0 , EI_∞ and EI_{var} at $N \neq 0$ kN are given in Figure 81. Note that the cracked zones for EI_0 and EI_∞ are imaginary and are only used to determine the cracked zones for EI_{var} . From this figure it can be observed that the cracked zones obtained with EI_{var} lie within the imaginary cracked zones obtained at the outer boundaries. The load distribution for EI_{var} is almost similar as for EI_0 . The reported values in Table 47 concern the maximum values for M_{Ed} , δ_v and U_x obtained at the 3 stiffnesses in the Plaxis 2D – Total Model. The right wall has the largest lateral displacement (in the direction of the braking force) for EI_0 , EI_∞ and EI_{var} . The M_{Ed} , δ_v and U_x obtained with EI_{var} are found to be lying within the outer boundaries. It is observed that the results with EI_{var} are heading towards the behaviour at EI_0 .

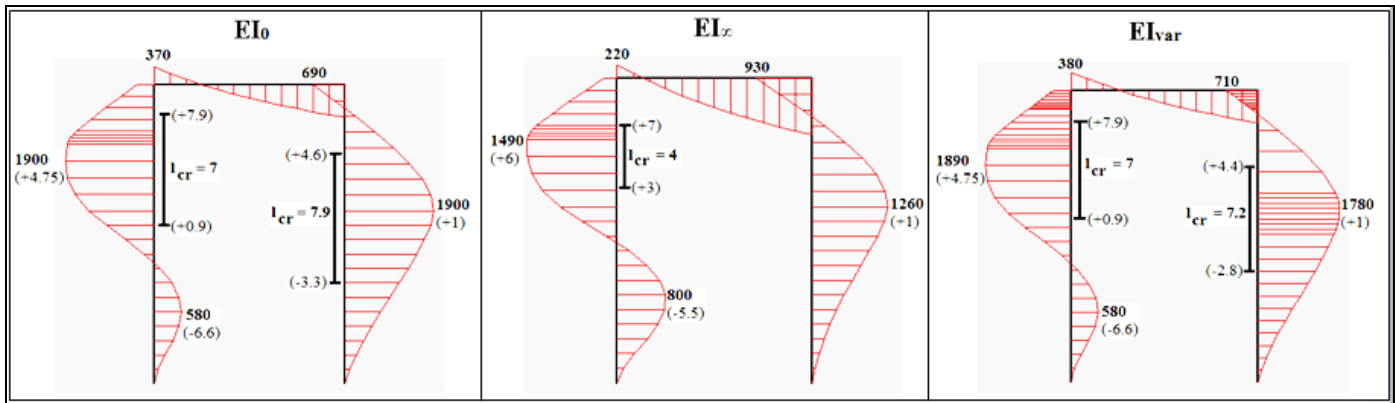


Figure 81: Clamped case – The M-line and cracked zones of the total structure for EI_0 , EI_∞ and EI_{var} at $N \neq 0$ kN

	M_{Ed} [kNm/m']	δ_v [mm]	U_v [mm]	
			Left wall	Right wall
EI_0	1900	97	-41	-54
EI_∞	1490	112	-54	-65
EI_{var}	1890	97	-41	-55

Table 47: Clamped case - Final results for the total structure for EI_0 , EI_∞ and EI_{var} at $N \neq 0$ kN

4.5.3. Impact roof stiffness

If one only considers the walls for the clamped case (see section 4.2), a relatively high $M_{clamped}$ (2100-2200 kNm) is obtained leading to an (almost) totally cracked stiffened region. Moreover, the right wall appears to be more heavily loaded in the field than the left wall. The opposite occurs by including the roof, noticing a drastical reduction of the $M_{clamped}$. From both Figure 80 and Figure 81 it can be stated that:

By including the roof the stiffened region does not crack anymore and the left wall is now more heavily loaded in the field. The roof stiffness is apparently so small that the connection acts more towards a hinged connection.

In Figure 82 a comparison in the bending moment distribution has been made for the realistic roof stiffness (equivalent beam model) and a very stiff roof with a $d_{eq} = 3.5$ m. This was especially done to find out the impact of the roof stiffness on the loading of the walls. The following is observed:

- The transition from the realistic roof stiffness to a very stiff roof leads to a change in the sign of the $M_{clamped}$ for the left wall. As the roof stiffness decreases the M-line of the left wall is positioned more outwards. Hereby, it is found that the maximum M_{field} of the left wall for the hinged case (for which the roof stiffness is irrelevant) lies in between the field moments obtained at the realistic roof stiffness and a very stiff roof for the clamped case. Based on this phenomenon the more heavily loaded left wall in case of the realistic roof stiffness can be attributed to the fact that:

“By including a roof with a low bending stiffness, the rotation of the roof leads to an extra deformation of the left wall as a result of which a higher load can be exerted on the left wall.”

- By introducing a very stiff roof, it is proven that the wall stiffness indeed has a great impact on the loading of the walls. The walls are now less loaded. The maximum $M_{clamped}$ increases with a factor 3, making it almost impossible to reinforce the roof structure. In practice it becomes difficult to reinforce a structure with an $M_{clamped}$ greater than 2000 kNm/m'. It can be stated that:

“Although a very stiff roof results in less heavily loaded walls, a very stiff roof should be avoided for it becomes practically impossible to reinforce the roof structure.”

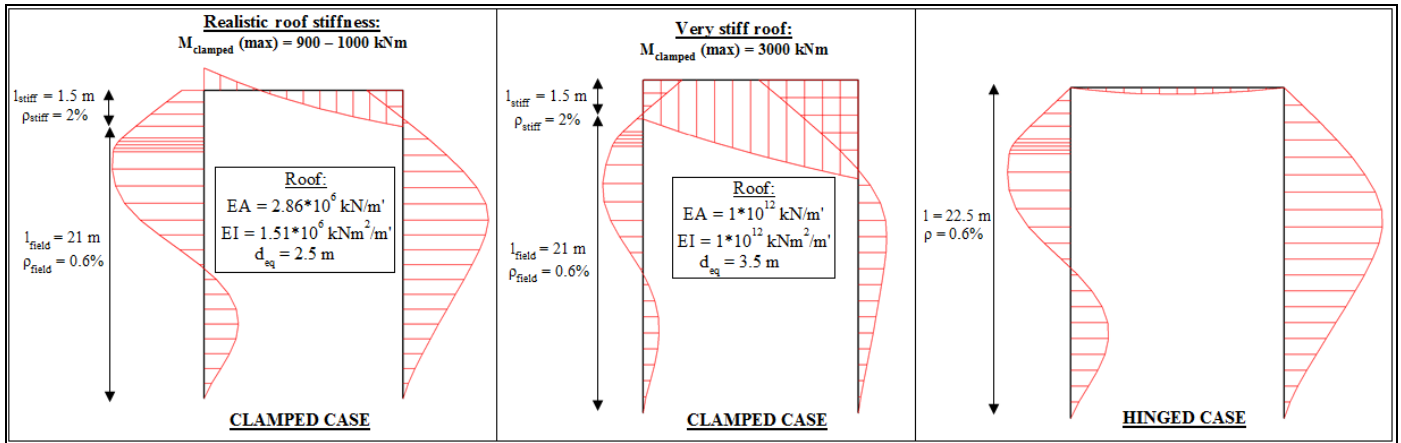


Figure 82: Impact roof stiffness on bending moment distribution

5. EVALUATION: SAFETY ANALYSIS

In this chapter a safety analysis is performed for EI_{var} . Therefore, a distinction is made between:

- The basic case : A basic reinforcement ratio is applied for the hinged and the clamped case;
- The hinged connection in particular: To determine whether the safety analysis for the hinged connection remains the same under different conditions, two extra variations are studied for the hinged case.

Throughout this research the reinforcement was the main input for determining the EI_{var} . For the hinged case a basic reinforcement ratio of $\rho_{l,tot} = 0.6\%$ per meter panel width was applied. For the clamped case a reinforcement pattern consisting of $\rho_{stiff} = 2\%$ over $l_{stiff} = 1.5$ m and $\rho_{field} = 0.6\%$ over $l_{field} = 21$ m, turned out to be the most strategic solution. These applied reinforcement ratios for the hinged and the clamped case are addressed to as *the basic reinforcement ratio*. First of all, the results obtained with the basic reinforcement ratio will be represented in section 5.1. This paragraph gives a total overview of the aimed results, in particular the maximum (absolute) values for the occurring bending moment (M_{Ed}), the settlement (δ_v) and the lateral wall displacement (U_x) for the different cases considered in chapter 4:

- Walls only; hinged
- Walls only; clamped
- Walls and roof; clamped.

For each case the results are represented at the 3 stiffnesses EI_0 , EI_∞ and EI_{var} at $N = 0$ kN and $N \neq 0$ kN. Based on these results a safety analysis is performed for EI_{var} at the basic reinforcement ratio.

Afterwards, two extra cases were investigated for the hinged connection in section 5.2. This concerns:

- A high reinforcement ratio of $\rho_{l,tot} = 1\%$ per meter panel width over the total wall height and;
- A different soil type.

The results obtained for EI_{var} at these two extra cases for the hinged connection are based on iteration procedure 2. For the clamped connection (“walls and roof”) no additional cases were investigated, because of the limited freedom of movement with regard to the reinforcement.

5.1. Basic reinforcement ratio – safety analysis

The results for the basic reinforcement ratio applied in the hinged and the clamped case are given in Table 48. For a good comparison with regard to the structural safety the results M_{Ed} , δ_v and U_x are plotted in Figure 83, Figure 84 and Figure 85, respectively.

	Case		Bending moment		Settlement		Lateral wall displacement	
			M_{Ed} [kNm/m']		δ_v [mm]		U_x [mm]	
	#	EI	N = 0	N ≠ 0	N = 0	N ≠ 0	N = 0	N ≠ 0
WALLS ONLY; HINGED	1	EI_0	2390	2430	91	101	62	63
	2	EI_∞	1750	1780	112	121	85	84
	3	EI_{var}	1470	1690	118	115	92	82
WALLS ONLY; CLAMPED	4	EI_0	2120	2250	54	69	37	42
	5	EI_∞	1820	1940	64	81	50	54
	6	EI_{var}	2140	2180	57	70	42	42
WALLS + ROOF; CLAMPED	7	EI_0	1890	1900	86	97	51	54
	8	EI_∞	1520	1490	101	112	63	65
	9	EI_{var}	1910	1890	89	97	55	55

Table 48: Basic reinforcement ratio – Overview of results for the hinged and clamped case

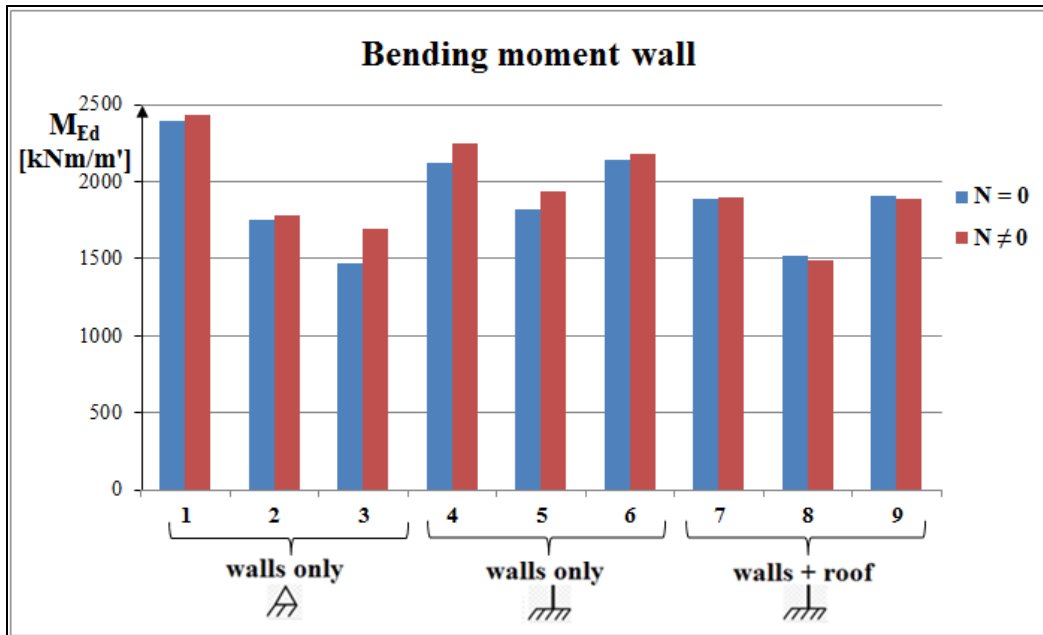


Figure 83: Basic reinforcement ratio – Maximum occurring bending moment of the walls for the hinged and clamped case

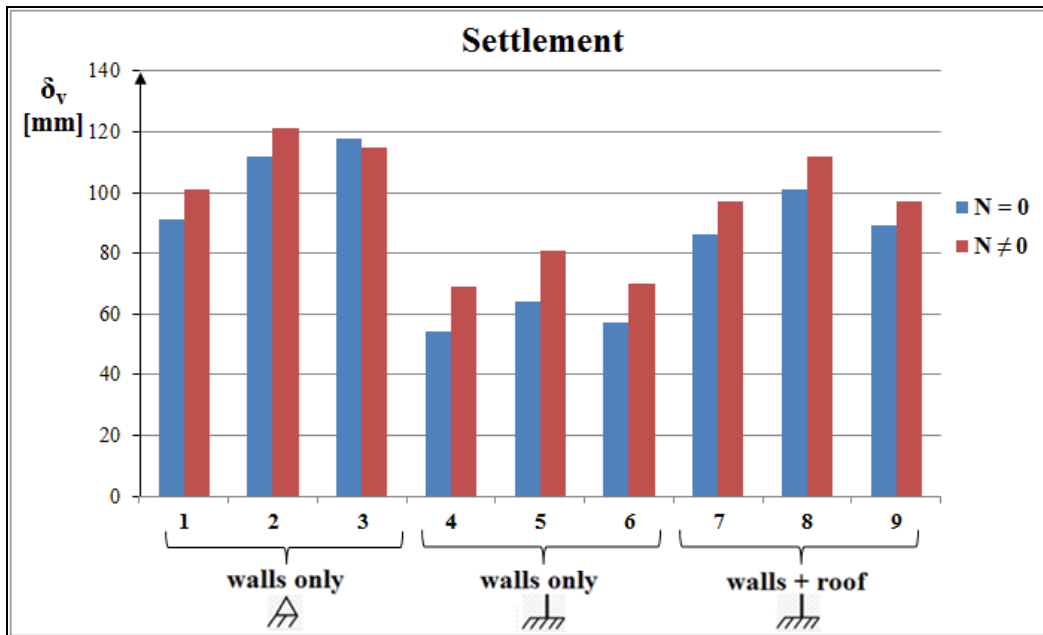


Figure 84: Basic reinforcement ratio – Maximum settlement of the foundation for the hinged and clamped case

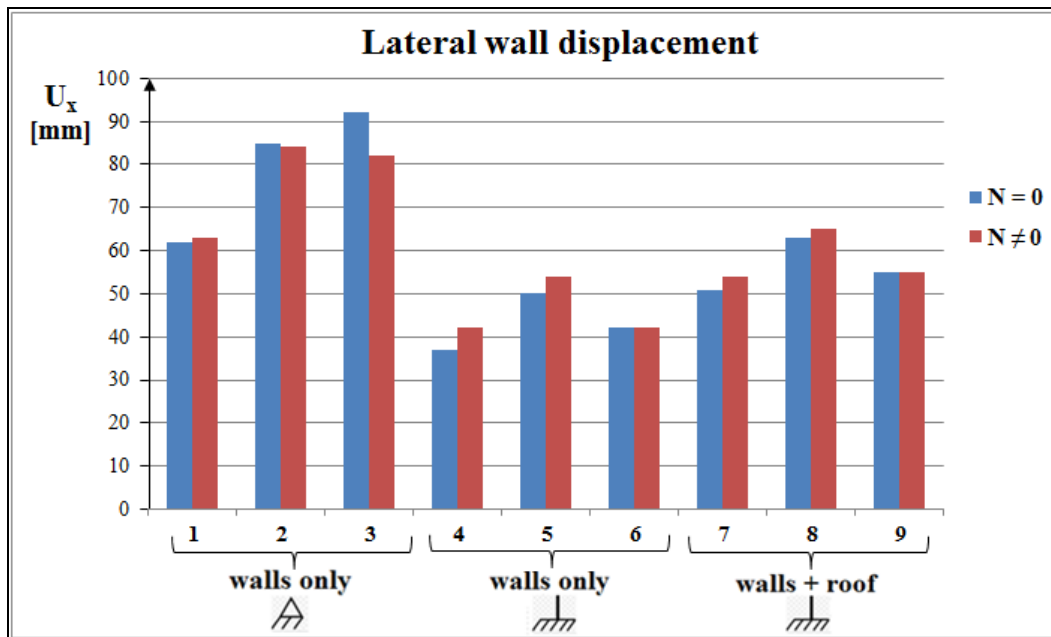


Figure 85: Basic reinforcement ratio – Maximum lateral wall displacement for the hinged and clamped case

Analysis of results:

From the results in Table 48 it follows that in general, the presence of an axial force does not have a significant impact on the occurring bending moment M_{Ed} of the diaphragm walls. This is evidenced by comparing Figure 42 and Figure 53 for the hinged case, and by comparing Figure 80 and Figure 81 for the clamped case ('walls and roof'). Based on these findings it can be stated that:

The axial force (N) does not have a significant influence on the realistic stiffness EI_{var} .

Based on the graphs in Figure 83, Figure 84 and Figure 85 a safety analysis is performed for EI_{var} . Herewith, a certain tendency is observed in the structural behaviour. The following can be stated for the:

▪ Walls only; hinged:

❖ EI_0 vs. EI_{var} (case 1 vs. 3):

- From Figure 83 it follows that M_{Ed} is higher for EI_0 than for EI_{var} . This implies that for a calculation based on EI_0 more reinforcement is required for the diaphragm wall, which is a safer approach;
- From Figure 84 it follows that δ_v is lower for EI_0 than for EI_{var} . This implies that the calculated settlements at EI_0 are lower than in reality;
- From Figure 85 it follows that U_x is lower for EI_0 than for EI_{var} . This implies that the calculated lateral wall displacements at EI_0 are lower than in reality.

❖ EI_∞ vs. EI_{var} (case 2 vs. 3):

- From Figure 83, Figure 84 and Figure 85 it can be stated that M_{Ed} , δ_v and U_x for the stiffnesses EI_∞ and EI_{var} are almost similar. From this it follows that the analysis with EI_∞ is a very good analysis for the hinged case; the iteration process for EI_{var} can be omitted since the results of $EI_{var} \approx EI_\infty$.

Based on the safety analysis for the case "Walls only; hinged" it can be stated that:

For the 'Waalbrug-project', where a hinged wall-roof connection has been applied, the packing structure could have been designed based on the totally cracked stiffness EI_∞ for the diaphragm walls.

▪ **Walls and roof; clamped:**

❖ **EI_0 vs. EI_{var} (case 7 vs. 9):**

- From Figure 83, Figure 84 and Figure 85 it can be stated that M_{Ed} , δ_v and U_x for the stiffnesses EI_0 and EI_{var} are almost similar. From this it follows that the analysis with EI_0 is a very good analysis for the clamped case; the iteration process for EI_{var} can be omitted since the results of $EI_{var} \approx EI_0$.

❖ **EI_∞ vs. EI_{var} (case 8 vs. 9):**

- From Figure 83 it follows that M_{Ed} is lower for EI_∞ than for EI_{var} . This implies that for a calculation based on EI_∞ the bending moment is underestimated with the risk of placing less reinforcement than required in reality;
- From Figure 84 it follows that δ_v is higher for EI_∞ than for EI_{var} . This implies that the calculated settlements at EI_∞ are higher than in reality, which is a safe approach (conservative);
- From Figure 85 it follows that U_x is higher for EI_∞ than for EI_{var} . This implies that the calculated lateral wall displacements at EI_∞ are higher than in reality, which is a safe approach (conservative).

▪ **Walls only; clamped:**

For this case no safety analysis has been performed for EI_{var} , since it was observed that (almost) the total stiffened region cracked. However, from the graphs in Figure 83, Figure 84 and Figure 85 it is obvious that the results for EI_{var} at “Walls and roof; clamped” lie in between the results for EI_{var} obtained for “Walls only; hinged” and “Walls only; clamped”. This phenomenon is observed for M_{Ed} , δ_v and U_x , where case 9 lies in between the cases 3 and 6. Noteworthy is that for the deformations δ_v and U_x the results obtained at each of the stiffnesses EI_0 , EI_∞ and EI_{var} for “Walls and roof; clamped” always lie in between the results for “Walls only; hinged” and “Walls only; clamped”. This does not hold for M_{Ed} .

From the safety analysis performed for EI_{var} at the “Walls only; hinged” and the “Walls and roof; clamped” the following can be stated:

For the hinged case, an analysis based on:

- EI_0 : - is a wrong analysis for δ_v and U_x
: - is a correct analysis for M_{Ed} (safe approach)
- EI_∞ : - is a very good analysis, since the results for $EI_{var} \approx EI_\infty$

For the clamped case (walls and roof), an analysis based on:

- EI_∞ : - is a wrong analysis for M_{Ed}
: - is a correct analysis for δ_v and U_x (safe approach)
- EI_0 : - is a very good analysis, since the results for $EI_{var} \approx EI_0$

The behaviour at the clamped case (walls and roof) is the exact opposite of the behaviour at the hinged case. It is remarkable that at both the hinged case and the clamped case an error can be made in the structural safety. For the hinged case the packing structure is totally safe if the walls are designed based on the totally cracked stiffness EI_∞ , while for the clamped case a totally safe design is reached by applying the totally uncracked stiffness EI_0 for the walls. Since from the analysis it is proven that the results with EI_{var} may also lie outside the outer boundaries EI_0 and EI_∞ , it can be concluded that:

A calculation procedure based on EI_{var} is always a safe method.

An incorrect way of thinking is that calculations based on EI_0 are always safe (conservative). This is especially emphasized by the hinged case, where the actual deformations are much greater than the

calculated deformations based on EI_0 . This can be logically explained by the fact that a more rigid structure deforms less. With EI_{var} there is a variation of stiff and less stiff parts over the wall height, as a result of which the load distribution and deformations will be different from a totally uncracked or totally cracked wall. The occurring load distribution and the displacements are a result of the mutual relationship between the wall stiffness, the soil stiffness and the applied wall – roof connection.

5.2. Variations hinged connection

In order to investigate whether the structural safety based on the basic reinforcement ratio of $\rho_{1,tot} = 0.6\%$ for the hinged case changes, two variations were made for the hinged case. This is dealt with in section 5.2.1 and 5.2.2. Eventually, a comparison is made between the basic case and the two variations in section 5.2.3.

5.2.1. High reinforcement ratio

For the first variation in the hinged case, the walls were made stiffer by introducing a high reinforcement ratio of $\rho_{1,tot} = 1\%$. The basic reinforcement ratio of $\rho_{1,tot} = 0.6\%$ is an optimized value calculated for the “Waalbrug-project”. If $\rho_{1,tot} < 0.6\%$, one encounters:

- Brittle failure by steel rupture (not enough reinforcement) or;
- An unstable diaphragm wall ($M_{Ed} > M_u$).

Therefore, the impact of EI_{var} on the structural safety had to be examined for $\rho_{1,tot} \geq 0.6\%$.

In this case:

- The soil properties remain the same, according to 3.4.2.1, Table 14;
- The realistic wall stiffness (EI_{var}) changes due to $\rho_{1,tot} = 1\%$. This implies that the structural behaviour at EI_{var} will be different compared to the basic case with $\rho_{1,tot} = 0.6\%$. Nevertheless, the behaviour for EI_0 and EI_{∞} will be the same for both reinforcement ratios, since the soil properties in the Plaxis 2D – Total Model are maintained.

The input and results obtained with iteration procedure 2 for EI_{var} based on $\rho_{1,tot} = 1\%$ at $N = 0$ kN and $N \neq 0$ are given in Appendix E1 and E2, respectively. The M-(N)- κ diagrams, the M-line and the cracked zones are included.

5.2.2. Different soil type

The second variation in the hinged case was made by introducing a different soil type, the so-called: ‘Soil Type 2’ (loose sand). In this case:

- The material properties of Soil Type 2 and the interfaces in Plaxis 2D are according to Table 49;
- The realistic wall stiffness (EI_{var}) is based on the basic reinforcement ratio $\rho_{1,tot} = 0.6\%$.

Parameter	Name	Value	Unit
Material model	Hardening soil model		[-]
Type of material behaviour	Drained		[-]
Soil unit weight above phreatic level	γ_{dry}	19	[kN/m ³]
Soil unit weight below phreatic level	γ_{sat}	20	[kN/m ³]
Permeability in horizontal direction	k_x	1	[m/day]
Permeability in vertical direction	k_y	1	[m/day]
Secant stiffness in standard drained triaxial test	E_{50}^{ref}	15000	[kN/m ²]
Tangent stiffness for primary oedometer loading	E_{oed}^{ref}	15000	[kN/m ²]
Unloading and reloading stiffness	E_{ur}^{ref}	45000	[kN/m ²]
Power for stress-level dependency of stiffness	m	0.55	[-]
Cohesion (constant)	c_{ref}	0.5	[kN/m ²]
Internal friction angle	ϕ	30	[°]
Dilatancy angle	ψ	0	[°]
Strength reduction factor	R_{inter}	1	[-]

Table 49: Material properties ‘Soil Type 2’ in Plaxis 2D

The input and results obtained for EI_0 , EI_∞ and EI_{var} at Soil Type 2 for $N = 0$ kN and $N \neq 0$ are given in Appendix F1 and F2, respectively. The M-(N)- κ diagrams, the M-line and the cracked zones are included.

5.2.3. Hinged case in particular – safety analysis

An overview of the results obtained for the hinged case at a basic reinforcement ratio ($\rho_{l,tot} = 0.6\%$), a high reinforcement ratio ($\rho_{l,tot} = 1\%$) and Soil Type 2 are given in Table 50. The reported values for the cracked zone in this table relate to the heaviest loaded wall for the hinged case, namely the right wall. For a good comparison with regard to the structural safety for the hinged case the results M_{Ed} , δ_v and U_x are plotted in Figure 86, Figure 87 and Figure 88, respectively.

	Case		Bending moment		Settlement		Lateral wall displacement		Cracked zone	
	#	EI	M_{Ed} [kNm/m']		δ_v [mm]		U_x [mm]		l_{crack} [m]	
			N = 0	N \neq 0	N = 0	N \neq 0	N = 0	N \neq 0	N = 0	N \neq 0
BASIC REINFORCEMENT RATIO	1	EI_0	2390	2430	91	101	62	63	-	-
	2	EI_∞	1750	1780	112	121	85	84	-	-
	3	EI_{var}	1470	1690	118	115	92	82	7	6.8
HIGH REINFORCEMENT RATIO	4	EI_0	2390	2430	91	101	62	63	-	-
	5	EI_∞	1750	1780	112	121	85	84	-	-
	6	EI_{var}	1810	1970	106	109	78	73	9.7	8.9
SOIL TYPE 2	7	EI_0	2860	2820	210	232	131	133	-	-
	8	EI_∞	2300	2300	245	268	166	167	-	-
	9	EI_{var}	1820	2020	267	274	191	177	10.4	9.8

Table 50: Overview of results for the hinged case at different reinforcement ratios and soil types

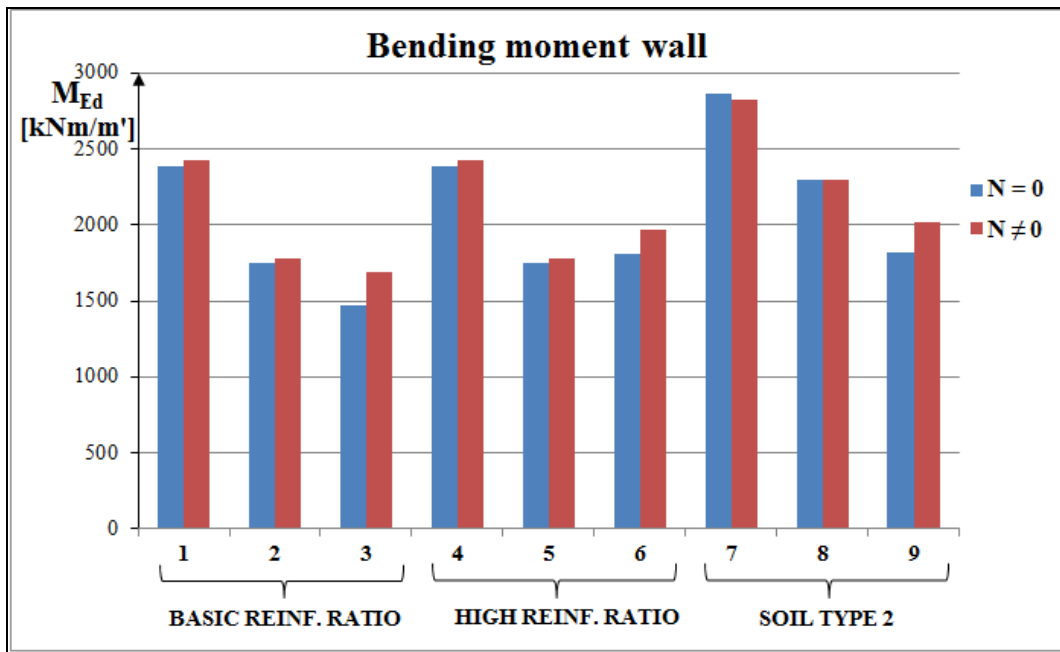


Figure 86: Maximum occurring bending moment of the walls for the hinged case at different reinforcement ratios and soil types

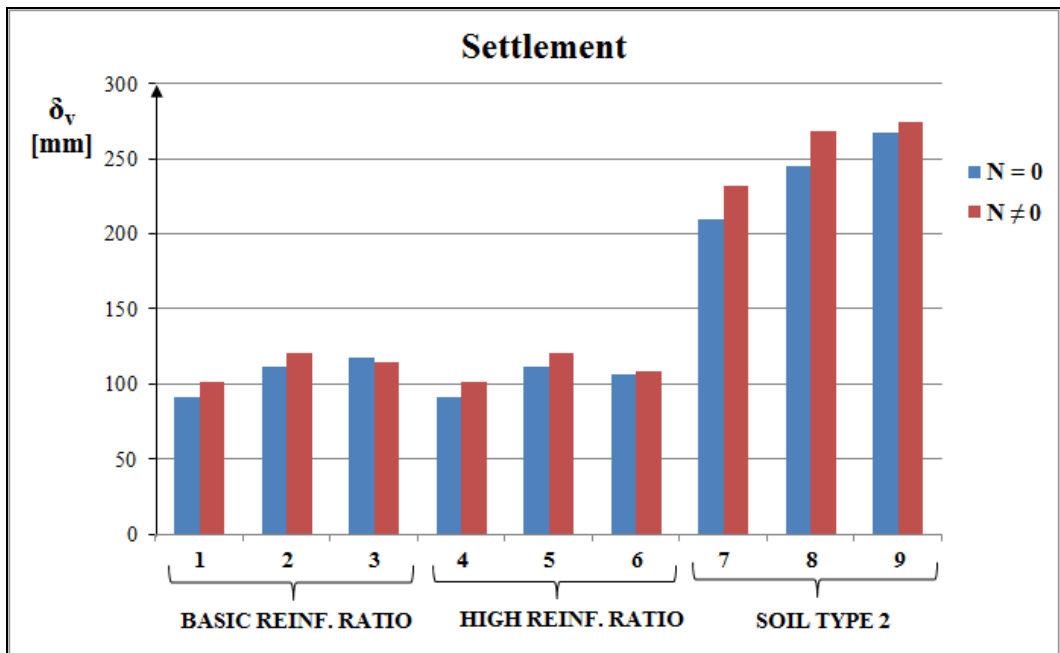


Figure 87: Maximum settlement of the foundation for the hinged case at different reinforcement ratios and soil types

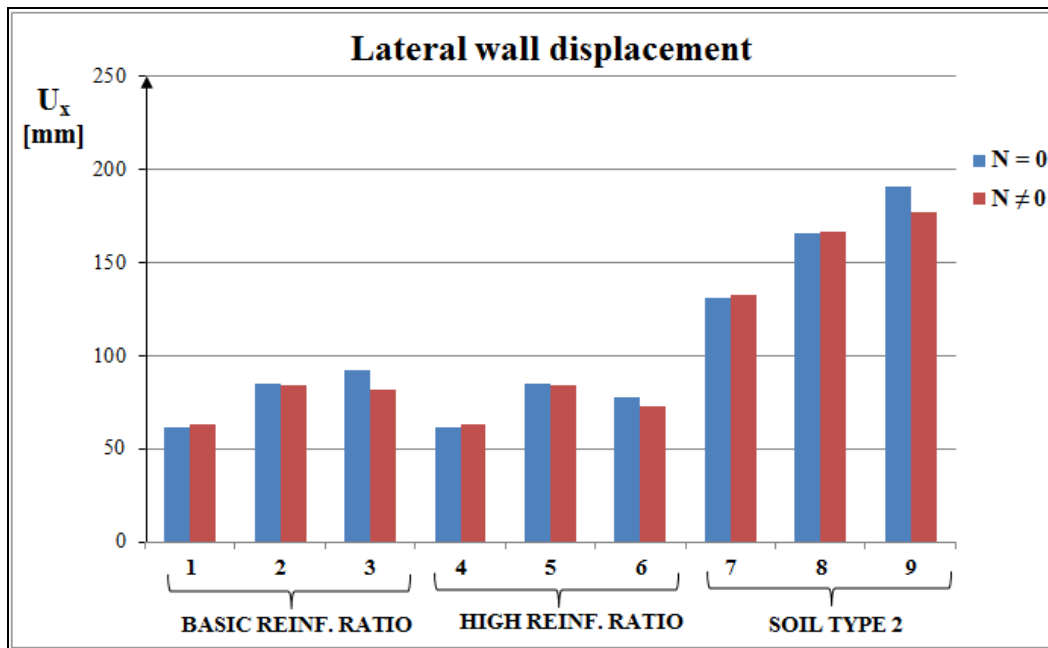


Figure 88: Maximum lateral wall displacement for the hinged case at different reinforcement ratios and soil types

Analysis of results:

In section 5.1 it was already determined that a safe structural design was obtained for the hinged case if the walls were designed based on the totally cracked stiffness EI_{∞} , since the results for $EI_{var} \approx EI_{\infty}$. With regard to the structural safety, the following was expected for:

- **A high reinforcement ratio:** At $\rho_{l,tot} = 1\%$ the diaphragm walls are expected to crack less, as a result of which the structural behaviour at EI_{var} will have a tendency to go towards the behaviour at EI_0 . However, this is not the case. From the cracked heights given in Table 50 it can be derived that a higher reinforcement ratio results in greater cracked zones, implying that the wall behaviour tends faster towards the behaviour at EI_{∞} . At $\rho_{l,tot} = 0.6\%$ an $l_{cracked} \approx 7$ m is noted, while at $\rho_{l,tot} = 1\%$ the $l_{cracked} \approx 9$ -10 m for the highest loaded wall (right wall). From Figure 86, Figure 87 and Figure 88 (cases 5 vs. 6) it is observed that M_{Ed} , δ_v and U_x for the stiffness EI_{var} tend to go towards EI_{∞} ;

Based on these findings it can be stated that:

The findings regarding the safety analysis for EI_{var} at a hinged wall-roof connection remains the same, irrespective of the reinforcement ratio applied for the diaphragm wall: the results for $EI_{var} \approx EI_{\infty}$. At a higher reinforcement ratio the behaviour tends even faster towards EI_{∞} .

- **Soil Type 2:** The total stiffness of the geotechnical structure, which can be regarded as a combined stiffness of the wall and the soil, is expected to decrease at a lower soil stiffness. Due to a lower stiffness of the geotechnical structure, larger cracked zones are expected for the wall. From Table 50 it is indeed found that $l_{cracked}$ increases from about 7 m to 10 m at a lower soil stiffness. This implies that the structural behaviour at EI_{var} tends towards the behaviour at EI_{∞} . This is confirmed by the results in Figure 86, Figure 87 and Figure 88 (cases 8 vs. 9). It is observed that M_{Ed} , δ_v and U_x for the stiffness EI_{var} are lying closer to EI_{∞} . Nevertheless, the deformations at EI_{var} for Soil Type 2 are greater than obtained with EI_{∞} . It is therefore better to calculate the deformations based on EI_{var} , since this is always safer.

At a lower soil stiffness the structural behaviour at EI_{var} still tends towards EI_{∞} for a hinged connection. However, the actual deformations prove that a calculation based on EI_{var} is always a safer method.

5.3. Risk analysis required reinforcement ratio for EI_{var}

Due to the strongly varying bending moment over the height of the diaphragm wall, it is usually not efficient to apply the same reinforcement over the entire height of the diaphragm wall. In practice, the reinforcement is therefore varied over different sections. For enough strength the reinforcement is based on the M-line following from EI_0 (totally uncracked wall). In general, the reinforcement is exactly designed based on this M-line. Therefore, the so-called ‘dekkingslijn’ is drawn to calculate the amount of reinforcement over different sections. For the “Waalbrug-project” this strategy was also applied by the contractor; an example of determining the reinforcement based on the dekkingslijn for the starter panel is depicted in Figure 89. This example shows that not only does the reinforcement differ over the wall height itself, but it also differs at both sides of the wall.

The remaining question now is whether the applied reinforcement variation over the wall height based on EI_0 is sufficient to cope with the M-line in accordance with EI_{var} . In other words:

What is the risk in designing the reinforcement exactly in conformity with the uncracked stiffness EI_0 ? Is it enough to cope with the actual load distribution according to EI_{var} ?

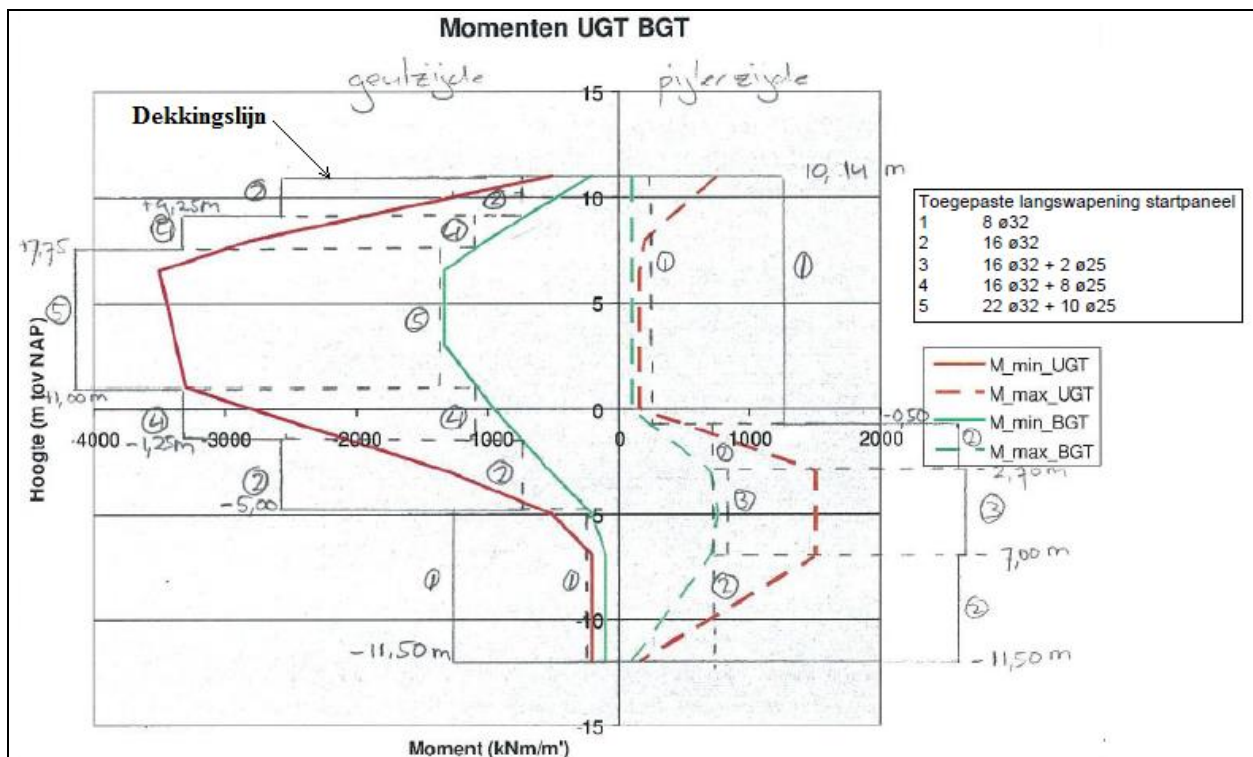


Figure 89: The ‘Waalbrug-project’: Example of ‘dekkingslijn’ bending moments used for reinforcement design over the wall height of the starter panel [11]³

In order to answer this question a comparison of the load distribution (M-line) at EI_0 and EI_{var} has been made for a number of cases. Since it concerns a mirrored situation (trains run in both directions), the basic

³ Source from Intranet (not publicly available) of Engineering Office of Rotterdam (IGR)

assumption here is that for both EI_0 and EI_{var} the highest occurring moment over a certain section of the wall height of both the left and the right wall is used to design the reinforcement. With this basic assumption the risk with regard to the required reinforcement ratio is determined for EI_{var} , which is represented in Table 51. Depending on the applied reinforcement ratio and the soil properties it is observed that in reality there is a risk of applying 20% - 47% less reinforcement at the bottom part of the walls in the hinged case. This highest risk occurs over a region from NAP -5 m to NAP -7 m. In the clamped case (walls and roof) there is a possible risk of applying a lower reinforcement ratio at the top of the wall (in the stiffened region) than required for a situation based on EI_{var} . In the clamped case this risk is very low compared to the hinged case. It is observed that for a lower soil stiffness in the hinged case an even higher amount of extra reinforcement (about 50%) is required for EI_{var} . This can be attributed to the fact that due to the lower soil stiffness the diaphragm wall will redistribute the forces more towards the stiffer bottom part. This same phenomenon occurs when the wall cracks at the upper part, the redistribution of forces then takes place towards the stiffer bottom part of the wall (see also section 4.1.1.7).

It is also not recommended to design the reinforcement based on the M-line configuration of both EI_0 and EI_{sc} , implying that the governing moments following from these stiffnesses should be considered over the real wall. This does not hold in all cases; it is observed that the bending moment for EI_{var} can be greater in some regions than the values following from both EI_0 and EI_{sc} . Therefore it can be concluded that:

It is necessary to always design the reinforcement based on a load distribution according to EI_{var} , otherwise there is a great risk of placing less reinforcement over a certain part of the wall than required for the actual situation. This applies primarily to the hinged case.

Studied case	Detailed info	EI_{var}	Reference	Risk at EI_{var}
Walls only; hinged	Basic reinforcement ratio	$EI (\kappa)$	<i>Section 4.1.1.7, Figure 42</i>	35% less reinforcement at bottom part wall
		$EI (\kappa, N)$	<i>Section 4.1.2.7, Figure 53</i>	30% less reinforcement at bottom part wall
Walls only; hinged	High reinforcement ratio	$EI (\kappa)$	<i>Appendix E1</i>	23% less reinforcement at bottom part wall
		$EI (\kappa, N)$	<i>Appendix E2</i>	20% less reinforcement at bottom part wall
Walls only; hinged	Soil Type 2 (lower soil stiffness)	$EI (\kappa)$	<i>Appendix F1</i>	45% less reinforcement at bottom part wall
		$EI (\kappa, N)$	<i>Appendix F2</i>	47% less reinforcement at bottom part wall
Walls and roof; clamped	Basic reinforcement ratio	$EI (\kappa)$	<i>Section 4.5.1, Figure 80</i>	Possible risk of less reinforcement at top of wall
		$EI (\kappa, N)$	<i>Section 4.5.2, Figure 81</i>	Possible risk of less reinforcement at top of wall

Table 51: Risk with regard to required reinforcement ratio for EI_{var}

Based on the analysis above it is clear that for the hinged case it is not a good philosophy to design the reinforcement based on EI_0 , since there is a high risk that a certain part of the wall will contain less reinforcement to take up the actual behaviour (M-line). The idea that an EI_0 based calculation is always correct, has thus proven not to be true. However, it should be noted that in reality there is a certain degree of safety, because for short-term loading (the braking force in this research) it generally holds that the soil behaves much stiffer (5-10 x the static stiffness). As a result a great part of the load is transferred directly

to the soil under the foundation level (within the packing structure). Based on this theorem the diaphragm wall is loaded less in reality. Ignoring the theorem of a higher soil stiffness in case of short-term loading, it can be stated that:

*The philosophy for designing the reinforcement based on EI_0 is conservative for the hinged case, **only if** the maximum occurring bending moment of both walls is considered over the total wall height for calculation of the reinforcement. However, this is a too safe approach!*

Of more practical relevance would be to design the reinforcement based on the 'dekkingslijn'-principle, where:

- EI_0 is used, but then placing 30-50% extra reinforcement at the bottom part of the wall;

- The bending moment envelope (in Dutch: omhullende M-lijn) based on different simulations with EI_{var} (e.g. variation in wall stiffness and soil stiffness) is used to design the required reinforcement.

For (similar) future projects this should be taken into account.

5.4. Evaluation cracked zones for EI_{var}

For LC3 (representative loading case with braking forces on the left wall and 1 m scour), the occurring cracked zones largely depend on the wall-roof connection. An overview is given in Table 52, where the cracked zones are identified at the top, middle and bottom part of the walls.

For the hinged case it is obvious that the right wall (without the braking forces) has the largest cracked zone compared to the left wall. The right wall cracks over approximately 30% of its height. This cracked zone is concentrated in the middle part of the right wall. For stiffer walls (higher reinforcement ratio) or a lower soil stiffness this increases to even 40-45%. For the clamped case, both walls seem to crack over a reasonable height of about 30%; the cracked zones are more concentrated at the top part of the left wall (below the stiffened region) and at the middle part of the right wall.

Studied case	Detailed info	EI_{var}	Cracked zones [m]	
			Left wall	Right wall
Walls only; hinged	Basic reinforcement ratio	$EI(\kappa)$	2.5 m (top) + 3.7 m (bottom)	7 m (middle)
		$EI(\kappa, N)$	2.7 m (top)	6.8 m (middle)
Walls only; hinged	High reinforcement ratio	$EI(\kappa)$	4 m (top)	9.7 m (middle)
		$EI(\kappa, N)$	3.7 m (top)	8.9 m (middle)
Walls only; hinged	Soil Type 2 (lower soil stiffness)	$EI(\kappa)$	3.2 m (top) + 1.1 m (bottom)	10.4 m (middle)
		$EI(\kappa, N)$	0.2 m (top)	9.8 m (middle)
Walls and roof; clamped	Basic reinforcement ratio	$EI(\kappa)$	8.1 m (top)	5.3 m (middle)
		$EI(\kappa, N)$	7 m (top)	7.2 m (middle)

Table 52: Cracked zones for EI_{var} as a function of the connection type, wall properties and soil properties

5.5. Overview and answering of research questions

In order to reach the aim of this research project, a number of research questions had to be answered in the first place. These were distinguished into two main streams. In the following, the research questions are listed and answered briefly, with reference to relevant sections of the thesis.

I. Determine the structural safety for different calculation models

1) What is the safety level for each of the calculation models with regard to:

- a) The diaphragm walls only;
- b) The total packing structure.

The safety level is not expressed in terms of a unity check, but it rather concerns an evaluation whether the structural behaviour at a realistic stiffness EI_{var} lies indeed within the behaviour of an uncracked (EI_0) and fully cracked structure (EI_∞), as indicated by the Eurocode 2. In this thesis the structural behaviour is expressed in terms of the bending moment (M_{Ed}), settlement (δ_v) and lateral wall displacement (U_x), which are calculated at the bending stiffnesses EI_0 , EI_∞ and EI_{var} as a function of both $N = 0$ kN and $N \neq 0$ kN. The structural safety was investigated for the following calculation models:

- Walls only; hinged
- Walls only; clamped
- Walls and roof; clamped.

In the above-mentioned models a *basic reinforcement ratio* was the main input for determining EI_{var} . For the hinged case a basic reinforcement ratio of $\rho_{l,tot} = 0.6\%$ per meter panel width was applied. For the clamped case a reinforcement pattern consisting of $\rho_{stiff} = 2\%$ over $l_{stiff} = 1.5$ m and $\rho_{field} = 0.6\%$ over $l_{field} = 21$ m turned out to be the most strategic solution. The results have been plotted into diagrams, for which reference is made to section 5.1. For the “Walls only; hinged” it was found that the packing structure was totally safe if the walls were designed based on EI_∞ , while for the “Walls and roof; clamped”- model a safe structure was reached if the walls were designed based on EI_0 . The “Walls only; clamped”- model showed that a fully clamped connection is only an academic case, which is not realizable.

- 2) *Should EI_{var} indeed be accounted for?*
 - a) *Should EI_{var} be accounted for as $EI(\kappa)$ or as $EI(\kappa, N)$?*
 - b) *What is the contribution of the axial force (N) to EI_{var} ?*

Yes, EI_{var} should be accounted for. From this research it is proven that for both a hinged and a clamped connection an error can be made in the structural safety. For the basic case (basic reinforcement ratio) it is found that for the hinged case a wrong analysis is obtained for the deformations based on EI_0 , while for the clamped case a wrong analysis is obtained for the bending moments based on EI_∞ . From the variations made for the hinged case it is also observed that the representative (highest) values for the bending moment and deformations following from both EI_0 and EI_∞ are *not always* a guarantee for a safe structure. Therefore, EI_{var} based calculations are necessary. It has been proven that the axial force (N) has no significant impact on EI_{var} .

- 3) *Are the applied models, based on EI_0 and EI_∞ , conservative?*

This depends on the chosen connection type, the wall properties (reinforcement ratio in particular) and the soil properties. At the basic reinforcement ratio it was found that:

- For a hinged wall-roof connection a model based on EI_∞ is conservative;
- For a clamped wall-roof connection a model based on EI_0 is conservative.

- 4) *Does the safety level change for stiffer diaphragm walls (e.g. thicker wall, higher reinforcement ratio), and if so how much does it change?*

If stiffer diaphragm walls, achieved by applying a high reinforcement ratio, are used in case of a hinged wall-roof connection it is obvious that a model based on EI_∞ is still conservative. At a higher reinforcement ratio the behaviour tends even faster towards EI_∞ (occurrence of greater cracked zones).

When the soil properties (lower soil stiffness) are changed in case of a hinged wall-roof connection, it is obvious that EI_∞ is still a safe approach for the bending moment. However, for the deformations an EI_{var} based calculation is a safer method, because the actual deformations prove to be larger than what follows from the lower bound stiffness EI_∞ .

- 5) *Based on the structural safety, which calculation model is the most adequate for this project and why?*

For the execution of the ‘Waalbrug-project’ the choice for a hinged connection was correct, since there was no integral model representing the internal forces in both the walls and the roof. In this research, an integral model has been studied for the clamped case, where the 3D-model of the roof is approached by an equivalent beam model. From the “Walls and roof; clamped”- case it has been proven that due to the relatively low stiffness of the roof, the situation can be approached by a hinged connection. Therefore, it can be concluded that it was not absolutely necessary to design the packing structure based on a hinged wall-roof connection, but that a clamped connection would also have been a good choice.

- 6) *Which parameters have an impact on the structural safety?*

As mentioned before, the obtained results prove that the chosen connection type, the wall properties and the soil properties have a large impact on the structural safety.

- 7) *If a calculation model forms an unsafe approach, how can this be dealt with?*

Throughout this research it has been observed that considering both the outer boundaries EI_0 and EI_∞ is not always a guarantee for a safe structure. The best way is to always consider EI_{var} for the load distribution and the deformations. Especially, when designing the reinforcement a load distribution according to EI_{var} should be considered. Otherwise, there is a great risk of placing less reinforcement over a certain part of the wall, in particular for the hinged case. An EI_0 based calculation for reinforcement design is only conservative if the maximum occurring bending moment of both walls is considered over the total wall height.

II. Knowledge building and guidelines for similar conditions as the ‘Waalbrug-project’

A. Interaction concrete structure (diaphragm wall) – soil:

- 1) *How is the EI-variation over the wall height and/ or how does the wall crack (location cracked zones):*
- As a function of the loading, soil condition and boundary condition?*
 - With/ without the roof structure at the given soil and loading condition?*

This has been dealt with in section 5.4.

- 2) *How does EI_{var} influence the soil reaction, e.g.: relaxation, settlements?*
- 3) *Does the interaction soil-wall change for another loading or soil condition, and if so, how does it change?*

In answer to research question II.A.2 and II.A.3:

Depending on the connection type, the settlements due to EI_{var} can be safely approached by:

- EI_∞ in the hinged case;
- EI_0 in the clamped case.

At a lower soil stiffness the settlements increase and the calculation of the settlements should then be based on the actual stiffness EI_{var} of the wall.

B. Boundary condition w.r.t. connection diaphragm wall – roof structure:

- 1) *What is the influence of the boundary condition on the diaphragm wall?*
- 2) *Was it necessary to consider the impact of the boundary condition?*

As concluded before, the chosen connection type is of great importance in the safety analysis of the diaphragm walls.

C. Response of total packing structure:

- 1) What is the influence of EI_{var} and the boundary condition on the safety of the total structure?
- 2) Under which circumstances is it (not) necessary to take EI_{var} into account?

In answer to research question II.C.1 and II.C.2:

This has been dealt with in section 5.1 and 5.2.3.

- 3) Which calculation model gives the most optimized design w.r.t. safety?

The most optimized design is obtained for the following models based on EI_{var} :

- “Walls only; hinged”, which is practically similar to the “Walls and roof; hinged”- model;
- “Walls and roof; clamped”- model.

The only exception is the “Walls only; clamped”- model. This model does not have to be considered.

6. CONCLUSIONS AND RECOMMENDATIONS

6.1. Introduction

In this thesis the impact of a realistic bending stiffness (EI_{var}) on the safety of a structure is investigated. According to the standards a safe structure is obtained by considering both the uncracked stiffness (EI_0) and the fully cracked stiffness (EI_∞), which is assumed to be $\frac{1}{3} EI_0$. In order to determine to which extent one is compromising the safety of the structure by calculating with EI_{var} and the impact of the boundary condition (hinged or clamped connection) in addition to that, different calculation models were set up:

- Walls only; hinged
- Walls only; clamped
- Walls and roof; clamped

The structural behaviour is expressed in terms of the bending moment (M_{Ed}), settlement (δ_v) and lateral wall displacement (U_x), which are calculated at the bending stiffnesses EI_0 , EI_∞ and EI_{var} as a function of both $N = 0$ kN and $N \neq 0$ kN. The EI_{var} was determined by means of the M-(N)- κ diagram of the reinforced concrete section.

6.2. Conclusions

Based on the results and discussion the following conclusions could be drawn with regard to:

- **A valid iteration procedure for EI_{var} :**

EI_{var} based calculations turned out to be an iterative procedure. During this research two iteration procedures were developed to find the actual EI-distribution over the diaphragm wall height. An evaluation of the load distribution and cracked zones according to both iteration procedures, finally led to the conclusion that the results of iteration procedure 2 were valid for EI_{var} and that too for every calculation model. In iteration procedure 2 the actual EI-distribution over the wall height is obtained by considering the average M-line and average cracked zones based on EI_0 and EI_∞ .

- **Safety analysis – basic reinforcement ratio:**

The safety level for EI_{var} was not expressed in terms of a unity check, but it rather concerned an evaluation whether the structural behaviour at EI_{var} lies indeed within the behaviour of an uncracked (EI_0) and fully cracked structure (EI_∞). In the above-mentioned models a *basic reinforcement ratio* was the main input for determining EI_{var} . For the hinged case a basic reinforcement ratio of $\rho_{l,tot} = 0.6\%$ per meter panel width was applied. For the clamped case a reinforcement pattern consisting of $\rho_{stiff} = 2\%$ over $l_{stiff} = 1.5$ m and $\rho_{field} = 0.6\%$ over $l_{field} = 21$ m, turned out to be the most strategic solution. The clamped case concerned a design case, for which it could be concluded that the reinforcement ratio to be applied in the stiffened region was limited. Application of a reinforcement ratio greater than 2% in the stiffened region led to an undesirable situation where concrete crushing (M_{pl}) occurred before yielding of the reinforcement (M_e).

Based on the applied basic reinforcement ratio for the hinged and the clamped case the following conclusions were drawn: For the “Walls only; hinged”- model it was found that the packing structure was totally safe if the walls were designed based on EI_∞ , while for the “Walls and roof; clamped”- model a safe structure was reached if the walls were designed based on EI_0 . The “Walls only; clamped”- model showed that a fully clamped connection is only an academic case, which is not realizable.

- **Safety analysis – hinged case in particular:**

For the “Walls only; hinged”- model it can be concluded that the safety analysis remains the same for a higher reinforcement ratio (stiffer walls). A model based on EI_∞ is still conservative. At a higher reinforcement ratio the behaviour tends even faster towards EI_∞ .

In case of a lower soil stiffness it is obvious that EI_{∞} is still a safe approach for the bending moment. However, for the deformations an EI_{var} based calculation is a safer method, because the actual deformations prove to be larger than what follows from the lower stiffness EI_{∞} .

▪ **Conservative design model:**

Whether a calculation model based on EI_0 or EI_{∞} is conservative depends totally on the boundary condition (hinged or clamped connection), the wall properties (reinforcement ratio in particular) and the soil properties. For the basic reinforcement ratio it could be concluded that:

- For a hinged wall-roof connection a model based on EI_{∞} is conservative;
- For a clamped wall-roof connection a model based on EI_0 is conservative.

▪ **Structural safety based on EI_{var} :**

From this research it has been proven that the results with EI_{var} *can* lie outside the outer boundaries, where especially the wall-roof connection has a significant impact on the results. Therefore, it can be concluded that EI_{var} based calculations are safe; these calculations are nearer the truth.

On the contrary, there is a chance that one is compromising the structural safety with EI_0 or EI_{∞} . But this totally depends on the boundary condition. For both a hinged and a clamped connection an error can be made in the structural safety. For the hinged case a wrong analysis is obtained for the deformations based on EI_0 , while for the clamped case a wrong analysis is obtained for the bending moments based on EI_{∞} . Therefore, EI_{var} based calculations are necessary. It has been proven that the axial force (N) has no significant impact on EI_{var} . In the hinged case the results for $EI_{\text{var}} \approx EI_{\infty}$, while for the clamped case the results for $EI_{\text{var}} \approx EI_0$.

▪ **Hinged or clamped wall-roof connection for “Waalbrug-project”:**

For the execution of the ‘Waalbrug-project’ the choice for a hinged connection was correct, since there was no integral model representing the internal forces in both the walls and the roof. In this research, an integral model has been studied for the clamped case, where the 3D-model of the roof is approached by an equivalent beam model. From the “Wall and roof; clamped” - model it has been proven that due to the relatively low stiffness of the roof, the situation can be approached by a hinged connection. Therefore, it can be concluded that it was not absolutely necessary to design the packing structure based on a hinged wall-roof connection, but that a clamped connection would also have been a good choice.

▪ **Risk w.r.t. required reinforcement ratio for EI_{var} :**

When designing the reinforcement a load distribution according to EI_{var} must be considered. Otherwise, there is a great risk of placing less reinforcement over a certain part of the wall, in particular for the hinged case. Depending on the wall properties and the soil properties a risk of applying 20% - 47% less reinforcement at the bottom part of the walls was determined for the hinged case. In the clamped case (walls and roof) there is a possible risk of applying a lower reinforcement ratio at the top of the wall (in the stiffened region) than required for a situation based on EI_{var} . But for the clamped case this risk is rather low.

6.3. Recommendations

For this research the following recommendations can be made with regard to:

▪ **Future projects:**

In this research iteration procedure 2 proved to be valid for EI_{var} based calculations. This iteration method, to find the variable EI-distribution over the diaphragm wall height, was validated for different calculation models used for the specific case of the “Waalbrug-project”. Iteration procedure 2 concerns a general procedure where it is assumed that the actual EI-distribution of the diaphragm wall lies in between EI_0 and

EI_{∞} . For *future projects* with diaphragm walls the following *general procedure* according to iteration procedure 2 is recommended to find the EI-distribution over the wall height of the diaphragm wall:

- Determine the M-line and the (imaginary) cracked zones of the wall for EI_0 . The cracked zones are defined where $M > M_r$;
- Determine the M-line and the (imaginary) cracked zones of the wall for EI_{∞} ;
- Determine the “average M-line” and the “average cracked zone” based on the results for EI_0 and EI_{∞} ;
- The average M-line is used to determine the EI-distribution of the wall. Based on the average bending moment, the EI and EA are determined for the average cracked zone. The uncracked stiffness is considered for the remaining part of the wall. The EI of the cracked and uncracked zones is determined by means of interpolation in the M-(N)- κ diagram;
- The obtained variable EI-distribution over the wall height is used as input in the Plaxis 2D model to find the final results (force distribution and deformations) for EI_{var} .

▪ **Iteration process:**

Throughout this research an iteration process based on the bending moment line was conducted to find the actual EI-distribution over the wall height of both walls. For this iteration process two programs were used, in particular PCSheetPileWall and Plaxis 2D. In Plaxis 2D a stiff structure was applied above the diaphragm walls to simulate the clamped connection. This resulted in equal forces and displacements at the top of both walls. In PCSheetPileWall, this fictitious stiff structure could also have been simulated by conducting an iteration process based on the shear forces at the top of the wall. Therefore, the interaction between two Half-Models (for the left and right wall) in PCSheetPileWall should be considered. Due to the loading on the left wall, a shear force occurs at the top of the left wall. This shear force is passed one on one via the roof structure to the right wall. The iteration process should then go on until the forces and displacements are equal for both Half-Models in PCSheetPileWall. This iteration procedure based on the shear forces obviously requires less effort than the applied iteration procedure based on the bending moments.

▪ **Reinforcement design:**

For (similar) future projects the contractor is recommended to use the ‘dekkingslijn’ strategy to design the reinforcement, considering the following points:

- Place 30-50% extra reinforcement at the bottom part of the wall when using EI_0 based calculations or;
- Use the bending moment envelope based on different simulations with EI_{var} (e.g. variation in wall stiffness and soil stiffness). This is a safe strategy.

▪ **Cyclic loading:**

In this research the braking force was considered on the left wall. However, it concerns a mirrored situation implying that at another point of time the braking force works on the right wall. In Plaxis 2D it is possible to take cyclic loading into account. Due to cyclic loading the soil in between the two walls can get under tension leading to higher bending moments in the wall. It is recommended to take the cyclic loading effect into account in a further study.

▪ **Crack width control:**

The crack width control was out of scope for this research. For the reinforcement design, especially in the cracked zone, this is of importance.

▪ **Roof structure:**

The variation in stresses of the roof structure (especially at the recess) as a function of the variable stiffness, boundary condition, temperature loading and roof inclination was out of scope for this research. It is recommended to gain more insight into this matter.

References

- [1] Van Hattum en Blankevoort. (05-03-2013). *Uitgangspunten notitie (Documentnummer: 4229-BER-001)*. Project: NASIN.
- [2] Van Hattum en Blankevoort. (19-07-2013). *Berekeningsrapport kapconstructie en schilconstructie (Documentnummer: 4229-BER-004)*. Project: NASIN.
- [3] Richards, T. (2005). *Diaphragm walls. 21st Central PA Geotechnical Conference*. Pennsylvania.
- [4] Chandra, S. (2014, December 3). Modelling of soil behaviour. Retrieved from http://home.iitk.ac.in/~peeyush/mth426/Lec4_schandra.pdf
- [5] <http://mfile.narotama.ac.id/files/Civil%20Engineering/Deep%20Excavation;%20Theory%20and%20Practice/Chapter%207%20%20Stress%20And%20Deformation%20Analysis;%20Beam%20On%20Elastic%20Foundation%20Method.pdf>
- [6] CUR committee C183. (2014). *Quay walls* (2nd ed.). Rotterdam, The Netherlands: CRC Press/Balkema.
- [7] Plaxis b.v. (2002). *Plaxis version 8 - Material Models Manual*. Delft, Netherlands: A. A. Balkema Publishers.
- [8] Ehsan, R. (2013). *A study of Geotechnical Constitutive Models using Plaxis 2D*. Retrieved from <http://www.indabook.org/d/A-Study-of-Geotechnical-Constitutive-Models-using-PLAXIS.pdf>
- [9] http://www.scielo.br/scielo.php?script=sci_arttext&pid=S1983-41952013000300008
- [10] Bamforth, P., Chisholm, D., Gibbs, J. & Harrison, T. (2008). *Properties of Concrete for use in Eurocode 2 - How to optimise the engineering properties of concrete in design to Eurocode 2*. Surrey: The Concrete Centre.
- [11] Van Hattum en Blankevoort. (08-03-2013). *Berekening wapening diepwanden (Documentnummer: 4229-BER-003)*. Project: NASIN.